PhD Program in
Translational and Molecular Medicine
DIMET

XXII Cycle, Academic Year 2008-2009

University of Milano-Bicocca
School of Medicine and Faculty of Science

New roles for the RNA processing factors CFI_m68 and SRPK2 highlight unexpected links in the control of mammalian gene expression

Silvia Vivarelli – No. 708258

A mio padre, Agostino

TABLE OF CONTENTS

Chapter 1

GENERAL INTRODUCTION

1. The Alternative Splicing

1.1 The Alternative Splicing Mechanism

Alternative splicing is a major mechanism for modulating the expression of cellular and viral genes and enables a single gene to increase its coding capacity, allowing the synthesis of several structurally and functionally distinct protein isoforms [1]. This mechanism takes place within the spliceosome, a large molecular complex composed of four small nuclear ribonucleoproteins (U1, U2, U4/U6 and U5 snRNPs) and approximately 50–100 non snRNP splicing factors [2]. Vertebrate genes have small exons separated by large introns, and interactions between the upstream 3′ splice site and the downstream 5′ splice site across the exon, facilitate exon recognition [3]. The mechanisms of splice-site selection in alternative and constitutive splicing appear to be closely connected because components of the splicing machinery essential for the constitutive splicing reaction, also have a role in the regulation of alternative splicing [4].

Splicing of regulated exons is modulated by trans-acting factors that recognize an arrangement of positive (splicing enhancers) and/or negative (splicing silencers) cis-acting sequence elements, which can be either exonic or intronic. Differences in

the activities or amounts of general splicing factors and/or gene-specific splicing regulators during development or in different tissues can cause differential patterns of splicing.

In fact, complexity, plasticity and functional specialization are distinctive features of multicellular eukaryotic organisms. Recently it was assumed that these features were mainly achieved through the differential turning on and off of a large number of genes. The realization that the human genome contains a smaller number of genes than expected, and the finding of multiple mechanisms that control the amount and quality of the encoded mRNAs enhance the contribution of pre-mRNA processing, and in particular of alternative splicing, to the observed complexity.

1.2 The Splicing Reaction

Commonly, alternative splicing patterns determine the inclusion of a portion of coding sequence in the mRNA, giving rise to protein isoforms that differ in their peptide sequence and hence chemical and biological activity [5]. Alternative splicing is a major contributor to protein diversity in metazoan organisms. Estimates of the minimum number of human gene products that undergo alternative splicing are as high as 70% [6]. Moreover, many gene transcripts have multiple splicing patterns and some have thousands [1], [7]

To understand this complexity of gene expression, we must study how changes in splice site choice come about.

In a typical multiexon mRNA, the splicing pattern can be altered in many ways (Figure 1). Most exons are constitutive; they are always spliced or included in the final mRNA. A regulated exon that is sometimes included and sometimes excluded from the mRNA is called a cassette exon. In certain cases, multiple cassette exons are mutually exclusive-producing mRNAs that always include one of several possible exon choices but no more. In these systems, special mechanisms must enforce the exclusive choice [8],[9]. Exons can also be lengthened or shortened by altering the position of one of their splice sites. One sees both alternative 5' and alternative 3' splice sites. The 5'-terminal exons of an mRNA can be switched through the use of alternative promoters and alternative splicing. Similarly, the 3'-terminal exons can be switched by combining alternative splicing with alternative polyadenylation sites. Alternative promoters are primarily an issue of transcriptional control. Control of polyadenylation appears mechanistically similar to control of splicing [10]. Finally, some important regulatory events are controlled by the failure to remove an intron, a splicing pattern called intron retention. Particular pre-mRNAs often have multiple positions of alternative splicing, giving rise to a family of related proteins from a single gene (Figure 1H).

Changes in splice site choice can have a wide range of effects on the encoded protein. Small changes in peptide sequence can alter ligand binding, enzymatic activity, allosteric regulation, or protein localization. In other genes, the synthesis of a whole polypeptide, or a large domain within it, can depend on a

particular splicing pattern. Genetic switches based on alternative splicing are important in many cellular and developmental processes, including sex determination, apoptosis, axon guidance, cell excitation and contraction, and many others. Errors in splicing regulation have been implicated in a number of different disease states. The roles played by alternative splicing in particular cellular processes and in disease have been reviewed extensively [5],[11-21].

Splices sites are designed as special sequences at the intron/exon junctions that direct the excision of introns from a pre-mRNA and the joining of exons. The 5' splice site marks the exon/intron junction at the 5' end of the intron. This includes a GU dinucleotide at the intron end encompassed within a larger, less conserved consensus sequence. At the other end of the intron, the 3' splice site region has three conserved sequence elements: the branch point, followed by a polypyrimidine tract, followed by a terminal AG at the extreme 3' end of the intron. Splicing is carried out by the spliceosome, a large macromolecular complex that assembles onto these sequences and catalyzes the two-transesterification steps of the splicing reaction (Figure 2). In the first step, the 2'-hydroxyl group of a special A residue at the branch point attacks the phosphate at the 5' splice site. This leads to cleavage of the 5' exon from the intron and the concerted ligation of the intron 5' end to the branch-point 2'-hydroxyl. This step produces two reaction intermediates, a detached 5' exon and an intron/3'-exon fragment in a lariat configuration containing a branched A

nucleotide at the branch point. The second transesterification step is the attack on the phosphate at the 3' end of the intron by the 3'-hydroxyl of the detached exon. This ligates the two exons and releases the intron, still in the form of a lariat.

The spliceosome assembles onto each intron from a set of five small nuclear ribonucleoproteins (snRNPs) and numerous accessory proteins. During assembly, the U1 snRNP binds to the 5' splice site via base pairing between the splice site and the U1 snRNA. The 3' splice site elements are bound by a special set of proteins. SF1 is a branch-point binding protein (also called BBP in yeast). The 65-kDa subunit of the dimeric U2 auxiliary factor (U2AF) binds to the polypyrimidine tract. In at least some cases, the 35-kDa subunit of U2AF binds to the AG at the intron/exon junction. The earliest defined complex in spliceosome assembly, called the E (early) or commitment complex, contains U1 and U2AF bound at the two intron ends [22]. The E complex is joined by the U2 snRNP, whose snRNA base-pairs at the branch point, to form the A complex. The A complex is joined by the U4/U5/U6 tri-snRNP to form the B complex. The B complex undergoes a complicated rearrangement to form the C complex, in which the U1 snRNP interaction at the 5' splice site is replaced with the U6 snRNP and the U1 and U4 snRNPs are lost from the complex. It is the C complex that catalyzes the two chemical steps of splicing (Figure 2B). There is also a minor class of spliceosome that excises a small family of introns that use different consensus sequences [23].

1.3 Alternative Splicing Regulation

The splice site consensus sequences are generally not sufficient information to determine whether a site will assemble a spliceosome and function in splicing. Other information and interactions are necessary to activate their use [3, 24].

Introns can range in size from less than 100 nucleotides to hundreds of thousands of nucleotides. In contrast, exons are generally short and have a fairly narrow size distribution of 50–300 nucleotides. Commonly, spliceosomal components binding on opposite sides of an exon can interact to stimulate excision of the flanking introns [25]. This process is called exon definition and apparently occurs in most internal exons [26]. Significantly, on top of this process, there are many non-splice site regulatory sequences that strongly affect spliceosome assembly. RNA elements that act positively to stimulate spliceosome assembly are called splicing enhancers. Exonic splicing enhancers (ESEs) are commonly found even in constitutive exons. Intronic enhancers (ISEs) also occur and appear to differ from exonic enhancers. Conversely, other RNA sequences act as splicing silencers or repressors to block spliceosome assembly and certain splicing choices. Again, these silencers have both exonic (ESSs) and intronic (ISSs) varieties. Some regulatory sequences create an RNA secondary structure that affects splice site recognition [27-29], but most seem to be protein binding sites.

ESEs are usually bound by members of the SR (Ser-Arg) protein family [30-32] (Table 1). ISSs and ESSs are commonly bound by heterogeneous nuclear RNPs (hnRNPs; Table 2), which have one or more RNA-binding domains and protein–protein interaction domains [33-34]. ISEs are not as well characterized as the other three types of element, although recently several proteins, such as hnRNP F, hnRNP H, neuro-oncological ventral antigen 1 (NOVA1), NOVA2, FOX1 and FOX2, have been shown to bind ISEs and to stimulate splicing [35-38].

Choices of alternative splicing have long been thought to be made at the stages of splice site recognition and early spliceosome assembly, and indeed this is frequently the case. However, several recent studies have shown that the decision can be made at different stages of spliceosome assembly, and even during conformational changes between the two transesterification steps [39-40]. In addition, there has been accumulating evidence showing the coupling of RNA transcription to splicing regulation [41-45].

What are the factors and the processes that are involved in the alternative splicing regulation?

In first instance, the correct alternative splicing depends on the stoichiometry and interactions of positive and negative regulatory proteins, including Core Splicing Proteins (CSPs) that represent the main protein components of the spliceosome complex, such as U1, U2 and U4/U6 snRNPs, as well as the U2AF heterodimer.

Each cell type has a unique repertoire of SR proteins and hnRNPs, and moderate changes in their relative stoichiometry can have great effects on the pattern of alternative splicing [46]. It is possible that changes in the stoichiometry of snRNPs can alter the complex network of splicing factors and the interactions between splicing factors and CSPs.

Early stages of spliceosome assembly occur around the exons owing to the large size of introns [47]. The exon definition must eventually be converted to intron definition, which occurs by cross-intron interactions between the U1 and U2 snRNPs [48-49].

Interestingly, the best-studied mechanisms of alternative splicing regulation involve controlling splice site recognition by facilitating or interfering with the binding of the U1 or U2 snRNP to the splice sites. SR proteins have important roles in facilitating splice site recognition. For example, they recruit the U1 snRNP to the 5′ splice site and the U2AF complex and U2 snRNP to the 3′ splice site by binding to an ESE and directly interacting with protein targets [50-53]. These interactions are mediated by their RS (Arg–Ser repeat-containing) domains [54-55], which have to be properly phosphorylated and dephosphorylated [56-57]. SR proteins also cooperate with other positive regulatory factors to form larger splicing enhancing complexes by interacting with other RS domain-containing proteins, such as transformer 2 (TRA2) and the SR-related nuclear matrix proteins SRm160 (also known as SRRM1) and SRm300 (also known as SRRM2) [58-60]. Binding

and recruiting can also be achieved by intronic binding proteins: for example, T cell-restricted intracellular antigen 1 (TIA1) binds a U-rich sequence downstream of weak 5′ splice sites to recruit the U1 snRNP [61-62]; and Src associated in mitosis 68 kDa protein (SAM68; also known as KHDRBS1) binds and recruits U2AF to the 3′ splice site of exon V5 of the transmembrane glycoprotein CD44 pre-mRNA [63].

There is also the possibility to inhibit splice site recognition. Inhibition of splice site recognition can be achieved in many ways. First, when splicing silencers are located close to splice sites or to splicing enhancers, inhibition can occur by sterically blocking the access of snRNPs or of positive regulatory factors. Splicing inhibitors also sterically block the binding of activators to enhancers.

Frequently, combinatorial or competitive effects of both activators and inhibitors control splicing and the final decision of whether an alternative exon is included is determined by the concentration or activity of each type of regulator, often by SR proteins and hnRNPs [64-66]. Also, the nature of the activity of cis-acting elements and their cognate binding proteins in some cases depends on their position relative to regulated exons. A new technique that combines CLIP and high-throughput sequencing, known as HITS-CIIP80 (CIIP-seq) [38, 67-68], not only verified the reproducibility of this mRNA map, but also provided genome-wide information on the target genes of NOVA1, NOVA2 and FOX2 as well as possibly mechanisms by which these proteins are regulated [69]. Why does the position

of splicing regulatory elements determine the action of cognate splicing factors? It is possible that enhancers are positioned so that when the splicing factors bind to them, the splice sites of the alternative exon are better presented to the splicing machinery by changing the local mRNA structure. By contrast, silencing elements function in the opposite manner, by competing with components of the splicing machinery or by changing the structure of the mRNA to impede splice site recognition.

The selection of the splice site can be influenced by secondary structures in the pre-mRNA as well. Secondary structures can affect alternative splicing by masking splice sites or by binding sites for splicing factors [70-71].

After the 5′ and 3′ splice sites are recognized and exons are defined, exon definition must be converted to intron definition, which involves cross-intron interaction between U1 and U2 snRNPs, to form a functional spliceosome. Several studies have shown that the commitment to splicing of at least some alternative exons occurs during splice site pairing in the A complex [48-49]. For example, ATP hydrolysis is required for splice site pairing, which locks splice sites into a splicing pattern after U2 snRNP binding to the branch site [48]. Additional studies also provided evidence that binding of U1 and U2 snRNPs to splice sites to define an exon does not necessarily commit the exon to splicing [39, 72].

Alternative splicing should be coupled with transcription. Two models have been proposed to explain the role of RNA

polymerase II (RNAP II) in the regulation of alternative splicing [73]. The first model is known as the recruitment model, in which RNAP II and transcription factors interact, directly or indirectly, with splicing factors [45, 73-74], thereby increasing or decreasing the efficiency of splicing. A second, kinetic model proposes that the rate of transcription elongation influences the inclusion of alternative exons by affecting whether the splicing machinery is recruited sufficiently quickly for spliceosome assembly and splicing to occur. In support of this model, an RNAP II with a reduced elongation rate caused by a point mutation was found to greatly stimulate the inclusion of an alternative exon that has weak splice sites [75].

Alternative splicing has an important role also in defining tissue specificity. Recent high-throughput studies have shown that, of the human tissues examined, 50% or more of alternative splicing isoforms are differently expressed among tissues [76], indicating that most alternative splicing is subject to tissue-specific regulation. Tissue-specific alternative splicing events can be explained in part by tissue-specific expression of splicing factors, and the corresponding regulation of their target mRNA transcripts [77-79]. Among all human tissues, brain is the most functionally diverse tissue, as it has the highest occurrence of tissue-specific alternative splicing isoforms. Accordingly, several brain specific factors have been identified, such as nPTB [80], NOVA1, NOVA2 [81] and Hu/Elav proteins [82-84]. In addition, region- and cell type specific expression of most of the >300 RNA-binding proteins examined was observed

in proliferating and post-mitotic mouse brain cells [85]. Alternative splicing should be also regulated by constitutive splicing factors. For example SR proteins originally discovered as general, or non-sequence-specific, splicing activators [31], can act as specific alternative splicing regulators in different cell types and tissues. Disruption of the genes that encode ASF/SF2 and SC35 specifically in the heart have shown that they have important but distinct roles in tissue development [86-87]. In addition, a recent study showed that mice with complete ablation of SRp38 survived through early embryogenesis and, strikingly, displayed only cardiac defects; these mice showed differences in alternative splicing [88].

CSPs are also involved in alternative splicing regulation. In fact, analysis of micro array based expression profiles from mouse, chimpanzee and human tissues revealed that snRNPs are differentially expressed in particular tissues [89]. This is consistent with results from an RNA interference (RNAi) screen in D. melanogaster, which showed that changing levels of CSPs leads to changes in alternative splicing. Notably, that differences in protein expression levels of either tissue-specific splicing regulators or CSPs may not fully explain how cells can change alternative splicing patterns rapidly, for example in response to cellular stress. Mounting evidence has shown that post-translational modification of splicing factors can affect alternative splicing. The best studied modification is phosphorylation, and consistent with this, several well studied cell signalling pathways have been shown to be involved in

alternative splicing regulation [90-91]. Phosphorylation has been shown to affect the local concentration of splicing factors that are adjacent to pre-mRNA substrates, by altering their intracellular localization [92-95], protein–protein [57] and protein–RNA interactions [63, 96] and even intrinsic splicing activity [51]. Phosphorylation can change the ability of splicing factors to interact with other proteins or mRNA substrates, leading to changes in splice site selection. Phosphorylation can also change the intracellular localization of splicing factors. Phosphorylation status can also, in one case, determine whether a splicing factor functions as a splicing repressor or activator [97-98].

Finally, alternative splicing regulatory networks have a branched architecture and the perturbation of any single step can lead to alternative splicing misregulation. Diverse mechanisms are used to ensure tissue and cell type-specific splicing regulation. Accumulating evidence has shown that alternative splicing plays an important part in defining tissue specificity. The action of sequence specific transcription factors has been thought to be the most robust way of defining tissue specificity [99]. Important goals of future studies of alternative splicing regulation include understanding how regulators switch key splicing events during development and in response to environmental stimuli, and how misregulation of alternative splicing leads to disease. Complete characterization of tissue-specific patterns of expression is of great importance to defining

mechanisms of alternative splicing regulation in different cell types.

1.4 The SR Family of Proteins

1.4.1 SR Proteins: an overview

The SR proteins, a group of highly conserved proteins in metazoans, are required for constitutive splicing and also influence alternative splicing regulation [3, 33]. They have a modular structure consisting of one or two copies of an RNA-recognition motif (RRM) and a C-terminal domain rich in alternating serine and arginine residues (the RS domain). The RRMs determine RNA-binding specificity, whereas the RS domain mediates protein–protein interactions that are thought to be essential for the recruitment of the splicing apparatus and for splice site pairing [4, 100]. Another class of RS domain-containing proteins involved in splicing are the SR-related proteins. These proteins, which might contain RRMs, include the U1-70K protein, both subunits of U2AF, SRm 160/300 (two SR-related nuclear matrix proteins of 160 and 300 kDa), as well as alternative splicing regulators such as Tra and Tra2 [33].

The SR family and SR-related proteins function in the recognition of exonic splicing enhancers (ESEs), thus leading to the activation of suboptimal adjacent 3′ splice sites [30]. The first SR proteins to be identified had similar effects on 5′ splice-site selection: increased concentrations of the proteins resulted in the selection of intron-proximal 5′ splice sites in pre-mRNAs that contain two or more alternative 5′ splice sites. Strikingly, an

excess of hnRNPA/B proteins had the opposite effect, promoting the selection of intron-distal 5′ splice sites. These effects have been observed with different pre-mRNA substrates both in vitro and in vivo [21, 55, 58]. Individual SR proteins can sometimes have opposite effects on alternative splice site selection too, as in the case of the antagonistic effects of SF2/ASF and SC35 in the regulation of β-tropomyosin [101], and of SF2/ASF and SRp20 on the regulation of SRp20 pre-mRNA alternative splicing [102]. The functional antagonism of SF2/ASF and hnRNPA1 in splice site selection is based on competitive binding to pre-mRNA. SF2/ASF interferes with hnRNPA1 binding and enhances U1 snRNP binding at both duplicated 5′ splice sites in a pre-mRNA model substrate. Thus, U1 snRNP simultaneous occupancy results in the selection of the proximal 5′ splice site. By contrast, hnRNPA1 binds cooperatively and indiscriminately to this pre-mRNA and interferes with U1 snRNP binding at both sites, resulting in a shift to the distal 5′ splice site [103]. The general activities of SR proteins and hnRNPA/B proteins on 5′ splice-site selection do not appear to require the recognition of specific target sequences. However, there are clear examples in which specific sequences have a role. For instance, the presence of high-affinity sites for hnRNPA1 between two 5′ splice sites shifts selection towards the intron-distal 5′ splice sites, but in this case the mechanism is unknown, because no corresponding change in U1 snRNP binding is observed [103-104]. By contrast, binding to specific sites is a clear requirement when these

proteins act at enhancers and silencers. Several models have been proposed to explain the function of SR proteins in enhancer-dependent splicing. SR family proteins bound to ESEs can promote U2AF recruitment to the polypyrimidine tract and activate an adjacent 3′ splice site. This activity involves an RS domain-mediated interaction between an enhancer-bound SR protein and the small subunit of U2AF (U2AF35) (U2AF recruitment model). Alternatively, ESE-bound SR proteins might interact with the splicing coactivator SRm160, an SR-related nuclear matrix protein of 160 kDa, establishing a set of interactions that are different from those required for the recruitment of U2AF65 (65 kDa) to the polypyrimidine tract (coactivator model) [30]. Biochemical and genetic evidence has shown that these interactions are important for optimal splicing activity and for proper development of the nematode Caenorhabditis elegans [105]. Finally, splicing enhancers can antagonize the negative activity of hnRNP proteins recognizing exonic splicing silencer (ESS) elements (inhibitor model) [106]. The relative abundance of SR and hnRNPA/B proteins could be important in regulating the patterns of alternative splicing in a tissue-specific manner. Indeed, there are tissue-specific variations in the total and relative amounts of SR proteins [60], and in particular the molar ratio of SF2/ASF to its antagonist, hnRNPA1, varies considerably in different rat tissues [107].

Moreover, SR and hnRNP protein activities are affected by phosphorylation; thus, protein kinases involved in the phosphorylation of these splicing regulators could have an

important role in linking alternative splicing regulation to extracellular signals. SR proteins appear to be functionally redundant in *in vitro* assays using constitutively spliced pre-mRNA substrates. However, differences observed in alternative splicing regulation suggest unique functions for individual SR proteins. SF2/ASF is essential for cell viability in the DT40 chicken cell line, and its depletion cannot be rescued by overexpression of other SR proteins [108]. SRp20 is essential for mouse development [109], and conditional deletion of the SR protein SC35 in the thymus causes a defect in T-cell maturation [110]. Genetic disruption of SRp55/B52 in Drosophila resulted in lethality during development; however, no general splicing defects were found in mutant larvae depleted of B52 [111-112]. It was later found that other SR family members are able to complement the loss of B52 in most tissues, except in the brain, where B52 is the predominant protein [113]. dsRNA-mediated interference (RNAi) experiments with C. elegans SR proteins have shown that, whereas the ortholog of the mammalian SF2/ASF (CeSF2/ASF) is an essential gene, functional knockouts of other SR genes result in no obvious phenotype, which is indicative of gene redundancy [114-115]. Simultaneous interference of two or more SR proteins in certain combinations caused lethality or other developmental defects. These results suggest that at least some SR proteins are functionally redundant and that the requirement for a particular SR protein might be due to specific

functions in the tissue or developmental stage in which a particular SR protein is predominant.

1.4.2 SR Proteins: a Vertical Integration of Gene Expression

Based on recent advances, it has become quite probable that RNA-binding SR proteins are critical to multiple steps in gene expression, from transcriptional elongation to mRNA splicing to RNA export to translation. The integration of these activities by single SR proteins may constitute the requirement of SR proteins for cell viability and proliferation.

Recent findings also suggest some unexpected roles of SR proteins in organizing gene networks in the nucleus and facilitating cell-cycle progression [116], maintaining genome stability [117-119].

Although it remains to be determined whether these functions reflect a degree of independent activities of SR proteins or are all intertwined with the function of SR proteins in pre-mRNA splicing, these recent discoveries emphasize key roles that SR proteins are likely to play in coupling various transcriptional and post-transcriptional gene expression events. Defects in these processes may directly contribute to developmental defects and onset of cancer. These findings, therefore, highlight the broader roles of SR proteins in vertical integration of gene expression and provide mechanistic insights into their contributions to genome stability and proper cell-cycle progression in higher eukaryotic cells.

1.4.3 SR Protein Kinases

Phosphorylation is essential for the SR family of splicing factors/regulators to function in constitutive and regulated pre-mRNA splicing; yet both hypo- and hyper-phosphorylation of SR proteins are known to inhibit splicing, indicating that SR protein phosphorylation must be tightly regulated in the cell. However, little is known how SR protein phosphorylation might be regulated during development or in response to specific signaling events. Consequently, it may not be surprising that experimental induction of both SR protein hypo- and hyper-phosphorylation inhibits splicing [120].

While these observations clearly suggest that SR protein phosphorylation is under precise control, little is known about the mechanism of such regulation in the cell.

Multiple protein kinases have been implicated in SR protein phosphorylation. Among the growing list of SR protein kinases, the SRPK and Clk/Sty families are best characterized. Mammalian cells express two SRPKs and four members of the Clk/Sty family of kinases. Interestingly, SRPK1 and SRPK2 were shown recently to differentially associate with U1 and tri-snRNP particles, respectively, indicating that these kinases have both overlapping and unique functions in mammalian cells [121].

Enzymatic analysis reveals that SRPKs use a highly processive mechanism to phosphorylate a defined region in the RS domain in each SR protein [122-123], and Clk/Sty can further

phosphorylate the remaining sites in the RS domain [124-125], suggesting the possibility that these kinases may catalyze a cooperative phosphorylation relay to modulate SR protein function at different biochemical steps and/or in various cellular locations [124, 126]. This idea is consistent with their cellular distributions: While members of the Clk/Sty family of kinases are predominately localized in the nucleus [127-128], the SRPK family of kinases are detected in both the cytoplasm and the nucleus [129-130]. Recently it was observed that SRPKs have the capacity to shuttle from cytoplasm to nucleus upon phosphorylation or osmotic stress signal [131-132].

Current data suggest that both the Clk/Sty and SRPK families of kinases are involved in the regulation of spliceosome assembly by mediating the localization and interaction of splicing factors in mammalian cells. It is, however, unlikely that they are completely redundant kinases, as each kinase may have a more defined spectrum of substrates. Alternatively, these kinases may be differentially expressed and/or regulated.

Despite its importance, little is known about how SR protein phosphorylation might be regulated in the cell and how a specific signal might be transduced to control RNA processing via modulation of SR protein phosphorylation.

Recent discoveries from the Manley laboratory shed a critical light on these important questions by revealing dramatic dephosphorylation of a specific SR protein (SRp38) in response to heat shock [133-134]. The regulation is achieved by an increased exposure of the protein to the activated protein

phosphatase PP1 in combination with limited accessibility of the protein to SR protein kinases under heat-shock conditions, underscoring the importance of a balanced action between SR protein kinases and phosphatases in controlling the phosphorylation state of SR proteins.

SRPK1 and SRPK2 are highly specific kinases for the SR family of splicing factors. SRPK1 is predominantly expressed in pancreas, whereas SRPK2 is highly expressed in brain, although both are coexpressed in other human tissues and in many experimental cell lines [130]. SRPK1 was originally identified as a kinase of SC35, a key pre-mRNA splicing factor in the nuclear speckles, in the extracts from HeLa cells [135-136]. Addition of purified SRPK1 to permeabilized cells or overexpression of SRPK1 in transfected cells results in an apparent disassembly of the nuclear speckles [135]. These results suggest that phosphorylation, or hyperphosphorylation, causes release of these factors from the speckles, or perhaps that the integrity of these structures is compromised.

In particular, SRPK2 is highly related in sequence, kinase activity, and substrate specificity to SRPK1. It is highly expressed in brain. SRPK2 possesses a large internal spacer sequence dividing its kinase domains into two parts, a structural feature unique among Ser/Thr protein kinases, its sequence is for more than two third unique in each kinase. SRPK2 contains also a proline-rich sequence at its N terminus, which is not present in SRPK1. This unique region of SRPK2 harbours consensus sites for binding to SH3 and WW domain-containing

proteins. SRPK2 efficiently phosphorylates serine/arginine-rich (SR) proteins, such as the splicing factors ASF/SF2, SC35, and SRp40, in their arginine/serine-rich (RS) domains in vitro. Overexpression of SRPK2 induces the phosphorylation-dependent relocalization of SR proteins from nuclear speckles to the nucleoplasm. Furthermore, SRPK2-mediated phosphorylation has been shown to regulate protein-protein interactions between RS domain-containing splicing factors in vitro [96, 137].

During these recent years scientists are shedding light on the regulation of the activity of SRPKs and on the mechanisms involving these kinases in stress response or cell cycle regulation. Nowadays there are not yet elucidated functions that have to be further explained.

1.5 Signal Transduction Pathways: from Extracellular Stimuli to Alternative Splicing

Pre-mRNA splicing is regulated in a tissue-specific or developmental stage-specific manner [138]. The selection of splice site can be altered by numerous extracellular stimuli such as hormones, immune response, neuronal depolarization, and cellular stress, through changes in synthesis/degradation, complex formation, and intracellular localization of regulatory proteins.

In the case of cellular stress, when cells are stressed by pH change, osmotic shock or lack of oxygen, cytoplasmic accumulation of splicing regulatory proteins such as hnRNP A1,

tra2-β, and SAM68 are observed, with alteration of splicing site selection in several genes [92]. The ICH-1 (interleukin-1h converting enzyme homologue 1) gene has an alternative exon 9, and the inclusion of exon 9 is repressed by SC35 and SF2/ASF [139]. After the ischemic event in the brain, inclusion of exon 9 is promoted, concomitant with the translocation of regulatory proteins. In NIH-3T3 fibroblasts, the MKK3/6–p38 pathway mediates the cytoplasmic accumulation of hnRNP A1 [94, 140]. However, activation of p38 is not observed in the ischemic model.

1.6 Stressful Splicing: the Effects of Paraquat

Paraquat (PQ, 1,1'-dimethyl-4,4'-bipyridinium), a widely-used herbicide, has been suggested as a potential etiologic factor for the development of Parkinson's disease and it is known to damage the lipid membrane via peroxidation [141], although the exact mechanism of PQ-induced oxidative cell damage is currently controversial. The assumption is that PQ promotes the production of ROS through a redox cycling process, which can then cause damage to cellular macromolecules [142]. Indeed, electron reduction of PQ, promoted by cellular diaphorases (that catalyses the oxidation of reduced NAD), results in the formation of a PQ radical, which in turn can transfer its electrons to molecular oxygen, forming elements such as superoxide anions. These properties make PQ exposure a useful experimental model for oxidative stress. Indeed, several

authors have used this compound to study the response and the sensitivity to oxidative damage *in vivo* and *in vitro* [143-147]. Recently, it was tested the hypothesis that mitochondrial damage modulates alternative splicing, not only of a few mRNAs, but also in a general manner. In fact, it was observed that PQ, affects the selection of pre-mRNA splice sites in general [143]. SH-SY5Y neuroblastoma cells treated with PQ represent a huge studied in vitro model to uncover neurodegeneration [145, 148-153] and to characterize the effect charged to alternative splicing after oxidative stress induction [143].

The recent commercialisation by Affymetrix of Exon 1.0 ST GeneChips (Exon GeneChips) allows the definition of both transcription patterns and of alternative pre-mRNA maturation events. Using this microarray platform our laboratory have profiled two *in vitro* models to identify the mRNA isoforms associated to ALS disease [Lenzken, C. et al., article in preparation]. The so-defined acute model, consisting in SH-SY5Y treated with a single dose of PQ, constituted the same that I used to perform the experiment contained in my project reported in Chapter 1.

2. The 3' End Formation and Export

2.1 Molecular mechanisms of Eukaryotic pre-mRNA 3'-end Processing Regulation

In eukaryotes, 3' end cleavage of transcripts generated by RNAP II is a universal step of gene expression that proceeds

through the recognition of cis-acting elements of the pre-messenger RNA (mRNA) [defined as the poly(A) signal] by a complex machinery. After cleavage, most pre-mRNAs, with the exception of histone replication-dependent transcripts, acquire a polyadenylated tail. 3' end processing is a nuclear co-transcriptional process that promotes transport of mRNAs from the nucleus to the cytoplasm and affects the stability and the translation of mRNAs.

The mRNA 3' end formation in vivo is an integral component of the coupled network in which the different machines carrying out separate steps of the gene expression pathway are tethered to each other to form a gene expression factory. In this network, 3' end processing cross-talks with the transcription and splicing steps to optimize the efficiency and specificity of each enzymatic reaction (Figure 3) [154]. The physical interconnections between the splicing/transcription and 3' end processing machineries create a strong functional interdependence. Indeed, 3' end polyadenylation factors (or pA factors, including factors involved in both cleavage and polyadenylation) and sequence elements of the poly(A) signal modulate transcription termination [155-158] and, in turn, transcription factors/activators affect processing at the poly(A) signal [159-162]. The phosphorylated carboxyl-terminal domain (CTD) of RNAP II also plays a major role in this coupling network by serving as a gathering/delivering platform of pA factors and is an integral component of the 3' end processing complex [163-164]. The functional interdependence between

splicing and 3' end processing is mediated by the molecular link between splicing factors bound at the last intron 3' splice site and pA factors associated to the poly(A) signal in the terminal exon [165-169] and contributes to define the last exon of a pre-mRNA [3].

In addition to playing an essential role in the extensive network that coordinates the activities of the different gene expression machineries, 3' end processing also participates in quantitative and qualitative regulatory aspects of gene expression.

In transcripts carrying a single poly(A) signal, the function of the regulatory factors is to define whether to process the transcript. The regulation of the efficiency of poly(A) signal recognition will determine the level of protein expression. Indeed, transcripts that are not processed at the 3' end will be degraded or not transported efficiently to the cytoplasm. In transcripts containing more than one poly(A) signal, that is the majority of the transcription units [170-172], the role of the regulatory factors is to define where to process the transcript. Alternative 3' end processing proceeds through the choice of alternative pA signals located in the same exon or in different exons. The consequence of this regulation is either to change the coding sequences, resulting in different protein isoforms, or the sequences included in the 3' untranslated region (UTR) region, resulting in transcripts which may differ in their stability, localization, transport and translation properties [173-176].

Processing at a single or multiple poly(A) signals not only can be influenced by physiological conditions (including cell growth,

cell cycle position, differentiation and development) but also can be altered in pathological situations (including cancer, immunity and inflammation and viral infection). The crucial role of 3' end processing in gene expression is highlighted by the increasing number of different disease entities caused by defects in the formation of proper mRNA ends [177]. Indeed, disruption of this process can profoundly perturb cell viability, growth and development.

2.2 Metazoan 3'-end Processing Machinery

The machinery leading to the formation of metazoan polyadenylated mRNAs contains several sub-complexes (Figure 4), including cleavage and polyadenylation specificity factor (CPSF), cleavage stimulation factor (CstF), cleavage factor I (CFIm), cleavage factor II (CFIIm), poly(A) polymerase (PAP), symplekin and the RNAP II. All these factors contribute to the cleavage reaction. The addition of the poly(A) tail, when tested in in vitro reconstituted assays, only requires CPSF, PAP and the poly(A) binding protein (PABP). PABP stimulates PAP to catalyze the addition of adenosine residues and controls poly(A) tail length by regulating the interaction between CPSF and PAP [178]. The poly(A) signal is defined by two primary sequence elements: the AAUAAA hexamer (or the more frequent variant AUUAAA) found 10–30 nt upstream of the cleavage site that binds CPSF and the U/GU-rich region located 30 nt downstream of the cleavage site (downstream sequence element or DSE) that associates with CstF. Recognition of the

poly(A) signal in the absence of the canonical A(A/U)UAAA element depends on the presence of an upstream UGUA sequence motif which functions in association with CFIm [179-180]. The optimal cleavage site is generally a CA dinucleotide and cleavage is catalyzed by the 73-kDa subunit of CPSF at the 3' side of the adenosine residue [181]. Recently, the purification and subsequent proteomic identification and structural characterization of the human 3' end processing complex revealed a complex architecture containing 85 proteins, including new essential factors and over 50 proteins that mediate the interplay with other processes. Among these factors, two proteins, the CPSF-associated factor, WDR33 (WD repeat domain 33), and the serine/threonine protein phosphatase 1 (PP1), have been shown to be required for the 3' end processing reactions [182].

The efficiency of the 3' end processing reaction is modulated by additional sequence elements located upstream (upstream sequence element or USE) or downstream (auxiliary downstream sequence element or AuxDSE) of the cleavage site. USEs are generally U-rich and serve as an additional anchor for the 3' end processing machinery by recruiting auxiliary or essential 3' end processing factors [183-192]. AuxDSEs are generally G-rich and function by binding regulatory factors resulting in enhanced mRNA 3' end formation [193-195].

Unlike polyadenylated mRNAs, histone pre-mRNAs 3' end processing is governed by a set of rigid constraints that allow a

precise coordination between regulation of their expression and DNA replication signals [196-197]. The replication-dependent histone processing signal lies within 100 nt downstream of the stop codon and is composed of a conserved stem–loop sequence and a more variable purine-rich element (histone downstream element or HDE) that begins 15–20 nt downstream of the stem–loop. The SLBP protein bound to the stem–loop structure acts to stabilize the binding of the U7 snRNA incorporated in the U7snRNP to the HDE. This interaction is bridged by a 100-kDa zinc finger protein (ZPF100) and involves Lsm11, a component of the U7snRNP that together with Lsm10 and the propaptotic protein FLASH, are required for histone 3' end processing [198-199]. The replication-dependent histone 3' end processing complex and the machinery producing polyadenylated mRNAs share a common cleavage site, the CA dinucleotide, and a core cleavage factor containing symplekin, CPSF100 and CPSF73 [200], with the endonuclease CPSF73 being the factor that cleaves the pre-mRNA [201]. CPSF100 is also important for the cleavage reaction but it lacks residues critical for catalysis [202]. Symplekin is the temperature-sensitive component of the essential heat-labile factor which also includes CPSF and CstF subunits. While using common catalytic core machinery, the histone processing reaction diverges from the process originating polyadenylated mRNAs in that it is a one-step process strictly dependent on specific signal elements and is incompatible with splicing. Although the transcription complex does not stimulate histone 3' end

processing [203], recent findings undercover a physical and functional link between transcription and 3' end processing factors playing a role in the choice of the correct cleavage site to achieve the stem-loop pathway [204].

2.3 Nuclear Export of mRNA

Cellular mRNAs are produced in the nucleus and must be exported to the cytoplasm to allow for their translation into proteins. Recruitment of export factors to nascent mRNA starts cotranscriptionally and involves elaborate systems of quality control. Correctly processed mRNAs are committed for export in the form of large ribonucleoprotein complexes (mRNPs). The nuclear-cytoplasmic transport occurs through Nuclear Pore Complexes (NPC), huge macromolecular assemblies inserted within the nuclear envelope. The translocation of mRNPs through the NPC is mediated by a conserved heterodimeric transport receptor (NXF1/p15 in metazoa and Mex67p/Mtr2p in yeast) that bridges the interaction between the mRNP and the NPC. Nuclear transport is energy-dependent and signal-mediated. The different classes of RNAs, including tRNAs, rRNAs, UsnRNAs and mRNAs, are exported through distinct pathways defined by specific signals present on the RNA and/or the RNA-bound proteins [205].

More generally, nuclear export of mRNAs in the form of mRNPs is expected to be more complex than export of proteins or small RNA molecules and transport directionality may be achieved through distinct mechanisms. A key issue in mRNA export is

the question of what factor(s) mediates the export-relevant interactions between the mRNP and the NPC. Currently, the most likely candidate is the essential yeast protein Mex67p and its human homologue TAP. Although not related in sequence to importin-β, Mex67p and TAP present the main features of mRNA export receptors. TAP and Mex67p shuttle between nucleus and cytoplasm, cross-links to poly(A)$^+$ RNA and interact directly with nucleoporins [206-208].

TAP and Mex67p are members of the NXF (Nuclear eXport Factor) family of putative mRNA export receptors, which has several members in most higher eukaryotes [209].

TAP/Mex67p exhibits low affinity RNA binding and is likely to interact with cellular mRNPs through protein–protein rather than protein–RNA interactions [208, 210].

Genetic and affinity purification methods in yeast identified Yra1p, an essential hnRNP-like protein that directly interacts with Mex67p. Yra1p belongs to the evolutionarily conserved REF (RNA and Export Factor binding) family of hnRNP-like proteins, which has several members in most species.

The intranuclear movement of an mRNP from its site of transcription to the NPC and its translocation through the pore are still poorly understood. Recent progress in defining the three-dimensional architecture and composition of NPCs gave important hints on how the NPC may guide transport complexes through its aqueous channel.

Diverse mechanisms regulate both protein nuclear import and export [211]. Increasing evidence suggests that mRNA export

may be subjected to regulation as well. For example, the efficiency of yeast mRNA export is linked to the phospholipase C-dependent inositol phosphate kinase signalling pathway [212]. There is also evidence that mRNA export rates may be modulated by arginine methylation of hnRNP proteins [213]. Finally, the non-essential yeast E3 ubiquitin ligase Tom1p was proposed to contribute to the selective export of transcripts associated with the mRNA binding protein Nab2, but not to those bound to Npl3p, suggesting the existence of differentially regulated mRNA export pathways in yeast [214]. Regulation of mRNA export also occurs under stress, when heat-induced transcripts are efficiently exported but non-heat shock mRNAs exhibit a reduced ability to reach the cytoplasm [215-218].

Main players involved in mRNA export have been identified in the few last years and start to get integrated into the network of interactions underlying this complex cellular process. Crystallizations and structure predictions have provided important tools for probing the function of some of these proteins and elucidating their mechanism of action. Despite these advances, it is still unclear how an mRNP travels from its site of transcription towards the pore, when and where TAP/Mex67p is recruited to the mRNP and whether proteins distinct from REF/Yra1p are involved in this recruitment. Another question concerns the mechanism by which TAP/Mex67p mediates directional transport of the mRNP through the pore; how interactions between the export receptor and FG nucleoporins are modulated and whether enzymatic

activities other than Dbp5 are involved in translocation and release of the mRNP from the pore. The diversity of NXF, REF and NXT family members in higher eukaryotes [209, 219] probably reflects greater substrate complexity in metazoan systems and is consistent with the existence of multiple and possibly differentially regulated export pathways. mRNA export may therefore provide an additional level of gene expression control. It seems probable that nuclear mRNA export will prove to be tightly coupled to mRNA transcription and processing, just as the various steps in mRNA processing are in turn tightly coupled to transcription and to each other.

2.4 Coupling Transcription, RNA Processing and mRNA Export

During expression of protein-coding genes, pre-mRNAs are transcribed in the nucleus and undergo several processing steps, including capping, splicing, 3'-end processing and polyadenylation. The mature mRNA is then exported through NPCs to the cytoplasm for translation. Although distinct and highly complex cellular machines carry out each of these steps in the gene-expression process, growing evidence suggests the existence of gene-expression factories in which individual machines are functionally coupled (Figure 5).

This coupling is obviously not obligatory, as virtually all of the coupled steps in gene expression can be uncoupled in various assays. Thus, coupling probably exists to enable the

proofreading and streamlining of the entire process of gene expression *in vivo*.

During the past year, important new insights into the mechanisms behind this coupling have been made. In addition, recent advances have revealed mechanisms for the co-transcriptional loading of the export machinery on to mRNAs. Finally, a newly identified link between the nuclear exosome and the machineries required for transcription, 3'-end formation and mRNA export suggests that proper mRNP formation is co-transcriptionally monitored.

Future directions will include a detailed characterization of the spliced mRNP and EJC that couples splicing to mRNA export. In addition the relationship between these processes and the nuclear exosome remain to be determined. Finally, the molecular basis for coupling 3'-end formation to mRNA export must be identified.

3. Confocal Microscopy

Confocal microscopy is an optical imaging technique used to increase micrograph contrast and/or to reconstruct three-dimensional images by using a spatial pinhole to eliminate out-of-focus light in specimens that are thicker than the focal plane (Figure 6). The principle of confocal imaging was patented by Marvin Minsky in 1957 and aims to overcome some limitations of traditional wide-fieldfluorescence microscopes. In a conventional (i.e., wide-field) fluorescence microscope, the entire specimen is flooded in light from a light source. All parts

of the specimen in the optical path are excited and the resulting fluorescence is detected by the microscope photodetector or camera as background signal. In contrast, a confocal microscope uses point illumination and a pinhole in an optically conjugate plane in front of the detector to eliminate out-of-focus information - the name "confocal" stems from this configuration. As only light produced by fluorescence very close to the focal plane can be detected the image resolution, particularly in the sample depth direction, is much better than that of wide-field microscopes. However as much of the light from sample fluorescence is blocked at the pinhole this increased resolution is at the cost of decreased signal intensity so long exposures are often required.

As only one point in the sample is illuminated at a time, 2D or 3D imaging requires scanning over a regular raster (i.e. a rectangular pattern of parallel scanning lines) in the specimen. The thickness of the focal plane is defined mostly by the inverse of the square of the numerical aperture of the objective lens, and also by the optical properties of the specimen and the ambient index of refraction. The thin optical sectioning possible make these types of microscopes particularly good at 3D imaging of samples. During my thesis, as it is reported in the next chapters, I used a Leica Laser Scan Microscope TCS SP2 AOBS.

FIGURES AND TABLES

Figure 1. Patterns of alternative splicing. Constitutive sequences are gray boxes. Alternative RNA segments are hatched boxes. (A) A cassette exon. (B) Mutually exclusive exons. (C, D) Alternative 5' and 3' splice sites. (E, F) Alternative promoters and alternative poly(A) sites. (G) A retained intron. (H) A single pre-mRNA with multiple sites of alternative splicing. (From: Black,D.L., *Annu.Rev.Biochem.*(2003)72:291–336)

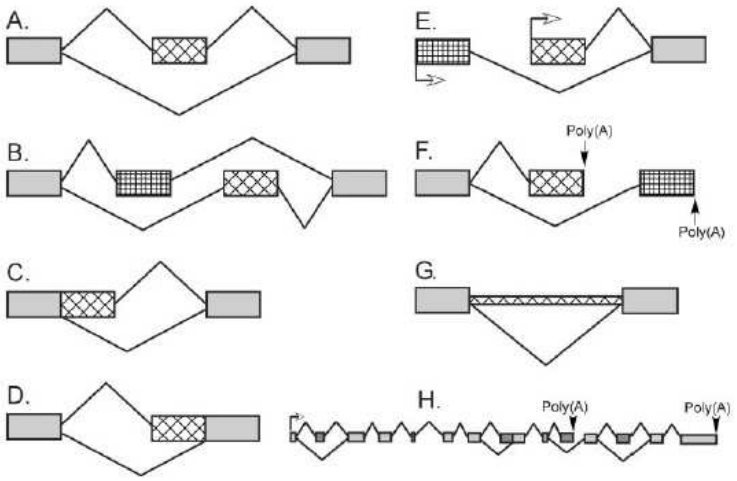

Figure 2. The two transesterification steps of the splicing reaction. (From: Black,D.L.; *Annu.Rev.Biochem.* (2003) 72:291–336)

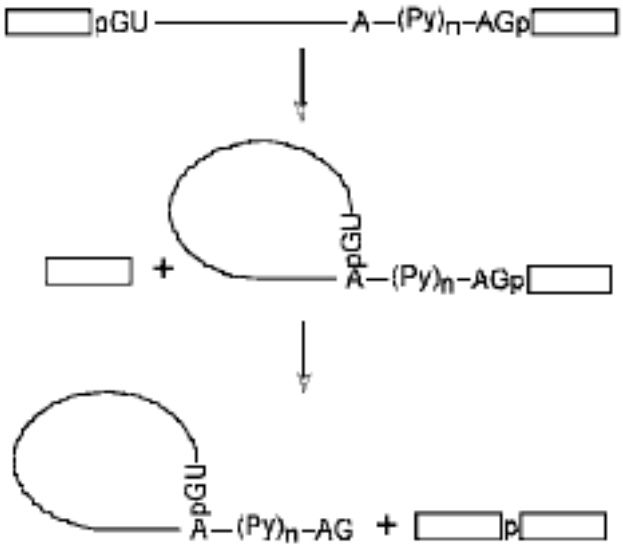

Figure 3. The 3'-end processing (at single or multiple pA signals) and its interconnections with splicing and/or transcription. The red/green dotted lines represent the physical and functional interdependence between the three processes. (From: Millevoi, S. et al.; *Nucleic Acids Research*, (2009) 1–18)

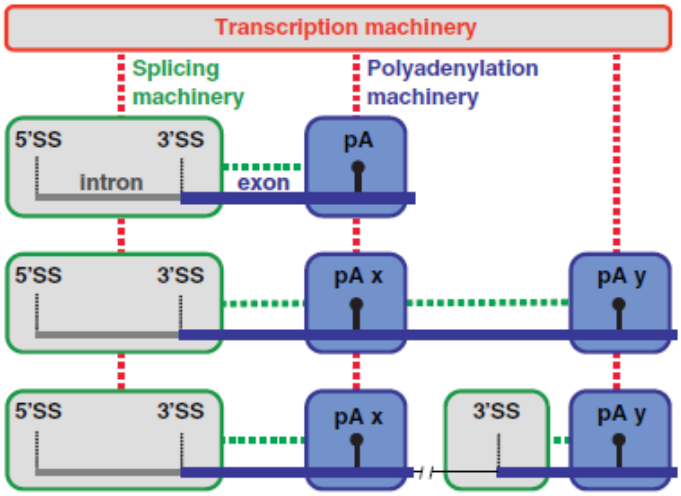

Figure 4. The eukaryotic 3'-end processing machineries. Known factors and cis-elements contributing to 3'-end processing of metazoan pre-mRNAs. In color: the homologous factors , in grey: the specific factors. The sequence elements comprising the poly(A) signals are indicated by black rectangles, and the site of cleavage is shown by a red dotted-line. (From: Millevoi, S. et al.; *Nucleic Acids Research*, (2009) 1–18)

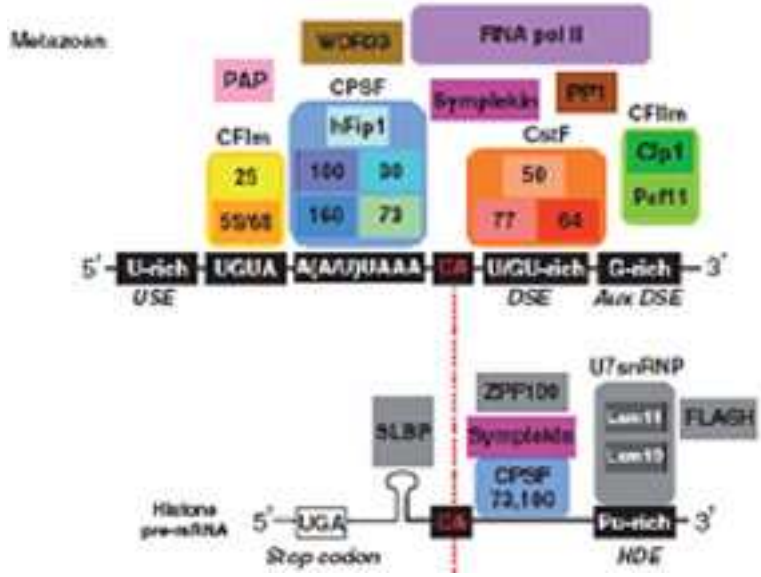

Figure 5. Splicing is coupled with a conserved export mechanism. UAP56 (Sub2 in yeast), which is present in the spliceosome, recruits Aly (Yra1 in yeast) to the mRNA during splicing. UAP56 is replaced by the mRNA export receptor TAP/p15 (Mex67/MTR2 in yeast). (From: Reed, R.; *Current Opinion in Cell Biology* (2003) 15:326–331)

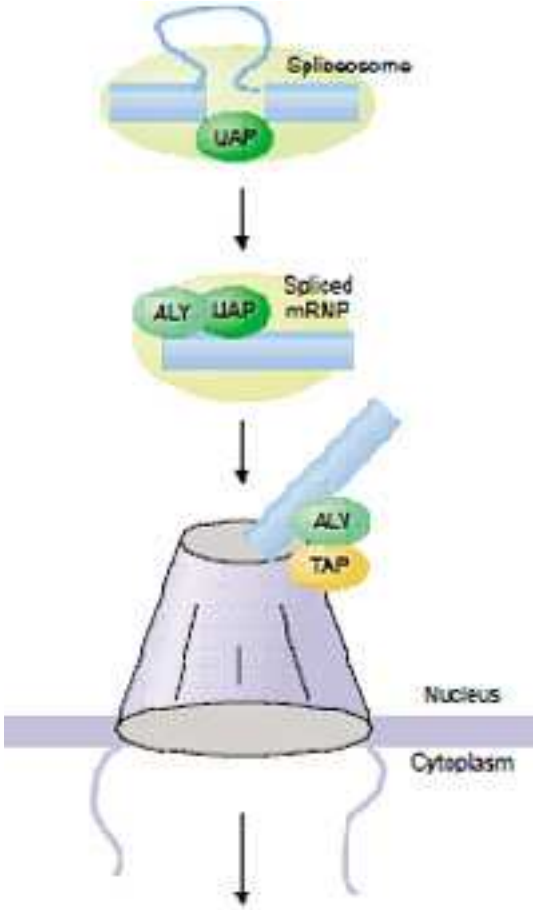

Figure 6. The path of the laser-light in a confocal microscope

(www.olympusfluoview.com/theory/images/theoryheader.jpg)

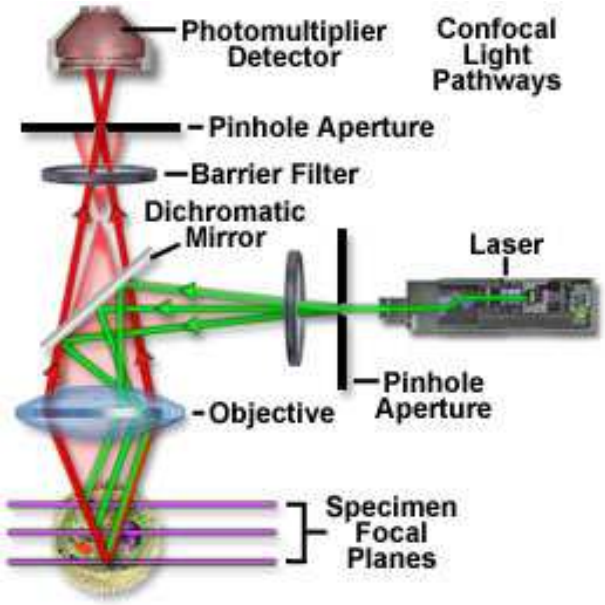

Table 1: The SR Protein Family

Name	Domains	Binding Sequence	Target Genes
Canonical SR Proteins			
SRp20 (SFRS3)	RRM and RS	GCUCCUCUUC	*SRP20*, *CALCA* and *INSR*
SC35 (SFRS2)	RRM and RS	UGCUGUU	*AChE* and *GRIA1–GRIA4*
ASF/SF2 (SFRS1)	RRM, RRMH and RS	RGAAGAAC	*hIPK3*, *CAMK2D*, HIV RNAs and *GRIA1–GRIA4*
SRp40 (SFRS5)	RRM, RRMH and RS	AGGAGAAGGGA	*hIPK3*, *PRKCB* and *FN1*
SRp55 (SFRS6)	RRM, RRMH and RS	GGCAGCACCUG	*TNNT2* and *CD44*
SRp75 (SFRS4)	RRM, RRMH and RS	GAAGGA	*FN1*, *E1A* and C*D45*
9G8 (SFRS7)	RRM, zinc finger and RS	(GAC)n	*TAu*, *GNRh* and S*FRS7*
SRp30c (SFRS9)	RRM, RRMH and RS	CUGGAUU	*BCL2L1*, *TAu* and *hNRNPA1*
SRp38 (FUSIP1)	RRM and RS	AAAGACAAA	*GRIA2* and *TRD*
Other SR Proteins			
SRp54	RRM and RS	ND	*TAu*
SRp46 (SFRS2B)	RRM and RS	ND	NA
RNPS1	RRM and Ser-rich	ND	*TRA2B*
SRrp35	RRM and RS	ND	NA
SRrp86 (SRrp508 and SFRS12)	RRM and RS	ND	NA
TRA2α	RRM and two Arg-rich	GAAARGARR	dsx
TRA2β	RRM and two RS	(GAA)n	*SMN1*, *CD44* and *TAu*
RBM5	RRM and RS	ND	*CD95*

CAPER (RBM39)	RRM and RS	ND	*VEGF*

Table 2: The hnRNP Family

Name	Other Name	Domains	Binding Sequence	Target Genes
hnRNP A1	NA	RRM, RGG and G	UAGGGA/U	SMN2 and RAS
hnRNP A2 hnRNP B1	NA	RRM, RGG and G	(UUAGGG)n	HIV tat and IKBKAP
hnRNP C1 hnRNP C2	AUF1	RRM	U rich	APP
hnRNP F	NA	RRM, RGG and GY	GGGA and G rich	PLP, SRC and BCL2L2
hnRNP G	NA	RRM and SRGY	CC(A/C) and AAGU	SMN2 and TMP1
hnRNP H hnRNP H′	DSEF1	RRM, RGG, GYR and GY	GGGA and G rich	PLP, HIV tat and BCL2L1
hnRNP I	PTB	RRM	UCUU and CUCUCU	PTB, nPTB, SRC, CD95, TNTT2, CALCA and GRIN3B
hnRNP L	NA	RRM	C and A rich	NOS and CD45
hnRNP LL	SRRF	RRM	C and A rich	CD45
hnRNP M	NA	RRM and GY	ND	FGFR2
hnRNP Q	NA	RRM and RGG	ND	SMN2

SCOPE OF THE THESIS

The main goal of my PhD research was to examine the role carried out by SRPK2 in the regulation of alternative splicing in an *in vitro* model of neurodegeneration (presented in the Chapter 2).

Besides, during these three years I also had the opportunity to participate in two other projects planning and performing several experiments that required the use of the confocal microscopy technology.

- For the first project, aimed to uncover the connection between pre-mRNA splicing, pre-mRNA 3' end processing and RNA export by examining the role performed by the mammalian cleavage factor I CFIm68, I designed and executed the RNA Fluorescence in Situ Hybridisation experiments (presented in the Chapter 3).

- For the second project, which purposed to dissect the role of CFIm68 in 3' end processing of animal histone mRNAs, I performed the Bimolecular Fluorescence Complementation experiments (presented in the Chapter 4).

REFERENCES

1. Black, D.L., *Protein diversity from alternative splicing: a challenge for bioinformatics and post-genome biology.* Cell, 2000. **103**(3): p. 367-70.
2. Kramer, A., *The structure and function of proteins involved in mammalian pre-mRNA splicing.* Annu Rev Biochem, 1996. **65**: p. 367-409.
3. Berget, S.M., *Exon recognition in vertebrate splicing.* J Biol Chem, 1995. **270**(6): p. 2411-4.
4. Horowitz, D.S. and A.R. Krainer, *Mechanisms for selecting 5' splice sites in mammalian pre-mRNA splicing.* Trends Genet, 1994. **10**(3): p. 100-6.
5. Grabowski, P.J. and D.L. Black, *Alternative RNA splicing in the nervous system.* Prog Neurobiol, 2001. **65**(3): p. 289-308.
6. Modrek, B. and C. Lee, *A genomic view of alternative splicing.* Nat Genet, 2002. **30**(1): p. 13-9.
7. Graveley, B.R., *Alternative splicing: increasing diversity in the proteomic world.* Trends Genet, 2001. **17**(2): p. 100-7.
8. Smith, C.W. and B. Nadal-Ginard, *Mutually exclusive splicing of alpha-tropomyosin exons enforced by an unusual lariat branch point location: implications for constitutive splicing.* Cell, 1989. **56**(5): p. 749-58.

9. Schmucker, D., et al., *Drosophila Dscam is an axon guidance receptor exhibiting extraordinary molecular diversity.* Cell, 2000. **101**(6): p. 671-84.
10. Colgan, D.F. and J.L. Manley, *Mechanism and regulation of mRNA polyadenylation.* Genes Dev, 1997. **11**(21): p. 2755-66.
11. Black, D.L., *Splicing in the inner ear: a familiar tune, but what are the instruments?* Neuron, 1998. **20**(2): p. 165-8.
12. Burge, P.S., et al., *Development of an expert system for the interpretation of serial peak expiratory flow measurements in the diagnosis of occupational asthma. Midlands Thoracic Society Research Group.* Occup Environ Med, 1999. **56**(11): p. 758-64.
13. Burgess, R.W., et al., *Alternatively spliced isoforms of nerve- and muscle-derived agrin: their roles at the neuromuscular junction.* Neuron, 1999. **23**(1): p. 33-44.
14. Burke, J.F., et al., *Alternative mRNA splicing in the nervous system.* Prog Brain Res, 1992. **92**: p. 115-25.
15. Cartegni, L., S.L. Chew, and A.R. Krainer, *Listening to silence and understanding nonsense: exonic mutations that affect splicing.* Nat Rev Genet, 2002. **3**(4): p. 285-98.
16. Cooper, T.A. and W. Mattox, *The regulation of splice-site selection, and its role in human disease.* Am J Hum Genet, 1997. **61**(2): p. 259-66.
17. Eckardt, N.A., *Alternative splicing and the control of flowering time.* Plant Cell, 2002. **14**(4): p. 743-7.

18. Jiang, Z.H. and J.Y. Wu, *Alternative splicing and programmed cell death.* Proc Soc Exp Biol Med, 1999. **220**(2): p. 64-72.
19. Matera, A.G., *RNA splicing: more clues from spinal muscular atrophy.* Curr Biol, 1999. **9**(4): p. R140-2.
20. Caceres, J.F. and A.R. Kornblihtt, *Alternative splicing: multiple control mechanisms and involvement in human disease.* Trends Genet, 2002. **18**(4): p. 186-93.
21. Blencowe, B.J., *Exonic splicing enhancers: mechanism of action, diversity and role in human genetic diseases.* Trends Biochem Sci, 2000. **25**(3): p. 106-10.
22. Das, R., Z. Zhou, and R. Reed, *Functional association of U2 snRNP with the ATP-independent spliceosomal complex E.* Mol Cell, 2000. **5**(5): p. 779-87.
23. Nilsen, T.W., *A parallel spliceosome.* Science, 1996. **273**(5283): p. 1813.
24. Black, D.L., *Finding splice sites within a wilderness of RNA.* RNA, 1995. **1**(8): p. 763-71.
25. Hoffman, B.E. and P.J. Grabowski, *U1 snRNP targets an essential splicing factor, U2AF65, to the 3' splice site by a network of interactions spanning the exon.* Genes Dev, 1992. **6**(12B): p. 2554-68.
26. Robberson, B.L., G.J. Cote, and S.M. Berget, *Exon definition may facilitate splice site selection in RNAs with multiple exons.* Mol Cell Biol, 1990. **10**(1): p. 84-94.
27. Libri, D., A. Piseri, and M.Y. Fiszman, *Tissue-specific splicing in vivo of the beta-tropomyosin gene:*

dependence on an RNA secondary structure. Science, 1991. **252**(5014): p. 1842-5.

28. Libri, D., et al., *RNA structural patterns and splicing: molecular basis for an RNA-based enhancer.* RNA, 1995. **1**(4): p. 425-36.
29. Jacquenet, S., et al., *Conserved stem-loop structures in the HIV-1 RNA region containing the A3 3' splice site and its cis-regulatory element: possible involvement in RNA splicing.* Nucleic Acids Res, 2001. **29**(2): p. 464-78.
30. Graveley, B.R., *Sorting out the complexity of SR protein functions.* RNA, 2000. **6**(9): p. 1197-211.
31. Tacke, R. and J.L. Manley, *Determinants of SR protein specificity.* Curr Opin Cell Biol, 1999. **11**(3): p. 358-62.
32. Long, J.C. and J.F. Caceres, *The SR protein family of splicing factors: master regulators of gene expression.* Biochem J, 2009. **417**(1): p. 15-27.
33. Smith, C.W. and J. Valcarcel, *Alternative pre-mRNA splicing: the logic of combinatorial control.* Trends Biochem Sci, 2000. **25**(8): p. 381-8.
34. Dreyfuss, G., V.N. Kim, and N. Kataoka, *Messenger-RNA-binding proteins and the messages they carry.* Nat Rev Mol Cell Biol, 2002. **3**(3): p. 195-205.
35. Hui, J., et al., *Intronic CA-repeat and CA-rich elements: a new class of regulators of mammalian alternative splicing.* EMBO J, 2005. **24**(11): p. 1988-98.
36. Mauger, D.M., C. Lin, and M.A. Garcia-Blanco, *hnRNP H and hnRNP F complex with Fox2 to silence fibroblast*

growth factor receptor 2 exon IIIc. Mol Cell Biol, 2008. **28**(17): p. 5403-19.

37. Ule, J., et al., *An RNA map predicting Nova-dependent splicing regulation.* Nature, 2006. **444**(7119): p. 580-6.
38. Yeo, G.W., et al., *An RNA code for the FOX2 splicing regulator revealed by mapping RNA-protein interactions in stem cells.* Nat Struct Mol Biol, 2009. **16**(2): p. 130-7.
39. House, A.E. and K.W. Lynch, *An exonic splicing silencer represses spliceosome assembly after ATP-dependent exon recognition.* Nat Struct Mol Biol, 2006. **13**(10): p. 937-44.
40. Lallena, M.J., et al., *Splicing regulation at the second catalytic step by Sex-lethal involves 3' splice site recognition by SPF45.* Cell, 2002. **109**(3): p. 285-96.
41. Batsche, E., M. Yaniv, and C. Muchardt, *The human SWI/SNF subunit Brm is a regulator of alternative splicing.* Nat Struct Mol Biol, 2006. **13**(1): p. 22-9.
42. de la Mata, M. and A.R. Kornblihtt, *RNA polymerase II C-terminal domain mediates regulation of alternative splicing by SRp20.* Nat Struct Mol Biol, 2006. **13**(11): p. 973-80.
43. Sims, R.J., 3rd, et al., *Recognition of trimethylated histone H3 lysine 4 facilitates the recruitment of transcription postinitiation factors and pre-mRNA splicing.* Mol Cell, 2007. **28**(4): p. 665-76.

44. Lin, S., et al., *The splicing factor SC35 has an active role in transcriptional elongation.* Nat Struct Mol Biol, 2008. **15**(8): p. 819-26.
45. Moldon, A., et al., *Promoter-driven splicing regulation in fission yeast.* Nature, 2008. **455**(7215): p. 997-1000.
46. Kashima, T. and J.L. Manley, *A negative element in SMN2 exon 7 inhibits splicing in spinal muscular atrophy.* Nat Genet, 2003. **34**(4): p. 460-3.
47. Sterner, D.A., T. Carlo, and S.M. Berget, *Architectural limits on split genes.* Proc Natl Acad Sci U S A, 1996. **93**(26): p. 15081-5.
48. Kotlajich, M.V., T.L. Crabb, and K.J. Hertel, *Spliceosome assembly pathways for different types of alternative splicing converge during commitment to splice site pairing in the A complex.* Mol Cell Biol, 2009. **29**(4): p. 1072-82.
49. Lim, S.R. and K.J. Hertel, *Commitment to splice site pairing coincides with A complex formation.* Mol Cell, 2004. **15**(3): p. 477-83.
50. Bourgeois, C.F., et al., *Identification of a bidirectional splicing enhancer: differential involvement of SR proteins in 5' or 3' splice site activation.* Mol Cell Biol, 1999. **19**(11): p. 7347-56.
51. Feng, Y., M. Chen, and J.L. Manley, *Phosphorylation switches the general splicing repressor SRp38 to a sequence-specific activator.* Nat Struct Mol Biol, 2008. **15**(10): p. 1040-8.

52. Graveley, B.R., K.J. Hertel, and T. Maniatis, *The role of U2AF35 and U2AF65 in enhancer-dependent splicing.* RNA, 2001. **7**(6): p. 806-18.
53. Zuo, P. and T. Maniatis, *The splicing factor U2AF35 mediates critical protein-protein interactions in constitutive and enhancer-dependent splicing.* Genes Dev, 1996. **10**(11): p. 1356-68.
54. Kohtz, J.D., et al., *Protein-protein interactions and 5'-splice-site recognition in mammalian mRNA precursors.* Nature, 1994. **368**(6467): p. 119-24.
55. Wu, J.Y. and T. Maniatis, *Specific interactions between proteins implicated in splice site selection and regulated alternative splicing.* Cell, 1993. **75**(6): p. 1061-70.
56. Pacheco, T.R., et al., *In vivo requirement of the small subunit of U2AF for recognition of a weak 3' splice site.* Mol Cell Biol, 2006. **26**(21): p. 8183-90.
57. Xiao, S.H. and J.L. Manley, *Phosphorylation of the ASF/SF2 RS domain affects both protein-protein and protein-RNA interactions and is necessary for splicing.* Genes Dev, 1997. **11**(3): p. 334-44.
58. Tacke, R. and J.L. Manley, *Functions of SR and Tra2 proteins in pre-mRNA splicing regulation.* Proc Soc Exp Biol Med, 1999. **220**(2): p. 59-63.
59. Blencowe, B.J., et al., *The SRm160/300 splicing coactivator subunits.* RNA, 2000. **6**(1): p. 111-20.
60. Longman, D., et al., *Multiple interactions between SRm160 and SR family proteins in enhancer-dependent*

splicing and development of C. elegans. Curr Biol, 2001. **11**(24): p. 1923-33.

61. Forch, P., et al., *The splicing regulator TIA-1 interacts with U1-C to promote U1 snRNP recruitment to 5' splice sites.* EMBO J, 2002. **21**(24): p. 6882-92.
62. Izquierdo, J.M., et al., *Regulation of Fas alternative splicing by antagonistic effects of TIA-1 and PTB on exon definition.* Mol Cell, 2005. **19**(4): p. 475-84.
63. Tisserant, A. and H. Konig, *Signal-regulated Pre-mRNA occupancy by the general splicing factor U2AF.* PLoS One, 2008. **3**(1): p. e1418.
64. Zhu, J. and A.R. Krainer, *Pre-mRNA splicing in the absence of an SR protein RS domain.* Genes Dev, 2000. **14**(24): p. 3166-78.
65. Zahler, A.M., et al., *SC35 and heterogeneous nuclear ribonucleoprotein A/B proteins bind to a juxtaposed exonic splicing enhancer/exonic splicing silencer element to regulate HIV-1 tat exon 2 splicing.* J Biol Chem, 2004. **279**(11): p. 10077-84.
66. Mayeda, A., D.M. Helfman, and A.R. Krainer, *Modulation of exon skipping and inclusion by heterogeneous nuclear ribonucleoprotein A1 and pre-mRNA splicing factor SF2/ASF.* Mol Cell Biol, 1993. **13**(5): p. 2993-3001.
67. Sanford, J.R., et al., *Splicing factor SFRS1 recognizes a functionally diverse landscape of RNA transcripts.* Genome Res, 2009. **19**(3): p. 381-94.

68. Sanford, J.R., et al., *Identification of nuclear and cytoplasmic mRNA targets for the shuttling protein SF2/ASF.* PLoS One, 2008. **3**(10): p. e3369.
69. Licatalosi, D.D., et al., *HITS-CLIP yields genome-wide insights into brain alternative RNA processing.* Nature, 2008. **456**(7221): p. 464-9.
70. Camats, M., et al., *P68 RNA helicase (DDX5) alters activity of cis- and trans-acting factors of the alternative splicing of H-Ras.* PLoS One, 2008. **3**(8): p. e2926.
71. Hiller, M., et al., *Pre-mRNA secondary structures influence exon recognition.* PLoS Genet, 2007. **3**(11): p. e204.
72. Yu, Y., et al., *Dynamic regulation of alternative splicing by silencers that modulate 5' splice site competition.* Cell, 2008. **135**(7): p. 1224-36.
73. Das, R., et al., *SR proteins function in coupling RNAP II transcription to pre-mRNA splicing.* Mol Cell, 2007. **26**(6): p. 867-81.
74. Auboeuf, D., et al., *Differential recruitment of nuclear receptor coactivators may determine alternative RNA splice site choice in target genes.* Proc Natl Acad Sci U S A, 2004. **101**(8): p. 2270-4.
75. de la Mata, M., et al., *A slow RNA polymerase II affects alternative splicing in vivo.* Mol Cell, 2003. **12**(2): p. 525-32.

76. Wang, E.T., et al., *Alternative isoform regulation in human tissue transcriptomes.* Nature, 2008. **456**(7221): p. 470-6.
77. Castle, J.C., et al., *Expression of 24,426 human alternative splicing events and predicted cis regulation in 48 tissues and cell lines.* Nat Genet, 2008. **40**(12): p. 1416-25.
78. David, C.J. and J.L. Manley, *The search for alternative splicing regulators: new approaches offer a path to a splicing code.* Genes Dev, 2008. **22**(3): p. 279-85.
79. Ohno, G., M. Hagiwara, and H. Kuroyanagi, *STAR family RNA-binding protein ASD-2 regulates developmental switching of mutually exclusive alternative splicing in vivo.* Genes Dev, 2008. **22**(3): p. 360-74.
80. Li, Q., J.A. Lee, and D.L. Black, *Neuronal regulation of alternative pre-mRNA splicing.* Nat Rev Neurosci, 2007. **8**(11): p. 819-31.
81. Ule, J., et al., *Nova regulates brain-specific splicing to shape the synapse.* Nat Genet, 2005. **37**(8): p. 844-52.
82. Perrone-Bizzozero, N. and F. Bolognani, *Role of HuD and other RNA-binding proteins in neural development and plasticity.* J Neurosci Res, 2002. **68**(2): p. 121-6.
83. Soller, M., M. Li, and I.U. Haussmann, *Regulation of the ELAV target ewg: insights from an evolutionary perspective.* Biochem Soc Trans, 2008. **36**(Pt 3): p. 502-4.

84. Zhu, H., et al., *A nuclear function of Hu proteins as neuron-specific alternative RNA processing regulators.* Mol Biol Cell, 2006. **17**(12): p. 5105-14.
85. McKee, A.E., et al., *A genome-wide in situ hybridization map of RNA-binding proteins reveals anatomically restricted expression in the developing mouse brain.* BMC Dev Biol, 2005. **5**: p. 14.
86. Xu, X., et al., *ASF/SF2-regulated CaMKIIdelta alternative splicing temporally reprograms excitation-contraction coupling in cardiac muscle.* Cell, 2005. **120**(1): p. 59-72.
87. Ding, J.H., et al., *Dilated cardiomyopathy caused by tissue-specific ablation of SC35 in the heart.* EMBO J, 2004. **23**(4): p. 885-96.
88. Feng, Y., et al., *SRp38 regulates alternative splicing and is required for Ca(2+) handling in the embryonic heart.* Dev Cell, 2009. **16**(4): p. 528-38.
89. Grosso, A.R., et al., *Tissue-specific splicing factor gene expression signatures.* Nucleic Acids Res, 2008. **36**(15): p. 4823-32.
90. Tarn, W.Y., *Cellular signals modulate alternative splicing.* J Biomed Sci, 2007. **14**(4): p. 517-22.
91. Shin, C. and J.L. Manley, *Cell signalling and the control of pre-mRNA splicing.* Nat Rev Mol Cell Biol, 2004. **5**(9): p. 727-38.
92. Daoud, R., et al., *Ischemia induces a translocation of the splicing factor tra2-beta 1 and changes alternative*

splicing patterns in the brain. J Neurosci, 2002. **22**(14): p. 5889-99.

93. Habelhah, H., et al., *ERK phosphorylation drives cytoplasmic accumulation of hnRNP-K and inhibition of mRNA translation.* Nat Cell Biol, 2001. **3**(3): p. 325-30.
94. van der Houven van Oordt, W., et al., *The MKK(3/6)-p38-signaling cascade alters the subcellular distribution of hnRNP A1 and modulates alternative splicing regulation.* J Cell Biol, 2000. **149**(2): p. 307-16.
95. Huang, Y., T.A. Yario, and J.A. Steitz, *A molecular link between SR protein dephosphorylation and mRNA export.* Proc Natl Acad Sci U S A, 2004. **101**(26): p. 9666-70.
96. Huang, C.J., et al., *Phosphorylation by SR kinases regulates the binding of PTB-associated splicing factor (PSF) to the pre-mRNA polypyrimidine tract.* FEBS Lett, 2007. **581**(2): p. 223-32.
97. Sanford, J.R. and J.P. Bruzik, *Developmental regulation of SR protein phosphorylation and activity.* Genes Dev, 1999. **13**(12): p. 1513-8.
98. Xiao, S.H. and J.L. Manley, *Phosphorylation-dephosphorylation differentially affects activities of splicing factor ASF/SF2.* EMBO J, 1998. **17**(21): p. 6359-67.
99. Hallikas, O., et al., *Genome-wide prediction of mammalian enhancers based on analysis of*

transcription-factor binding affinity. Cell, 2006. **124**(1): p. 47-59.

100. Fu, X.D., *The superfamily of arginine/serine-rich splicing factors.* RNA, 1995. **1**(7): p. 663-80.
101. Mayeda, A. and A.R. Krainer, *Regulation of alternative pre-mRNA splicing by hnRNP A1 and splicing factor SF2.* Cell, 1992. **68**(2): p. 365-75.
102. Caceres, J.F., et al., *Regulation of alternative splicing in vivo by overexpression of antagonistic splicing factors.* Science, 1994. **265**(5179): p. 1706-9.
103. Yang, X., et al., *The A1 and A1B proteins of heterogeneous nuclear ribonucleoparticles modulate 5' splice site selection in vivo.* Proc Natl Acad Sci U S A, 1994. **91**(15): p. 6924-8.
104. Gallego, M.E., et al., *The SR splicing factors ASF/SF2 and SC35 have antagonistic effects on intronic enhancer-dependent splicing of the beta-tropomyosin alternative exon 6A.* EMBO J, 1997. **16**(7): p. 1772-84.
105. Jumaa, H. and P.J. Nielsen, *The splicing factor SRp20 modifies splicing of its own mRNA and ASF/SF2 antagonizes this regulation.* EMBO J, 1997. **16**(16): p. 5077-85.
106. Eperon, I.C., et al., *Selection of alternative 5' splice sites: role of U1 snRNP and models for the antagonistic effects of SF2/ASF and hnRNP A1.* Mol Cell Biol, 2000. **20**(22): p. 8303-18.

107. Hastings, M.L. and A.R. Krainer, *Pre-mRNA splicing in the new millennium.* Curr Opin Cell Biol, 2001. **13**(3): p. 302-9.
108. Zhu, J., A. Mayeda, and A.R. Krainer, *Exon identity established through differential antagonism between exonic splicing silencer-bound hnRNP A1 and enhancer-bound SR proteins.* Mol Cell, 2001. **8**(6): p. 1351-61.
109. Zahler, A.M., et al., *Distinct functions of SR proteins in alternative pre-mRNA splicing.* Science, 1993. **260**(5105): p. 219-22.
110. Hanamura, A., et al., *Regulated tissue-specific expression of antagonistic pre-mRNA splicing factors.* RNA, 1998. **4**(4): p. 430-44.
111. Jumaa, H., G. Wei, and P.J. Nielsen, *Blastocyst formation is blocked in mouse embryos lacking the splicing factor SRp20.* Curr Biol, 1999. **9**(16): p. 899-902.
112. Wang, J., Y. Takagaki, and J.L. Manley, *Targeted disruption of an essential vertebrate gene: ASF/SF2 is required for cell viability.* Genes Dev, 1996. **10**(20): p. 2588-99.
113. Wang, H.Y., et al., *SC35 plays a role in T cell development and alternative splicing of CD45.* Mol Cell, 2001. **7**(2): p. 331-42.
114. Peng, X. and S.M. Mount, *Genetic enhancement of RNA-processing defects by a dominant mutation in B52, the Drosophila gene for an SR protein splicing factor.* Mol Cell Biol, 1995. **15**(11): p. 6273-82.

115. Ring, H.Z. and J.T. Lis, *The SR protein B52/SRp55 is essential for Drosophila development.* Mol Cell Biol, 1994. **14**(11): p. 7499-506.
116. Loomis, R.J., et al., *Chromatin binding of SRp20 and ASF/SF2 and dissociation from mitotic chromosomes is modulated by histone H3 serine 10 phosphorylation.* Mol Cell, 2009. **33**(4): p. 450-61.
117. Li, X. and J.L. Manley, *Inactivation of the SR protein splicing factor ASF/SF2 results in genomic instability.* Cell, 2005. **122**(3): p. 365-78.
118. Li, X. and J.L. Manley, *Cotranscriptional processes and their influence on genome stability.* Genes Dev, 2006. **20**(14): p. 1838-47.
119. Li, X., J. Wang, and J.L. Manley, *Loss of splicing factor ASF/SF2 induces G2 cell cycle arrest and apoptosis, but inhibits internucleosomal DNA fragmentation.* Genes Dev, 2005. **19**(22): p. 2705-14.
120. Prasad, J., et al., *The protein kinase Clk/Sty directly modulates SR protein activity: both hyper- and hypophosphorylation inhibit splicing.* Mol Cell Biol, 1999. **19**(10): p. 6991-7000.
121. Mathew, R., et al., *Phosphorylation of human PRP28 by SRPK2 is required for integration of the U4/U6-U5 tri-snRNP into the spliceosome.* Nat Struct Mol Biol, 2008. **15**(5): p. 435-43.

122. Aubol, B.E., et al., *Processive phosphorylation of alternative splicing factor/splicing factor 2.* Proc Natl Acad Sci U S A, 2003. **100**(22): p. 12601-6.
123. Ngo, J.C., et al., *A sliding docking interaction is essential for sequential and processive phosphorylation of an SR protein by SRPK1.* Mol Cell, 2008. **29**(5): p. 563-76.
124. Ngo, J.C., et al., *Interplay between SRPK and Clk/Sty kinases in phosphorylation of the splicing factor ASF/SF2 is regulated by a docking motif in ASF/SF2.* Mol Cell, 2005. **20**(1): p. 77-89.
125. Velazquez-Dones, A., et al., *Mass spectrometric and kinetic analysis of ASF/SF2 phosphorylation by SRPK1 and Clk/Sty.* J Biol Chem, 2005. **280**(50): p. 41761-8.
126. Hagopian, J.C., et al., *Adaptable molecular interactions guide phosphorylation of the SR protein ASF/SF2 by SRPK1.* J Mol Biol, 2008. **382**(4): p. 894-909.
127. Colwill, K., et al., *The Clk/Sty protein kinase phosphorylates SR splicing factors and regulates their intranuclear distribution.* EMBO J, 1996. **15**(2): p. 265-75.
128. Nayler, O., et al., *The cellular localization of the murine serine/arginine-rich protein kinase CLK2 is regulated by serine 141 autophosphorylation.* J Biol Chem, 1998. **273**(51): p. 34341-8.
129. Ding, J.H., et al., *Regulated cellular partitioning of SR protein-specific kinases in mammalian cells.* Mol Biol Cell, 2006. **17**(2): p. 876-85.

130. Wang, H.Y., et al., *SRPK2: a differentially expressed SR protein-specific kinase involved in mediating the interaction and localization of pre-mRNA splicing factors in mammalian cells.* J Cell Biol, 1998. **140**(4): p. 737-50.
131. Jang, S.W., et al., *Interaction of Akt-phosphorylated SRPK2 with 14-3-3 mediates cell cycle and cell death in neurons.* J Biol Chem, 2009. **284**(36): p. 24512-25.
132. Zhong, X.Y., et al., *Regulation of SR protein phosphorylation and alternative splicing by modulating kinetic interactions of SRPK1 with molecular chaperones.* Genes Dev, 2009. **23**(4): p. 482-95.
133. Shin, C., Y. Feng, and J.L. Manley, *Dephosphorylated SRp38 acts as a splicing repressor in response to heat shock.* Nature, 2004. **427**(6974): p. 553-8.
134. Shi, Y. and J.L. Manley, *A complex signaling pathway regulates SRp38 phosphorylation and pre-mRNA splicing in response to heat shock.* Mol Cell, 2007. **28**(1): p. 79-90.
135. Gui, J.F., et al., *Purification and characterization of a kinase specific for the serine- and arginine-rich pre-mRNA splicing factors.* Proc Natl Acad Sci U S A, 1994. **91**(23): p. 10824-8.
136. Gui, J.F., W.S. Lane, and X.D. Fu, *A serine kinase regulates intracellular localization of splicing factors in the cell cycle.* Nature, 1994. **369**(6482): p. 678-82.

137. Kuroyanagi, N., et al., *Novel SR-protein-specific kinase, SRPK2, disassembles nuclear speckles.* Biochem Biophys Res Commun, 1998. **242**(2): p. 357-64.
138. Stamm, S., *Signals and their transduction pathways regulating alternative splicing: a new dimension of the human genome.* Hum Mol Genet, 2002. **11**(20): p. 2409-16.
139. Jiang, Z.H., et al., *Regulation of Ich-1 pre-mRNA alternative splicing and apoptosis by mammalian splicing factors.* Proc Natl Acad Sci U S A, 1998. **95**(16): p. 9155-60.
140. Allemand, E., et al., *Regulation of heterogenous nuclear ribonucleoprotein A1 transport by phosphorylation in cells stressed by osmotic shock.* Proc Natl Acad Sci U S A, 2005. **102**(10): p. 3605-10.
141. Melchiorri, D., et al., *Paraquat toxicity and oxidative damage. Reduction by melatonin.* Biochem Pharmacol, 1996. **51**(8): p. 1095-9.
142. Bonneh-Barkay, D., et al., *Redox cycling of the herbicide paraquat in microglial cultures.* Brain Res Mol Brain Res, 2005. **134**(1): p. 52-6.
143. Maracchioni, A., et al., *Mitochondrial damage modulates alternative splicing in neuronal cells: implications for neurodegeneration.* J Neurochem, 2007. **100**(1): p. 142-53.

144. Bishop, A.L., et al., *Phenotypic heterogeneity can enhance rare-cell survival in 'stress-sensitive' yeast populations.* Mol Microbiol, 2007. **63**(2): p. 507-20.
145. Bonilla, E., et al., *Paraquat-induced oxidative stress in drosophila melanogaster: effects of melatonin, glutathione, serotonin, minocycline, lipoic acid and ascorbic acid.* Neurochem Res, 2006. **31**(12): p. 1425-32.
146. Cicchetti, F., et al., *Systemic exposure to paraquat and maneb models early Parkinson's disease in young adult rats.* Neurobiol Dis, 2005. **20**(2): p. 360-71.
147. Senator, A., et al., *Prion protein protects against DNA damage induced by paraquat in cultured cells.* Free Radic Biol Med, 2004. **37**(8): p. 1224-30.
148. Moran, J.M., et al., *Identification of genes associated with paraquat-induced toxicity in SH-SY5Y cells by PCR array focused on apoptotic pathways.* J Toxicol Environ Health A, 2008. **71**(22): p. 1457-67.
149. Gonzalez-Polo, R.A., et al., *Inhibition of paraquat-induced autophagy accelerates the apoptotic cell death in neuroblastoma SH-SY5Y cells.* Toxicol Sci, 2007. **97**(2): p. 448-58.
150. Ortiz-Ortiz, M.A., et al., *Nitric oxide-mediated toxicity in paraquat-exposed SH-SY5Y cells: a protective role of 7-nitroindazole.* Neurotox Res, 2009. **16**(2): p. 160-73.
151. Yang, W., et al., *Paraquat activates the IRE1/ASK1/JNK cascade associated with apoptosis in human*

neuroblastoma SH-SY5Y cells. Toxicol Lett, 2009. **191**(2-3): p. 203-10.

152. Yang, W. and E. Tiffany-Castiglioni, *Paraquat-induced apoptosis in human neuroblastoma SH-SY5Y cells: involvement of p53 and mitochondria.* J Toxicol Environ Health A, 2008. **71**(4): p. 289-99.
153. Dupiereux, I., et al., *Protective effect of prion protein via the N-terminal region in mediating a protective effect on paraquat-induced oxidative injury in neuronal cells.* J Neurosci Res, 2008. **86**(3): p. 653-9.
154. Maniatis, T. and R. Reed, *An extensive network of coupling among gene expression machines.* Nature, 2002. **416**(6880): p. 499-506.
155. Proudfoot, N.J., A. Furger, and M.J. Dye, *Integrating mRNA processing with transcription.* Cell, 2002. **108**(4): p. 501-12.
156. Buratowski, S., *Connections between mRNA 3' end processing and transcription termination.* Curr Opin Cell Biol, 2005. **17**(3): p. 257-61.
157. Rosonina, E., S. Kaneko, and J.L. Manley, *Terminating the transcript: breaking up is hard to do.* Genes Dev, 2006. **20**(9): p. 1050-6.
158. Kaneko, S., et al., *The multifunctional protein p54nrb/PSF recruits the exonuclease XRN2 to facilitate pre-mRNA 3' processing and transcription termination.* Genes Dev, 2007. **21**(14): p. 1779-89.

159. Dantonel, J.C., et al., *Transcription factor TFIID recruits factor CPSF for formation of 3' end of mRNA.* Nature, 1997. **389**(6649): p. 399-402.
160. Rosonina, E., et al., *Role for PSF in mediating transcriptional activator-dependent stimulation of pre-mRNA processing in vivo.* Mol Cell Biol, 2005. **25**(15): p. 6734-46.
161. Rosonina, E., et al., *Transcriptional activators control splicing and 3'-end cleavage levels.* J Biol Chem, 2003. **278**(44): p. 43034-40.
162. McCracken, S., et al., *The C-terminal domain of RNA polymerase II couples mRNA processing to transcription.* Nature, 1997. **385**(6614): p. 357-61.
163. Hirose, Y. and J.L. Manley, *RNA polymerase II is an essential mRNA polyadenylation factor.* Nature, 1998. **395**(6697): p. 93-6.
164. Ryan, K., et al., *Requirements of the RNA polymerase II C-terminal domain for reconstituting pre-mRNA 3' cleavage.* Mol Cell Biol, 2002. **22**(6): p. 1684-92.
165. Gunderson, S.I., et al., *Involvement of the carboxyl terminus of vertebrate poly(A) polymerase in U1A autoregulation and in the coupling of splicing and polyadenylation.* Genes Dev, 1997. **11**(6): p. 761-73.
166. Vagner, S., C. Vagner, and I.W. Mattaj, *The carboxyl terminus of vertebrate poly(A) polymerase interacts with U2AF 65 to couple 3'-end processing and splicing.* Genes Dev, 2000. **14**(4): p. 403-13.

167. Millevoi, S., et al., *A novel function for the U2AF 65 splicing factor in promoting pre-mRNA 3'-end processing.* EMBO Rep, 2002. **3**(9): p. 869-74.
168. Millevoi, S., et al., *An interaction between U2AF 65 and CF I(m) links the splicing and 3' end processing machineries.* EMBO J, 2006. **25**(20): p. 4854-64.
169. Kyburz, A., et al., *Direct interactions between subunits of CPSF and the U2 snRNP contribute to the coupling of pre-mRNA 3' end processing and splicing.* Mol Cell, 2006. **23**(2): p. 195-205.
170. Koscielny, G., et al., *ASTD: The Alternative Splicing and Transcript Diversity database.* Genomics, 2009. **93**(3): p. 213-20.
171. Tian, B., et al., *A large-scale analysis of mRNA polyadenylation of human and mouse genes.* Nucleic Acids Res, 2005. **33**(1): p. 201-12.
172. Yan, J. and T.G. Marr, *Computational analysis of 3'-ends of ESTs shows four classes of alternative polyadenylation in human, mouse, and rat.* Genome Res, 2005. **15**(3): p. 369-75.
173. Barabino, S.M. and W. Keller, *Last but not least: regulated poly(A) tail formation.* Cell, 1999. **99**(1): p. 9-11.
174. Edwalds-Gilbert, G., K.L. Veraldi, and C. Milcarek, *Alternative poly(A) site selection in complex transcription units: means to an end?* Nucleic Acids Res, 1997. **25**(13): p. 2547-61.

175. Lutz, C.S., *Alternative polyadenylation: a twist on mRNA 3' end formation.* ACS Chem Biol, 2008. **3**(10): p. 609-17.
176. Zhao, J., L. Hyman, and C. Moore, *Formation of mRNA 3' ends in eukaryotes: mechanism, regulation, and interrelationships with other steps in mRNA synthesis.* Microbiol Mol Biol Rev, 1999. **63**(2): p. 405-45.
177. Danckwardt, S., M.W. Hentze, and A.E. Kulozik, *3' end mRNA processing: molecular mechanisms and implications for health and disease.* EMBO J, 2008. **27**(3): p. 482-98.
178. Kuhn, U., et al., *Poly(A) tail length is controlled by the nuclear poly(A)-binding protein regulating the interaction between poly(A) polymerase and the cleavage and polyadenylation specificity factor.* J Biol Chem, 2009. **284**(34): p. 22803-14.
179. Brown, K.M. and G.M. Gilmartin, *A mechanism for the regulation of pre-mRNA 3' processing by human cleavage factor Im.* Mol Cell, 2003. **12**(6): p. 1467-76.
180. Venkataraman, K., K.M. Brown, and G.M. Gilmartin, *Analysis of a noncanonical poly(A) site reveals a tripartite mechanism for vertebrate poly(A) site recognition.* Genes Dev, 2005. **19**(11): p. 1315-27.
181. Mandel, C.R., et al., *Polyadenylation factor CPSF-73 is the pre-mRNA 3'-end-processing endonuclease.* Nature, 2006. **444**(7121): p. 953-6.

182. Shi, Y., et al., *Molecular architecture of the human pre-mRNA 3' processing complex.* Mol Cell, 2009. **33**(3): p. 365-76.
183. Brackenridge, S. and N.J. Proudfoot, *Recruitment of a basal polyadenylation factor by the upstream sequence element of the human lamin B2 polyadenylation signal.* Mol Cell Biol, 2000. **20**(8): p. 2660-9.
184. Danckwardt, S., et al., *The prothrombin 3'end formation signal reveals a unique architecture that is sensitive to thrombophilic gain-of-function mutations.* Blood, 2004. **104**(2): p. 428-35.
185. Gilmartin, G.M., et al., *CPSF recognition of an HIV-1 mRNA 3'-processing enhancer: multiple sequence contacts involved in poly(A) site definition.* Genes Dev, 1995. **9**(1): p. 72-83.
186. Graveley, B.R. and G.M. Gilmartin, *A common mechanism for the enhancement of mRNA 3' processing by U3 sequences in two distantly related lentiviruses.* J Virol, 1996. **70**(3): p. 1612-7.
187. Hall-Pogar, T., et al., *Specific trans-acting proteins interact with auxiliary RNA polyadenylation elements in the COX-2 3'-UTR.* RNA, 2007. **13**(7): p. 1103-15.
188. Hu, J., et al., *Bioinformatic identification of candidate cis-regulatory elements involved in human mRNA polyadenylation.* RNA, 2005. **11**(10): p. 1485-93.

189. Legendre, M. and D. Gautheret, *Sequence determinants in human polyadenylation site selection.* BMC Genomics, 2003. **4**(1): p. 7.
190. Moreira, A., et al., *The upstream sequence element of the C2 complement poly(A) signal activates mRNA 3' end formation by two distinct mechanisms.* Genes Dev, 1998. **12**(16): p. 2522-34.
191. Natalizio, B.J., et al., *Upstream elements present in the 3'-untranslated region of collagen genes influence the processing efficiency of overlapping polyadenylation signals.* J Biol Chem, 2002. **277**(45): p. 42733-40.
192. Xie, X., et al., *Systematic discovery of regulatory motifs in human promoters and 3' UTRs by comparison of several mammals.* Nature, 2005. **434**(7031): p. 338-45.
193. Arhin, G.K., et al., *Downstream sequence elements with different affinities for the hnRNP H/H' protein influence the processing efficiency of mammalian polyadenylation signals.* Nucleic Acids Res, 2002. **30**(8): p. 1842-50.
194. Bagga, P.S., G.K. Arhin, and J. Wilusz, *DSEF-1 is a member of the hnRNP H family of RNA-binding proteins and stimulates pre-mRNA cleavage and polyadenylation in vitro.* Nucleic Acids Res, 1998. **26**(23): p. 5343-50.
195. Chen, F. and J. Wilusz, *Auxiliary downstream elements are required for efficient polyadenylation of mammalian pre-mRNAs.* Nucleic Acids Res, 1998. **26**(12): p. 2891-8.

196. Dominski, Z. and W.F. Marzluff, *Formation of the 3' end of histone mRNA: getting closer to the end.* Gene, 2007. **396**(2): p. 373-90.
197. Marzluff, W.F., E.J. Wagner, and R.J. Duronio, *Metabolism and regulation of canonical histone mRNAs: life without a poly(A) tail.* Nat Rev Genet, 2008. **9**(11): p. 843-54.
198. Godfrey, A.C., et al., *The Drosophila U7 snRNP proteins Lsm10 and Lsm11 are required for histone pre-mRNA processing and play an essential role in development.* RNA, 2009. **15**(9): p. 1661-72.
199. Yang, X.C., et al., *FLASH, a proapoptotic protein involved in activation of caspase-8, is essential for 3' end processing of histone pre-mRNAs.* Mol Cell, 2009. **36**(2): p. 267-78.
200. Sullivan, K.D., M. Steiniger, and W.F. Marzluff, *A core complex of CPSF73, CPSF100, and Symplekin may form two different cleavage factors for processing of poly(A) and histone mRNAs.* Mol Cell, 2009. **34**(3): p. 322-32.
201. Dominski, Z., X.C. Yang, and W.F. Marzluff, *The polyadenylation factor CPSF-73 is involved in histone-pre-mRNA processing.* Cell, 2005. **123**(1): p. 37-48.
202. Kolev, N.G., et al., *Conserved motifs in both CPSF73 and CPSF100 are required to assemble the active endonuclease for histone mRNA 3'-end maturation.* EMBO Rep, 2008. **9**(10): p. 1013-8.

203. Adamson, T.E. and D.H. Price, *Cotranscriptional processing of Drosophila histone mRNAs.* Mol Cell Biol, 2003. **23**(12): p. 4046-55.
204. Narita, T., et al., *NELF interacts with CBC and participates in 3' end processing of replication-dependent histone mRNAs.* Mol Cell, 2007. **26**(3): p. 349-65.
205. Jarmolowski, A., et al., *Nuclear export of different classes of RNA is mediated by specific factors.* J Cell Biol, 1994. **124**(5): p. 627-35.
206. Bachi, A., et al., *The C-terminal domain of TAP interacts with the nuclear pore complex and promotes export of specific CTE-bearing RNA substrates.* RNA, 2000. **6**(1): p. 136-58.
207. Bear, J., et al., *Identification of novel import and export signals of human TAP, the protein that binds to the constitutive transport element of the type D retrovirus mRNAs.* Mol Cell Biol, 1999. **19**(9): p. 6306-17.
208. Katahira, J., et al., *The Mex67p-mediated nuclear mRNA export pathway is conserved from yeast to human.* EMBO J, 1999. **18**(9): p. 2593-609.
209. Herold, A., et al., *TAP (NXF1) belongs to a multigene family of putative RNA export factors with a conserved modular architecture.* Mol Cell Biol, 2000. **20**(23): p. 8996-9008.
210. Santos-Rosa, H., et al., *Nuclear mRNA export requires complex formation between Mex67p and Mtr2p at the nuclear pores.* Mol Cell Biol, 1998. **18**(11): p. 6826-38.

211. Komeili, A. and E.K. O'Shea, *Nuclear transport and transcription.* Curr Opin Cell Biol, 2000. **12**(3): p. 355-60.
212. York, J.D., et al., *A phospholipase C-dependent inositol polyphosphate kinase pathway required for efficient messenger RNA export.* Science, 1999. **285**(5424): p. 96-100.
213. Shen, E.C., et al., *Arginine methylation facilitates the nuclear export of hnRNP proteins.* Genes Dev, 1998. **12**(5): p. 679-91.
214. Duncan, K., J.G. Umen, and C. Guthrie, *A putative ubiquitin ligase required for efficient mRNA export differentially affects hnRNP transport.* Curr Biol, 2000. 10(12): p. 687-96.
215. Vainberg, I.E., K. Dower, and M. Rosbash, Nuclear export of heat shock and non-heat-shock mRNA occurs via similar pathways. Mol Cell Biol, 2000. 20(11): p. 3996-4005.
216. Saavedra, C.A., et al., Yeast heat shock mRNAs are exported through a distinct pathway defined by Rip1p. Genes Dev, 1997. 11(21): p. 2845-56.
217. Krebber, H., et al., Uncoupling of the hnRNP Npl3p from mRNAs during the stress-induced block in mRNA export. Genes Dev, 1999. 13(15): p. 1994-2004.
218. Gallouzi, I.E., et al., HuR binding to cytoplasmic mRNA is perturbed by heat shock. Proc Natl Acad Sci U S A, 2000. 97(7): p. 3073-8.

219. Stutz, F., et al., REF, an evolutionary conserved family of hnRNP-like proteins, interacts with TAP/Mex67p and participates in mRNA nuclear export. RNA, 2000. 6(4): p. 638-50.

Chapter 2

Manuscript In Preparation

Gain insight Mammalian SR Protein Kinase 2 (SRPK2) functions: mutational analysis and characterization of its involvement in paraquat damage response

S. Vivarelli[1], S.C. Lenzken[1], D. Bonanno[1], S. Paro[2], R. Alvarez[1], A. Bachi[3] and S.M.L. Barabino[1*]

[1]Department of Biotechnology and Biosciences, University of Milano-Bicocca, Piazza della Scienza, 2, Italy

[2]Medical Research Council Human Genetics Unit Western General Hospital Crewe Road Edinburgh EH4 2XU

[3]Biological Mass Spectrometry Unit, Division of Genetics and Cell Biology, San Raffaele Scientific Institute, Via Olgettina 58, 20132 Milano, Italy

*Correspondence to: Silvia M.L. Barabino, Department of Biotechnology and Biosciences, University of Milano-Bicocca, Piazza della Scienza, 2; I-20126 Milano, Italy; Phone: +39-02-6448 3352; Fax: +39-02-6448 3569; Email: silvia.barabino@unimib.it

Keywords: *Paraquat, Neuroblastoma, Alternative Splicing, SR Proteins, SR Protein Specific Kinase 2*

Running Title: *SRPK2: The S581 residue is important for the nuclear translocation after paraquat treatment*

ABSTRACT

The herbicide paraquat is a model substance implicated in neurodegeneration, affecting the selection of pre-mRNA splice sites in general. Administered to SH-SY5Y neuroblastoma cells it represents a well-characterised *in vitro* model to uncover neurodegeneration and to characterize the effects upon alternative splicing after oxidative stress induction.

Here we report that paraquat treatment induces hyper-phosphorylation and translocation of SRPK2 from the cytoplasm to the nucleus. Also we can observe a speckled-enlarged pattern and a differential phosphorylation of SR proteins coupled with the alteration of splice site selection. SRPK2 mutational analysis brings us to identify Serine 581 (S581) residue as the required for the nuclear translocation of the kinase. Moreover S581 when phosphorylated mimics the paraquat effect on splicing changes.

These findings support insights into the complex modulation of SR protein phosphorylation in response to stress and damage signalling thereby providing new informations upon the regulation pathways involving the neuron-specific SR Protein Kinase 2.

INTRODUCTION

Tissue-specific alternative splicing deeply affects animal physiology, development and disease, and this is nowhere more evident than in the nervous system. This process represents a versatile form of genetic control whereby a common precursor messenger RNA (pre-mRNA) is processed into multiple mRNA isoforms differing in their precise combination of exon sequences. In the nervous system, thousands of alternatively spliced mRNAs are translated into their protein counterparts where specific isoforms play roles in learning and memory, neuronal cell recognition, neurotransmission, ion channel function, and receptor specificity. This is a highly regulated process. Therefore the essential nature of alternative splicing is underscored by the finding that its misregulation is a common feature of human disease, including neurodegenerative diseases [1].

Paraquat (PQ, 1,1'-dimethyl-4,4'-bipyridinium), a widely-used herbicide, has been suggested as a potential etiologic factor for the development of Parkinson's disease. It is known to damage the lipid membrane via peroxidation [2], although the exact mechanism of PQ-induced oxidative cell damage is presently controversial. The assumption is that PQ promotes the production of ROS through a redox cycling process, which can then cause damage to cellular macromolecules [3]. These properties make PQ exposure a useful experimental model for oxidative stress. Indeed, several authors have used this

compound to study the response and the sensitivity to oxidative damage *in vivo* and *in vitro* [4-8]. Recently, it was tested the hypothesis that mitochondrial damage modulates alternative splicing, not only of a few mRNAs, but also in a general manner [7]. SH-SY5Y neuroblastoma cells treated with PQ represent a huge studied *in vitro* model to uncover neurodegeneration and to characterize the effect on alternative splicing after oxidative stress induction [9-14].

SR proteins are key regulators of both constitutive and alternative splicing [15]. They have a modular structure consisting of one or two copies of an RNA-recognition motif (RRM) and a C-terminal domain rich in alternating Serine and Arginine residues (the RS domain) that should be subjected to extensive phosphorylation. The RRMs determine RNA-binding specificity, whereas the RS domain mediates protein-protein interactions that are thought to be essential for the recruitment of the splicing apparatus and for splice site pairing [16-17]. Recent studies reveal a broad vertical integration of SR proteins functions in gene expression from transcriptional elongation to protein synthesis, from organizing gene networks in the nucleus and facilitating cell-cycle progression [18] to maintaining genome stability ([19-21], for a review see [22]). Although it remains to be cleared whether these last functions reflect levels of independent activities of SR proteins or are all interconnected with pre-mRNA splicing, these recent discoveries underline the central role carry out by SR proteins in coupling various transcriptional and post-transcriptional gene

expression events. These functions make SR proteins essential for viability of proliferating cells [23-25]. Defects in these processes may directly contribute to developmental defects and onset of cancer [26-29]. SR proteins are regulated during development, which are translocated from the cytoplasm to the nucleus during zygotic activation of gene expression [30]. Individual SR proteins are also self-regulated, suggesting critical importance in maintaining their homeostasis in somatic cells [31]. This set of observations indicates that SR proteins must be tightly regulated and each sort of alteration on SR proteins has deep consequences on the cell fate.

The activity of SR proteins is deeply affected by RS domain cycles of phosphorylation/dephosphorylation thus, protein kinases involved in the phosphorylation of these splicing regulators could have an important role in linking alternative splicing regulation to extracellular signals. SR protein phosphorylation is essential for nuclear import of SR proteins as well as for their functions in mediating spliceosome assembly [32-33]. Whereas partial dephosphorylation of SR proteins is critical for progression of the assembled spliceosome to catalysis [34] and for a series of post-splicing events from the interaction with the mRNA transport machinery to SR protein-mediated translational control [25, 35]. As an unsurprising consequence, the experimental induction of both SR protein hypo- and hyperphosphorylation inhibits splicing [36]. While these observations clearly suggest that SR protein

phosphorylation is narrowly controlled, the mechanisms of such regulation in the cell have to be more outlined.

Many protein kinases have been implicated in SR protein phosphorylation. The SRPK and Clk/Sty families are the well studied among the growing list of SR protein kinases. Mammalian cells express two SRPKs and four Clk/Sty members of each family of kinases. Interestingly, SRPK1 and SRPK2 were shown recently to differentially associate with U1 and tri-snRNP particles, respectively, indicating that these kinases have overlapping as well as unique functions in mammalian cells [37].

The SRPK family of kinases are detected in both the cytoplasm and the nucleus [38-39]. Recent studies showed that SRPK1 can translocate in the nucleus upon osmotic stress induction [40] and SRPK2 can translocate in the nucleus when phosphorylated by Akt [41].

Despite its importance, little is known about how SR protein phosphorylation might be regulated in the cell and how a specific signal might be transduced to control RNA processing via modulation of SR protein phosphorylation. Interestingly, recent discoveries gained increasing data about how the SRPKs compartmentalization should be coupled with the tightly SR protein phosphorylation, observations that have to be further investigated.

In this report we show how SRPK2 respond to paraquat stress induction. It has been previously reported that SRPK2 is a constitutively active kinase highly expressed in the brain with a

conserved bipartite kinase domain divided by a unique spacer sequence and also a specific amino-terminus Proline-rich region that has shown the capacity to interact with WW domain or SH3 domain containing proteins *in vitro* [42-44].

We now demonstrate that SRPK2 is phosphorylated and moves into the nucleus upon paraquat treatment, thereby inducing an alternative splice site selection and a differential SR protein phosphorylation. These findings reveal the underlying mechanisms modulating SR protein phosphorylation in response to stress and damage signalling thereby providing new understanding concerning the regulation pathways that involve the neuron-specific SR Protein Kinase 2.

MATERIALS AND METHODS

Plasmids construction

pME-HAmSRPK2 was a kind gift from Masatoshi Hagiwara Laboratory [45]; all the SRPK2 mutants were obtained using the pME-mSRPK2 as a template. The spacer-deleted mutant was obtained by double digestion of pME-HAmSRPK2 (BamHI and HindIII) followed by fill-in and ligation of the vector. The N-terminus deleted was obtained by a first amplification with the oligos Nterm-FW and HindIII-REV, then a cleavage and cloning HindIII/SalI in pME-HAmSRPK2 vector. All other mutants were obtained thorough site directed mutagenesis using the four oligos method: a list of the oligos used is comprised in supplementary table 1. The general method consisted in a two-step PCR. For the first round of PCR we used pME-HAmSRPK2 as a template (exception made for the A50D and A581D mutations obtained by the use of pME-HAmSRPK2S50A or S581A as template respectively) with one matching external and one degenerated oligo for each of the two PCRs. Then we performed a second round of PCR using as a template the mix of the previously gel-purified PCR degenerated products amplified with the two more external oligos together. The resulting PCR product was purified from agarose gel and cloned NotI in pME-HAmSRPK2, after a subcloning step in pGEM-T-Easy vector system (A3600, Promega). The Taq used for the PCRs was the Phusion Hot Start High-Fidelity DNA Polymerase (F-540S, Finnzymes). The

amplification conditions for each PCR were reported in supplementary table 2. All the resulting plasmids were verified by nucleotide sequencing. pEGFPhRNPA1, pEGFPASF/SF2 and PCMV-SV40-E1A were a kind gift from Giuseppe Biamonti laboratory. The plasmid p-hSRPK2-FLAG was obtained by inserting FLAG tag in hSRPK2 (from pCMV6-XL5-hSRPK2, SC107542, OriGene) by PCR with oligos hSRPK2-fw (5'TATGTCAGTTAACTCTGAGAAGTCGT3') and hSRPK2-rev (5'ACTACTTATCGTCGTCATCCTTGTAATCAATGTTAACAGA ATTCAACCAAGGAT3'), by using the following amplification conditions: 98°C 30 sec; 30 cycles of 98°C 8 sec, 64,5°C 30 sec, 72°C 40 sec; 72°C 8 min. The Taq used for the PCR was the Phusion Hot Start High-Fidelity DNA Polymerase (F-540S, Finnzymes). The PCR product was first subcloned in pGEM-T-Easy vector system, then cleaved NotI and finally inserted in pCDNA3 vector. The resulting plasmids was verified by nucleotide sequencing.

Cells culture, transfections, drug treatments

Cells were maintained in Dulbecco's modified Eagle's medium (M0080541, EuroClone) supplemented with antibiotics (100 U/mL streptomycin and 100 µg/mL penicillin; M0081913, EuroClone), 2,5 mM L-Glutamine (M0080054, EuroClone) and 10% Foetal Bovine Serum (S0060094, EuroClone) at 37 °C with 5% CO2. For RNA extraction and immunoblotting, 1,5 x 106 SH-SY5Y cells were plated on a 10 cm plate, and the next day plasmid DNA (20 µg) was transfected using

Polyethylenimine (PEI, 40,872-7, Sigma, 100 mM in H_20 pH 7.00) according to the manufacturer's instruction. The transfected cells were incubated for further 48 hours before lysis. For immunofluorescence, 3 × 105 SH-SY5Y cells were plated in each well containing a coverslip in a 6-well plate. The next day plasmid DNA (3 µg) was transfected using Transfast (Promega). In drug treated samples paraquat (Methylviologen Hydrat, 85,617-7, Sigma, 100 mM in H2O) was added to the medium at a final concentration of 750 µm.

Immunofluorescence and confocal microscopy analysis

Cells grown on the glass coverslips were fixed with 4% paraformaldehyde in PBS (137 mM NaCl; 2,7 mM KCl; 4,3 mM Na2HPO4; 1,47 mM KH2PO4, pH 7.4) for 10 min and permeabilized with CKS solution (Hepes 20 mM, Sucrose 300 mM, NaCl 50 mM, MgCl2 3 mM, Triton 0,2 %) cold for 5 min. After blocking with FBS 10% in PBS with 0,05% Tween for 30 min, coverslips were incubated for 1 hour in a humid chamber with the following primary antibodies in PBS containing 0,2% BSA: goat polyclonal anti-SRPK2 (P-19, sc-11308, Santa Cruz Biotechnologies) at 1:100, mouse monoclonal anti-SRPK2 (611118, BD Biosciences) at 1:1000, mouse monoclonal anti-HA (Clone 6E2, 2367, Cell Signaling Technology) at 1:250, rabbit polyclonal anti-HA (Y-11, sc-805, Santa Cruz Biotechnologies) at 1:100, mouse monoclonal anti-SC35 (S4045, Ascites Fluid, Sigma) at 1:500. After washing three times with PBS plus 0.2% BSA, the coverslips were stained

with the respective fluor-conjugated secondary antibody diluted 1:2000 in PBS and 0,2% BSA. Alexa 488-conjugated donkey anti-goat IgG (H+L) (A11055, Molecular Probes), Alexa 488-conjugated goat anti-mouse IgG (H+L) (A11001, Molecular Probes), Alexa 488-conjugated goat anti-rabbit IgG (H+L) (A-11070, Molecular Probes), or Alexa 546-conjugated donkey anti-mouse IgG (H+L) (A10036, Molecular Probes) respectively were used. After dark incubation for 1 hour, coverslips were washed three times with PBS plus 0.2% BSA, incubated in a solution containing 4,6-diamidino-2-phenylindole (DAPI, D9542, Sigma) 1 µg/mL in PBS for 10 min at RT, and mounted with FluorSave Reagent (345789, 20mL, Calbiochem). The fluorescence 8-bit images were collected with a Leica TCS SP2 AOBS confocal microscope with the 63X oil immersion objective. Quantification of the data was done using LSC software: 12-bit images were acquired by using the same setting parameters for all the samples (gain, offset); for each field, five different xy sections along the z axis were acquired. Measurements were obtained for the nuclear fluorescence (Sn), the total cell fluorescence (Sc), the area of the nucleus (An), and area of the cell (Ac). The cytoplasmic (C') amount of signal was calculated as: C'=1 - [(An Sn)/(Ac Sc)]. C/N ratios were calculated as C/N = C'/(1 – C').

Immunoblotting and Co-Immunoprecipitation assays

For total protein extracts cells on 10 cm plate were lysed in 1 mL of Lysis buffer (Tris HCl 50 mM pH 6.80, NaCl 150 mM, 1%

NP40, 5 mM EGTA, 5 mM EDTA) with protease inhibitors (Complete PIC, 04 693 116 001, Roche) and phosphatase inhibitors (PhIC-1, P2850, Sigma; PhIC-2 P5726, Sigma) added. For fractionated protein extracts cells on 10 cm plate were lysed using the ProteoJET cytoplasmic and nuclear protein extraction kit (K0311, Fermentas) with protease inhibitors (Complete PIC, 04 693 116 001, Roche) and phosphatase inhibitors (PhIC-1, P2850, Sigma; PhIC-2 P5726, Sigma) added, following the manufacturer's instructions. For immunoprecipitation assays, Flag-tagged proteins were immunoprecipitated from the pre-cleared total cell lysate with M2 anti-Flag agarose affinity gel (A2220, Sigma) following manufacturer's instructions. For phosphatase treatment of total protein lysates Alkaline Phosphatase was used (Alkaline Phosphatase, Calf Intestinal, CIP, M0290L, New England Biolabs) following manufacturer's instructions.

Proteins were separated in 8% or 12% SDS-polyacrylamide gels (classic Laemli conditions) and transferred to nitrocellulose membranes (Protran-Nitrocellulose, 10401197, Whatman GmbH), in Transfer buffer (25 mM Tris, 192 mM Glicine, 20% Methanol) overnight at 4℃ at 15 Volts. Membranes were blocked using 5% non fat dried milk in PBST (0.1% (v/v) Tween 20 in 1x PBS) for 1 hour at room temperature and incubated with a primary antibody diluted in PBST 1 hour at RT for mAb104 (mouse IgM, [46]; CRL-2067, American Type Culture Collection, Manassas, VA; 1:500 dilution of hybridoma culture supernatant, kind gift by Daniel Shumperli laboratory), mouse

monoclonal anti SR proteins (clone 16H3, 33-9300, Invitrogen, 1:200 dilution), mouse monoclonal anti SRp20 (clone 7B4, 33-4200, Invitrogen, 1:500 dilution), mouse monoclonal anti ASF/SF2 (clone 96, 32-4500, Invitrogen, 1:500 dilution), mouse monoclonal anti-β-actin (ab8226, Abcam, 1:5000 dilution), mouse monoclonal anti-SRPK2 (611118, BD Biosciences, 1:1000 dilution), mouse monoclonal anti-hnRNP K/J (clone 3C3, R8903, Sigma, 1:10000 dilution), mouse monoclonal anti-hnRNP A1 (clone 4B10, AB10685, Abcam, 1:5000 dilution), rabbit anti-hnRNP H (NB-100-385, Novus Biological, 1:10000 dilution), mouse monoclonal anti-hRNP C1/C2 (clone 4F4, R5028, Sigma 1:10000 dilution), goat anti-LDH (AB1222, Chemicon International 1:5000 dilution), mouse monoclonal anti FLAG-M2 (F1804, Sigma, 1:1000 dilution) mouse monoclonal anti-HA (Clone 6E2, 2367, Cell Signaling Technology, 1:1000 dilution). After washing 3 times with PBST, membranes were incubated with peroxidase-conjugated secondary antibody anti-mouse IgG (H+L) (NXA931, GE Healthcare, 1:10000 dilution), anti-goat IgG (H+L) (31402, Pierce, 1:5000 dilution), anti-rabbit IgG (H+L) (31460, Pierce, 1:10000 dilution), anti-mouse IgM (sc-2064, Santa Cruz Biotechnologies, 1:5000 dilution) in PBST with 3% non fat dried milk for 45 minutes at room temperature. After washing as above, the chemio-luminescent signals developed by ECL reagents (RPN2106, GE Healthcare) were detected using films Amersham Hyperfilm ECL (28-9068-35, GE Healthcare). We made quantifications using Photoshop program: first for each band obtained (defined with the lasso

tool) we multiplied each pixel number for the average grey value thus obtaining an absolute intensity value. Second we normalized every absolute value obtained with the corresponding housekeeping band intensity, thus obtaining relative intensity values.

E1A splicing reporter assays

Total RNA was extracted using Trizol (15596-026, Invitrogen) for cell lysis until the phenol chloroform step, once obtained the RNA fraction, after adding equal volume of 70% ethanol, the solution was passed into RNeasy Mini Kit columns (74106, Qiagen) for total RNA washing and purification by following manufacturer's instructions. After DNase treatment (RQ1, RNase-free Dnase, M610A, Promega; 30 minutes at 37℃ and then 10 minutes at 65℃ after adding stop solution), cDNA was synthesized by reverse transcription (RT) using oligo-dT primer (C110A, Promega) and Reverse Transcriptase (M-MLV RT, M170B, Promega) 42 ℃ for 1 hour with 1 µg of RNA template in 20 µL reaction volume. An aliquot (1 µL) was then used for PCR reaction (12,5 µL) with GoTaq Flexi DNA Polymerase (M8301, Promega). The E1A splice isoforms were detected by PCR using the following E1A primers (5′TGAGTGCCAGCGAGTAGAGTTTTCT3′ and 5′TCTGGCTCGGGCTCAGGCTCAGGTT3′) and the following PCR amplification conditions: 1 cycle of 95 ℃ for 2 min, 27 cycles of 95 ℃ for 30 s, 55 ℃ for 30 s and 72 ℃ for 1 min, and 1 cycle of 72 ℃ for 5 min. The amounts of the isoforms were

measured using a 2100 Bioanalyzer (Agilent Technologies, Palo Alto, CA) and expressed as the molar ratio.

Maldi-Tof MS analysis

Total protein extracts form SH-SY5Y transfected with pCDNA3-SRPK2-FLAG or the pCDNA3-FLAG-emty control were characterized by SDS-PAGE electrophoresis. Polyacrylamide gel electrophoresis experiments were carried out with 7.5% acrylamide gels. Coomassie blue (Sigma-Aldrich Corporation) was used to stain the protein bands. For protein identification, the bands of interest were excised from Coomassie-stained gels, reduced, alkylated, and digested overnight with bovin trypsin as described elsewhere [47]. Supernatant (1 µl) of the digestion was used for MALDI-TOF MS analysis using the dried droplet technique and cyano-4-hydroxycinnamic acid (HCCA) as matrix. All analyses were performed using a Voyager-DE STR (Applied Biosystems, Framingham, MA, USA) time of flight (TOF) mass spectrometer operated in the delayed extraction mode. Peptides were measured in the mass range from 750 to 4000 Da; all spectra were internally calibrated and processed via Data Explorer software. Proteins were unambiguously identified by searching a comprehensive nonredundant protein database using the program ProFound [48].

Statistical analysis

Continuous variables are expressed as means ± SEM. The averages and SEMs were calculated from at least three

independent experiments. Means of two-groups experiments were compared with t-test (unpaired or paired, according to the fact that data were respectively coupled or not). Means of multiple-groups experiments were compared using one-way ANOVA (matched or not, according to the fact that data were matched or not) and Turkey post-test analysis. All the analyses were performed using GraphPad prism 5.0 and GraphPad Instat 3.

A P value of *P < 0.05 was considered statistically significant, **P < 0.001 was considered very significant, ***P < 0.0001 was considered extremely significant.

RESULTS

SRPK2 translocated in the nucleus in response to paraquat treatment

It has been previously reported that at the steady state SRPK endogenous kinases were present in both cytoplasmic and nuclear cellular compartments. The localization of the SRPK family of kinases in the cytoplasm is interesting because many kinases with a nuclear function are regulated by nuclear translocation. It was the case of Dsk1, an SRPK family member from fission yeast, also found to localize predominantly in the cytoplasm in interphase, but in the nucleus during mitosis (note that the yeast nuclear envelope does not break down in mitosis; [49]), in a cell cycle dependent fashion [50].

Consequently, we wondered if the neuron-specific SRPK2 could translocate in the nucleus in cell treated with paraquat.

In order to assess if SRPK2 could translocate from the cytoplasm into the nucleus after 18 hours of 750 μM paraquat treatment in SH-SY5Y neuroblastoma cells, thus being responsive to this kind of stress stimulus, in first instance we performed immunofluorescence studies by using confocal microscopy.

Actually we found that upon paraquat treatment the nuclear fluorescence for endogenous SRPK2 increased (figure 1 A). To further substantiate this finding, we also transiently transfected the SH-SY5Y cells with pME-HAmSRPK2 (HA tagged SRPK2). After 24 hours of transfection and 18 hours of drug treatment

(started 6 hours after transfection) we observed a nuclear translocation also for the exogenously overexpressed protein (figure 1 B). We therefore quantified the data by using confocal microscopy analysis (as described in methods) and interestingly we observed a significant shift of the fluorescent signal in the nucleus in the order of the 35% more in treated cells compared to the untreated (37% for the endogenous SRPK2, 35% for the overexpressed kinase; figure 1 C and D, right panels). But if we considered the ratio between the nuclear and the cytoplasmic signal, we assessed a 1,7 fold increase in the nuclear signal for the endogenous kinase versus only 1 fold for the HA tagged one (figure 1 C and D, left panels). Although the reason for such different behaviour is not clear, we could attribute this to the fact that endogenous SRPK2 signal was due to the addiction of the effect of both the SRPK2 existing splicing isoforms. On the contrary the transfected protein is specifically the b isoform. A supplementary meaning should be the fact that by overexpressing SRPK2 we forced the system and we had a highest level of SRPK2 under the strong plasmid promoter thereby there was a displacement of the physiological equilibrium in the cell and the resulting noticed shift was different in terms of fold change.

Paraquat treatment induced changes upon SR proteins

It has been previously well evidenced that paraquat treatment on SH-SY5Y induced a global change at the alternative splicing level [7]. Consequently the induction of SRPK2 nuclear

translocation as an outcome of stress signalling suggested that SR protein phosphorylation status might be orderly altered. We first examined this possibility by immunofluorescence comparison of untreated and paraquat treated SH-SY5Y. In first instance we used the S4045 antibody (Sigma) that recognized a phospho-epitope on the SR protein SC-35 and also it was reactive with the related SF2/ASF [51]. We clearly detected a speckled enlarged pattern in paraquat treated cells if compared with the untreated (figure 2 A, from a to b'). We also observed a brighter nuclear speckled distribution of transiently transfected GFP-ASF after treatment (figure 2 A, from c to d'). In case of stress (heat shock, osmotic) it was documented the shuttling of hnRNPA1 from nucleus to cytoplasm thereby having consequences on splicing trans-acting proteins nuclear equilibrium in HeLa cells [52]. In order to exclude any influence of hnRNPA1 after paraquat treatment in neuroblastoma cells we also checked for the GFP-hnRNPA1 signal and we did not observe neither changes in the intracellular distribution of the shuttling hnRNP protein hnRNPA1, nor any different nuclear pattern (figure 2 A, from e to f').

In order to better understand what was the status of SR protein phosphorylation, we used mAb104 for western blot analysis of total protein extracts from both untreated and treated cells. In fact this antibody was raised for its specific recognition of common SR-phospho-epitopes in all higher eukaryotic cells, thereby becoming an useful tool to probe the SR protein phosphorylation state [53]. What we observed in response to

paraquat treatment in SHSY5Y treated for 18 hours with paraquat 750 μM was a strong increase of the SRp55 (2,4 fold), SRp20 (2 fold), and SRp75 (1,7 fold) band signals and also an elevation for the SRp40 (1,2 fold) and SRp30 (1,1 fold) signals, (figure 2 B, left panel) as is quantified in the graph (data represented mean ± SEM of 3 independent experiments; figure 2 C). Endogenous β-actin was the loading control (figure 2 B, lower left panel). In order to ascertain that the increase in phosphorylation was really due to an increase in quantity of phospho-epitopes in the cells after the treatment, we normalized the results by measuring also the level of SR proteins expression. In fact, we tested both treated and untreated extracts by WB analysis with the 16H3 antibody recognizing SRp75, SRp55 and SRp40 (the antibody did not recognize SRp30a and SRp30b, but recognized also 20 different nuclear proteins, such as U1-70K and both the U2AF subunits); also with ASF/SF2 antibody and with SRp20 antibody and we did not find any difference after the drug treatment for each protein observed (figure 2 B, central panel).

In order to exclude any increase in hnRNP principal proteins expression, we tested the same protein extracts with anti hnRNP A1, C1/C2, H and K/J antibodies and we did not detect any increase in signal in total extracts after the treatment compared with the untreated samples. Endogenous β-actin was the loading control (figure 2 B, left panel).

Paraquat showed an effect on splice site selection

The E1A minigene is a well-characterized splicing reporter system ([54], see also www.ebi.ac.uk). We transfected the E1A reporter plasmid in SH-SY5Y cells (as described in methods); after 48 hours of transfection we collected and retrotranscribed the RNA and we performed the PCRs with the oligos annealing with all the isoforms (figure 3 A). Then we analysed the output of the experiments both by running the products on a 2% agarose gel, and by analysing the same samples with the 2100 Bioanalyzer instrument (see methods) in order to correctly quantify the product isoforms in terms of molarity. We compared three different whole of biological samples from three independent sets of experiments in order to render reproducible the assay. Every single set of RNA was then retrotranscribed (and analysed by RT-PCR) 2 times thereby making more robust the results. By observing the gel we noticed an increase of the 9S isoform band (Figure 3 B), thus confirmed by Bioanalyzer quantification. In fact we had an increasing amount of the 9S isoform ratio (from 1,5 to 2,7) due to an augment in the 9S isoform percentage (from 59% to 72%) respect to the other isoforms (figure 3 C). This result could be explained because of the hyper-phosphorylation of certain SR proteins, that overall brought to a splicing inhibition [36]. Finally we could speculate that after paraquat treatment the effect of hnRNPA1 prevailed on competitor SR proteins and the final effect was the distal splice site choice and the consequent increase in the 9S isoform synthesis. In fact, hnRNPA1 did not shuttle in

cytoplasm after treatment, therefore remaining available in nuclear spliceosomes [55].

SRPK2 became phosphorylated upon paraquat treatment

We further compared the endogenous SRPK2 protein expression level before and after the drug treatment by western blot analysis (see methods). We observed a bands pair at apparent mass weights of 116 and 120 KDa. We also noticed a strong increase in the upper band signal and a concomitant decrease in the lower band signal in paraquat treated samples (figure 4 A, left panel). This result has been verified by Calf Intestinal Phosphatase treatment, after which the upper bands of both samples disappeared thereby the lower bands persisted (figure 4 A, right panel). Our observation underlined that actually the upper bands were attributable to heaviest hyper-phosphorylated SRPK2 forms. Then, in order to better assess how the level changed and in which cellular compartment the phosphorylation took place, we obtained the nuclear and the cytoplasmic protein fractions of untreated and treated samples. After a western blot analysis we observed that the phosphorylated form prevalently localized in the nucleus in untreated cells, while the phosphorylated SRPK2 increased in all the compartments after the paraquat treatment. Overall we observed an increase of the phosphorylated form in the whole cell after the treatment. It should be that the phosphorylation would have been place in the cytoplasm therefore bringing to a

SRPK2 post-translational modified form capable to translocate in the nucleus.

SRPK2 mutational analysis

In order to uncover what was the link connecting SRPK2 phosphorylation and nuclear translocation, we undertaken the mutational analysis strategy. As well described in methods, we created a series of mutants to better understand what was the feature of the translocating SRPK2. In first instance we created an inactive kinase mutant by generating the K108R mutation in the catalytic site. Then we selected many putative phosphorylation sites by the presence along the sequence of consensus motifs as well as by exploiting informations available on the on-line tools [56]. We exploited these informations and finally we generated a series of unphosphorylable and constitutively phosphorylated-like counterparts (this approach is described in methods). We created the S50, S581 mutants (by analogy with SRPK1 [57]), and Y318 mutants. This latter Tyrosine is inserted in the spacer sequence and it was predicted as a possible phosphorylation site specific only for SRPK2. All the mutants were HA-tagged as well as the wild type template (see methods). We also constructed deletion mutants lacking of the N-terminus or the spacer region dividing the two halves kinase-domains (see a scheme in figure 5 A and B).

We tested their expression, intracellular localization and response to paraquat treatment after transient transfection in

SH-SY5Y cells (see figure 6 and figure S1). We found a mutation responsible for the nuclear translocation: the one upon the S581 residue, localized in the second half kinase domain of SRPK2. The same residue had seen to be phosphorylated in SRPK1 by CK2 therefore increasing the SRPK1 activity of six fold *in vitro* [57]. Until now this mutation was never seen connected to any translocation neither to any increased activity *in vivo*. We also observed that the other examined mutations had the general effect to render the kinase less responsive to paraquat treatment in terms of nuclear translocation. At the same time they also appeared less localized in cytoplasm at the steady state condition if compared with the wild type kinase (for a summary of the results obtained see the figure S1). This should be explained by the fact that SRPK2 could be also undertaken to other post-transcriptional modifications after external stimuli that perturbed its physiological balance into the cell. Moreover this phosphorylation could be matched with other intermolecular interactions or intramolecular modifications important for other responses. We also observed a particular nuclear speckled concentration of the spacer deleted mutant already previously observed for SRPK1 in untreated HeLa cells [38].

Through confocal microscopy we also acquired the SC-35 signal from cells overexpressing the mutants compared with untransfected cells in the same field. We therefore observed that only wild type SRPK2 re-localized SC-35 signal in transfected cells, whereas spacer deleted mutant

overexpression brought to a nuclear condensation of both SC-35 and itself together in few and very enlarged speckled structures. We observed this behaviour in paraquat treated cells thus indicating that the spacer region could be important in nuclear kinase functions. We could postulate that this spacer region should be involved in the correct nucleoplasmic localization of the kinase.

SRPK2 phosphorylation at S581 residue is required for the nuclear translocation after paraquat treatment in SH-SY5Y cells

S581A/D were the mutations that we found as the responsible for the nuclear translocation of SRPK2. Particularly, we found that S581A mutation (that rendered the 581 residue unphosphorylable) clearly prevented the nuclear translocation upon paraquat treatment. Accordingly the A581D counterpart (mimicking of a constitutive phosphorylation) resided in the nucleus already if overexpressed in untreated cells (figure 6 A).
We also quantified these observations by confocal analysis (performed as described in methods) and we found an extremely significant decrease in the nuclear signal in the treated S581A mutants compared with the treated controls (the percentage of nuclear signal in S581A mutant overexpressing cells was only 22,5% versus the 55,3% in control treated cells and the nuclear/cytoplasmic ratio was 1 fold less in S581A mutant overexpressing cells). We observed also an extremely significant increase in the nuclear fluorescence for the

untreated A581D mutants if compared with the untreated wild type controls, although less than the control both in treated and untreated samples (in fact, the percentage of nuclear signal grew from 20,2% to 38,8%, correspondingly the nucleus/cytoplasm signal ratio was 0,4 fold plus in A581D mutant overexpressing cells if compared with the controls, figure 6 B). We could explain this response if we considered that the S581 phosphorylation was the necessary but not the unique modification required for the nuclear translocation. Finally, equilibrium of modifications caused the different SRPK2 compartmentalization in normal condition and after a stress induction. It is important also to notice that we observed a reduced increase in the nuclear signal when we treated cells overexpressing the kinase death SRPK2 (a 5% less, corresponding to 0,25 fold less, if compared with the treated wild type protein) thus underlining that the kinase activity could in a little but significant way influence the nuclear translocation.
Considering the SC-35 corresponding signal, we observed only a partial SC-35 nuclear redistribution after the A581D mutant overexpression compared to the wild type dealing. On the contrary, we couldn't observe any relocalization overexpressing the S581A unphosphorylable mutant (figure 6 A).

Mutational analysis: the effects of mutants on alternative splicing before and after paraquat treatment

In order to better connect the nuclear translocation of the kinase with a proper effect on alternative splicing, we transfected each

kinase - wild type, kinase dead, S581A and A581D mutants or the mock empty vector control - with the same quantity of E1A minigene reporter plasmid, we further isolated, retrotranscribed the RNA, after we performed an RT-PCR on the samples (as described in methods). In figure 7A we reported the 2% agarose gel of the PCR product samples. We therefore quantified the same samples by using the Bioanalyzer instrument (as described in methods; figure 7 B). We observed that wild type and kinase dead mutant overexpression had no *per se* effect on the splice site choice thereby they did not differ significantly between each other and if compared with their mock controls (as it was already reported after the overexpression of the same plasmids in HeLa cells [58]). We also observed that the A581D mutant overexpression brought to an extremely significant increase of the 9S isoform (corresponding to the distal splice site choice) ratio and percentage if compared to the other isoforms already in untreated samples (1 fold increase, corresponding to an increase of 12 percent), thereby confirming the existence of a close connection between the effect on alternative splicing regulation and the SRPK2 nuclear translocation. In addiction, we obtained an extremely significant decreased signal in the same 9S isoform values for the S581A treated samples if compared with the controls (1,2 fold decrease, corresponding to a decrease of 13 percent). Hence, the cytoplasmic presence of this unphosphorylable SRPK2 mutant was likely to have a cytoplasmic sequestering effect on something else important for

splicing fulfilment in the nucleus, thereby contrasting, and in such way overcoming the effect of the endogenous SRPK2 (which was anyhow present in transfected samples and that could go into nucleus after treatment).

Mass spectrometric analysis of protein immunoprecipitates after overexpression of FLAG tagged SRPK2 in SH-SY5Y cells

Once determined that phosphorylated SRPK2 went into the nucleus then modifying splicing response after paraquat treatment, we wanted to better assess what could be the nuclear functions gained by this kinase. In particular we wanted to deeply uncover if nuclear SRPK2 could have also other targets and functions yet unknown.

In order to further assess which could be the SRPK2 interactors, we overexpressed FLAG tagged SRPK2 in neuroblastoma cells (or the FLAG empty vector as mock control) and then we performed a FLAG based immunoprecipitation (see methods). Therefore we analysed two SDS-PAGE electrophoresis gels, from two independent experiments, previously stained with Coomassie (see methods). In each experiment we observed some specific bands when compared with the unspecific pattern bands derived from the mock control.

The analysis by MALDI-TOF MS of these main bands of proteins separated by SDS-PAGE gel allowed further characterization of their composition. We reported a synthesis

of the result obtained in Table 1. As expected we found classical SR proteins as well as SR-related proteins. In addiction we also found splicing factors, hnRNP proteins, RNA binding proteins, transcription / replication-involved proteins, ribosomal proteins and translation-related proteins. These last interactors could be also due to RNA-mediated interactions, thus not direct. Surprisingly we also found heat shock proteins and also proteins involved in DNA damage repair, so indicating the possible existence of some undiscovered function gained by SRPK2 kinase maybe carried out in distinct cellular compartments.

We have to further validate these results by performing WB analysis both before and after RNAse A treatment, in order to exclude all the indirect RNA-mediated interactions. Also we have to compare these interactions before and after paraquat treatment in order to substantiate if there is some enrichment charged to any co-IP signal after the treatment.

DISCUSSION

Previous studies have established that SR protein activities are deeply affected by phosphorylation [33, 59]. We know also that each experimental induction of both SR protein hypo- and hyperphosphorylation inhibits splicing reaction [36]. Hence, protein kinases involved in the phosphorylation of these splicing regulators may have an important role in linking alternative splicing regulation to extracellular signals.

A novel study provides insight into a complex signalling pathway that controls the phosphorylation status of an SR related protein (SRp38) which functions as a splicing repressor following heat shock-dependent dephosphorylation. This effect is principally due to the activation of a protein phosphatase (PP1) and to the differential activity of SR protein kinases on different SR proteins [60]. Further recent studies connected the nuclear translocation of SRPKs with protein-protein interactions or post-transcriptional phosphorylation events, thus regulating the kinase cellular localization and activity in response to extracellular stimuli [22, 41].

Our present study shows how SRPK2 can be regulated in response to paraquat damage in a neuroblastoma cellular model. In particular our research connects the nuclear translocation of the kinase with the effect on SR protein phosphorylation and also with the changes affecting the alternative splice site choice, as a consequence of the phosphorylation at S581 residue. These observations represent

a further step toward the comprehension of these not totally uncovered regulatory systems.

In particular, our data correlate the cellular damage induced by paraquat to a general effect on SR proteins. In fact we only observed changes involving SR proteins intranuclear distribution and excluding hnRNPA1 (it was saw to redistribute in the cytoplasm in response to extracellular signals [52]). In particular we noted a brighter speckled nuclear signal with a concomitant increase in phosphorylation of SR classical proteins. Nuclear speckles are dynamic structures that are enriched in splicing factors and are located in the interchromatin regions of the nucleoplasm of mammalian cells. These sub-nuclear structures are traditionally considered as storage/modification sites of pre-mRNA splicing factors [61]. At the level of activation of some specific genes, it has been demonstrated that speckles serve as pools of splicing factors that are recruited to the transcription and splicing sites [62]. Thus the speckles enlargement could be connected with the hyperphosphorylation of SR proteins (observed by WB analysis) and their following accumulation in the speckles-enlarged storage sites, as it is suggested by the phospho-SC35 epitope immunofluorescence staining in our neuroblastoma cells after the paraquat treatment.

By using the minigene reporter system we documented a different splice site selection after this treatment, thereby confirming the link existing between SR protein phosphorylation and alternative splicing changes.

In parallel, we show that upon paraquat treatment SRPK2 is phosphorylated and translocates from the cytoplasm to the nucleus.

In order to connect these two events, thereby detecting if there is any posttranslational modification that can bring the kinase in the nucleus, we planned to perform an extensive mutational analysis. A panel of mutants was screened and finally we identified the S581 residue as the responsible for the nuclear translocation.

To further link the role performed by this mutation and the function gained by SRPK2 in the nucleus we analysed the splicing changes also due to the mutants. We show that when the S518 residue was constitutively phosphorylated the kinase relocalized in the nucleus regardless of the drug treatment, with a concomitant increase in the 9S isoform of the E1A reporter. This finding links the nuclear redistribution of the kinase (due to the posttranslational S581 phosphorylation in response to paraquat) with the change in the alternative splicing bands pattern of the E1A reporter thus mimic the paraquat cellular treatment.

We can hypothesize a model: upon paraquat treatment SRPK2 is phosphorylated and the phosphorylation at the S581 residue is required for the nuclear translocation of the kinase. This translocation displaces the nuclear balance existing between nuclear SR proteins kinases and phosphatases and the final effect is the distal splice site choice in our E1A alternative splicing reporter (as it is reported in figure 8).

Until now it was clear the physiological role of SRPK2 in the cytoplasm as a SR protein kinase involved in the phosphorylation of SR proteins that by this way could be re-imported into the nucleus to be further recruited in spliceosomes. We have discovered that SRPK2 can carry out some function also in the nucleus. In particular, a cytoplasm-to-nucleus translocation is now linked to an extracellular signal having as consequences both specific hyperphosphorylation of SR kinases as well as specific splicing effects.

It will be interesting to understand who is the upstream kinase that phosphorylates SRPK2. Also to clarify what are the effects deriving from the hyperphosphorylation on SR proteins. Finally, it will be necessary to discover if the nuclear SRPK2 can have also other not-canonical targets. Future work will be directed to answer to these basic questions. We have already performed a mass spectrometric analysis (as it is described in results) and we are now trying to characterize these new predicted interactors and the new foresaw pathways specifically involving SRPK2 function after paraquat treatment.

In conclusion, our work assessed a specific SRPK2-mediated response to paraquat drug treatment. This response finally brings to the regulation of both SR proteins activity and alternative splice site choice in the nucleus hence uncovering any possible compartmentalised-dependent regulation of the kinase.

Acknowledgements

We gratefully acknowledge Marc David Ruepp for the production of mAb104 antibody.

FIGURE LEGENDS

Figure 1

SRPK2 nuclear translocation in response to paraquat treatment

A, B. Induction of SRPK2 nuclear translocation in SH-SY5Y cells after 18 hours of 750 μM paraquat treatment (a, d). Corresponding nuclei were stained with DAPI (b, e; merged signal: c, f).

C, D. Quantification of the results: plots for endogenous SRPK2 (upper panels) and transiently transfected HA-SRPK2 (bottom panels) showed an extremely significant increase in the nuclear fluorescence. Data represented the mean ± SEM of 50 cells for endogenous SRPK2, and 10 positive cells for transfected SRPK2. ***P < 0,0001 treated vs. control group by unpaired t-test.

Figure 2

Paraquat treatment induced change charged to SR proteins

A. Endogenous SC-35 and GFP-ASF showed a speckled-enlarged pattern in SH-SY5Y cells after 18 hours of 750 μM paraquat treatment (a, b, c, d). On the contrary, GFP-hRNPA1 did not redistribute in the cytoplasm and its intranuclear localization appeared the same after the drug treatment (e, f). Corresponding nuclei were stained with DAPI (merged signal: a', b', c', d', e', f').

B. Left Panel: phosphorylation of SR proteins before and after the drug treatment: we showed mAb104 Western Blot pattern of

typical SR proteins in response to 18 hours of 750 μM paraquat treatment. β-actin was probed as loading control.

Central panel: WB analysis to probe SR corresponding protein levels before and after the drug treatment. Signals corresponding to: 16H3 antibody (detecting the SRp75, SRp55, SRp40 proteins), anti-ASF/SF2 and anti SRp20.

Right Panel: WB analysis to probe principal hnRNP protein levels. Signals corresponding to: hnRNP A1, C1/C2, H and K/J antibodies.

C. Here we reported the plot representing the fold change of the phosphorylation-specific signal for each specific band after the drug treatment. Data represented mean ± SEM of 3 independent experiments.

Figure 3

The effect of paraquat treatment on splice site selection

A. Representative scheme of the well-characterized E1A minigene reporter system, with its alternative 5' selection sites.

B. Paraquat induced an E1A alternative splicing in SH-SY5Y transfected cells (2% agarose gel).

C. Quantification of the results from transfected SH-SY5Y cells (2100 Bioanalyzer, Agilent Technologies): we observed an increase of the 9S isoform ratio (left) as well as of the 9S band percentage (right) after 18 hours of 750 μM paraquat treatment. Data represented the mean ± SEM of 3 independent biological replicates each double repeated. **P < 0,001 and ***P < 0,0001 treated vs. control group by paired t-test.

Figure 4

SRPK2 became phosphorylated upon paraquat treatment

A. Western Blot analysis of SH-SY5Y protein extracts before and after 18 hours of 750 μM paraquat treatment showed a bands pair for SRPK2 signal (left). The upper band matched to a hyper-phosphorylated form, as the Calf Intestinal Phosphatase treatment of the same protein extracts confirmed (right).

B. Western Blot analysis of total, nuclear and cytoplasmic SH-SY5Y protein extracts before and after 18 hours of 750 μM paraquat, with they proper loading controls.

C. Quantification of the ratio between phosphorylated versus unphosphorylated SRPK2 in total, nuclear and cytoplasmic protein extracts before and after the treatment.

Figure 5

Mutational analysis of SRPK2

A. Schematic representation of SRPK2 domains organization. SRPK2 showed a Proline-rich region at the amino-terminal (instead of the SRPK1 basic region here acting as NLS). SRPK2 presented also a typical bipartite kinase domain separated by a SRPK2 specific spacer region, characterized by the presence of a basic region and an acidic domain.

B. Scheme of the mutants cloned and tested.

Figure 6

SRPK2 phosphorylation at the 581 amino-acidic residue is required for the nuclear translocation in SH-SY5Y cells

A. Intracellular localization of HA-tagged SRPK2 wild type and its mutants before and after 18 hours of 750 μM paraquat treatment. HA-SRPK2 (a, b) and HA-SRPK2K108R (Kinase Dead; c, d) translocated into the nucleus after the drug treatment. HA-SRPK2S581A (e, f) was unable to translocate, whereas HA-SRPK2A581D (g, h) translocated also in untreated cells. Endogenous phosphorylated SC-35 staining revealed a nuclear relocalization in cells overexpressing HA-SRPK2 (both before and after drug treatment; a', b'), also there was visible a decrease in SC-35 signal in cells overexpressing HA-SRPK2A581D (both before and after drug treatment; g', h'). No changes in SC-35 signal were observed in cell overexpressing HA-SRPK2K108R and HA-SRPK2S581A (c' and d'; e' and f'). Merged signal between HA-tagged proteins and both SC-35 signal (from a'' to h'') and DAPI staining was also reported (from a''' to h''').

B. Quantification of the nucleus / cytoplasm ratio (left plot) and of the nuclear fluorescence percentage signal (right plot). We observed an increase in the nuclear fluorescence of untreated HA-SRPK2A581D transfected cells and a decrease in the signal for the treated HA-SRPK2S581A transfected cells, compared respectively with the untreated and treated wild type transfected control. Data represented the mean ± SEM of 10 positive cells for each condition. ***P < 0,0001 of groups compared by one-way ANOVA and Turkey post-test analysis.

Figure 7

The effect of the SRPK2 (wild type and mutants) overexpression on splice site selection before and after 18 hours of 750 μM paraquat treatment

A. Impact of overexpressed SRPK2 wild type and mutants on E1A alternative splicing before and after the drug treatment (upper panel). SH-SY5Y were transfected with the same amount of plasmids-expressing proteins. These expressions were verified by Western Blot analysis (as shown in the two bottom panels). While the wild type and the kinase dead mutant had no per se effect on splice site selection, the S581A mutant interfered with the preferential proximal 9S choice after drug treatment, whereas the A581D mutant showed an increase of the same splice site selection already in the untreated sample.

B. Quantification of the results (2100 Bioanalyzer, Agilent Technologies): 9S isoform ratio (up) and percentage of 9S product (bottom) in the presence of the overexpressed proteins. We observed an extremely significant increase in both the ratio and the percentage of the 9S isoform in S581A mutant overexpressing cells before Paraquat treatment. We also observed a substantial decrease of the 9S isoform ratio and percentage in A581D overexpressing cells after the drug treatment. Data represented the mean ± SEM of 3 independent biological replicates each double repeated. ***P < 0,0001 of groups compared by repeated measures (matched) one-way ANOVA and Turkey post-test analysis.

Figure 8

Model of the SRPK2 mediated response after paraquat treatment

Effects observed on alternative splicing choice using an E1A minigene reporter system before (left half) and after (right half) paraquat treatment. SRPK2: SR protein Kinase 2; PQ: paraquat treatment; PPases: Protein Phosphatases; SR: SR Proteins unphosphorylated; SR-P: SR Proteins phosphorylated; K?: unknown kinase.

Table 1

Result obtained by Maldi-Tof MS analysis

FLAG tagged SRPK2 or the mock control were transfected in SH-SY5Y cells. The overexpressed proteins were immunoprecipitated and the immunoprecipitated samples were separated on a SDS-page, Coomassie stained and specific lanes were further analysed by mass spectrometric analysis as described.

Supplementary Figure S1

A. We screened the effect of 18 hours of 750 μM paraquat treatment on the intracellular localization for all the SRPK2 mutants obtained and transiently transfected in SH-SY5Y cells.

B. Table of the observed results summarized.

Supplementary Table T1

Primer sequences used in SRPK2 four oligos mutagenesis

Supplementary Table T2

SRPK2 mutagenesis: PCR amplification conditions

FIGURES AND TABLES

Figure 1

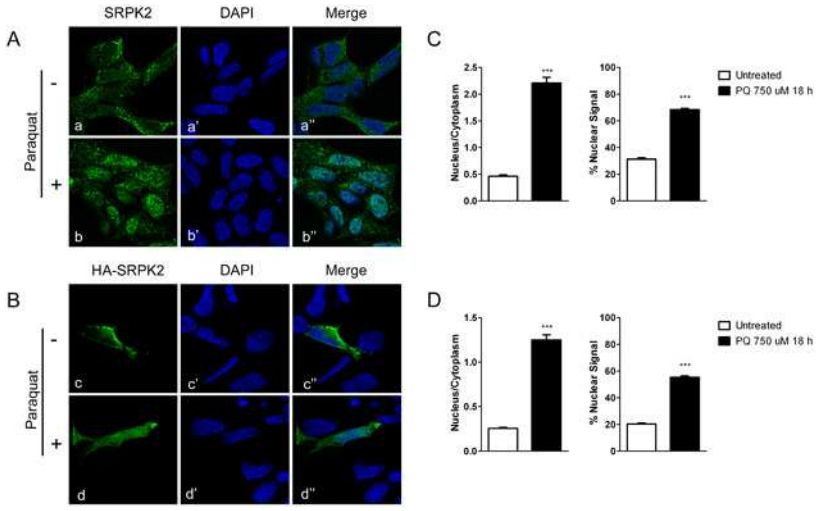

Figure 2

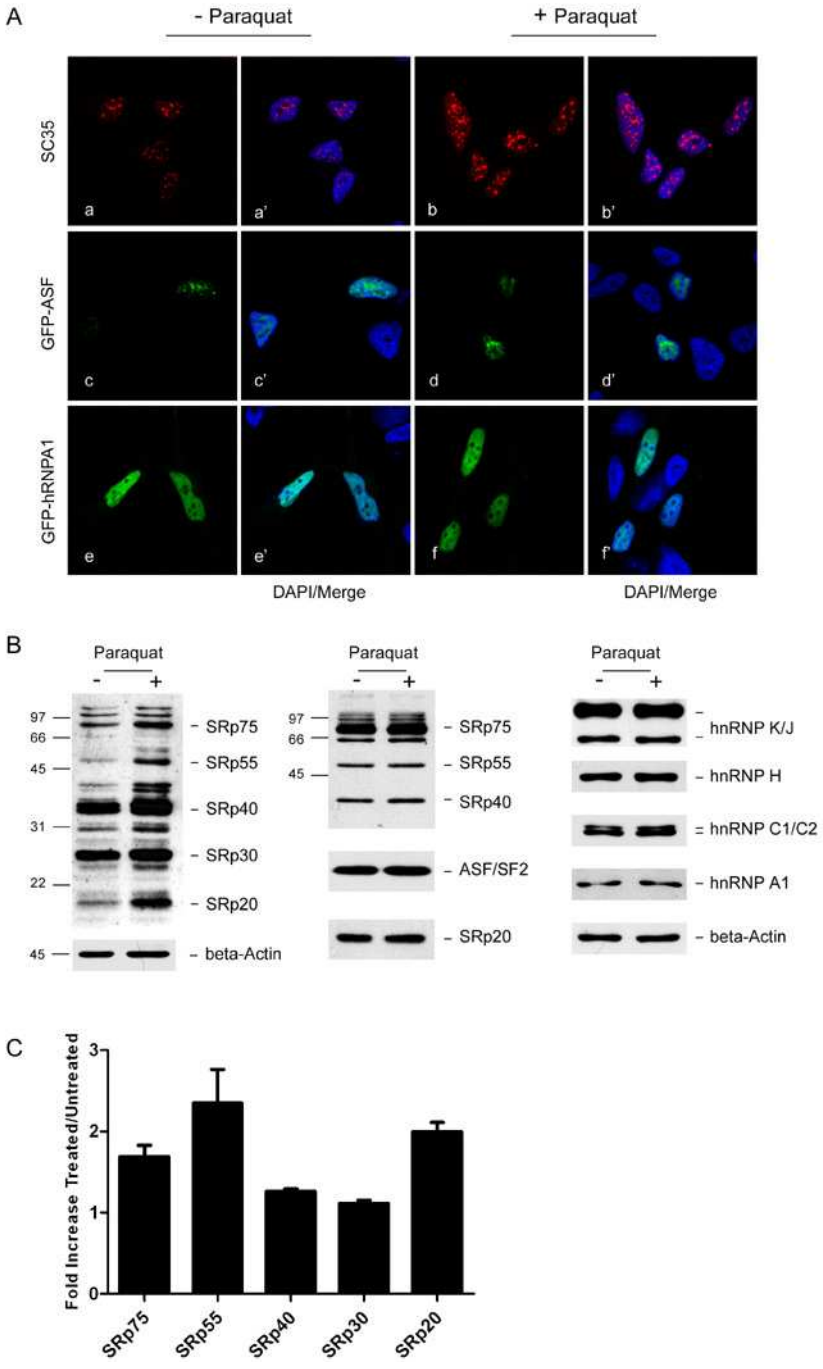
A
- Paraquat
+ Paraquat
SC35
GFP-ASF
GFP-hRNPA1
a
a'
b
b'
c
c'
d
d'
e
e'
f
f'
DAPI/Merge
DAPI/Merge
B
Paraquat
- +
97
66
45
31
22
45
SRp75
SRp55
SRp40
SRp30
SRp20
beta-Actin
ASF/SF2
hnRNP K/J
hnRNP H
hnRNP C1/C2
hnRNP A1
C
Fold Increase Treated/Untreated
0
1
2
3
SRp75
SRp55
SRp40
SRp30
SRp20

Figure 3

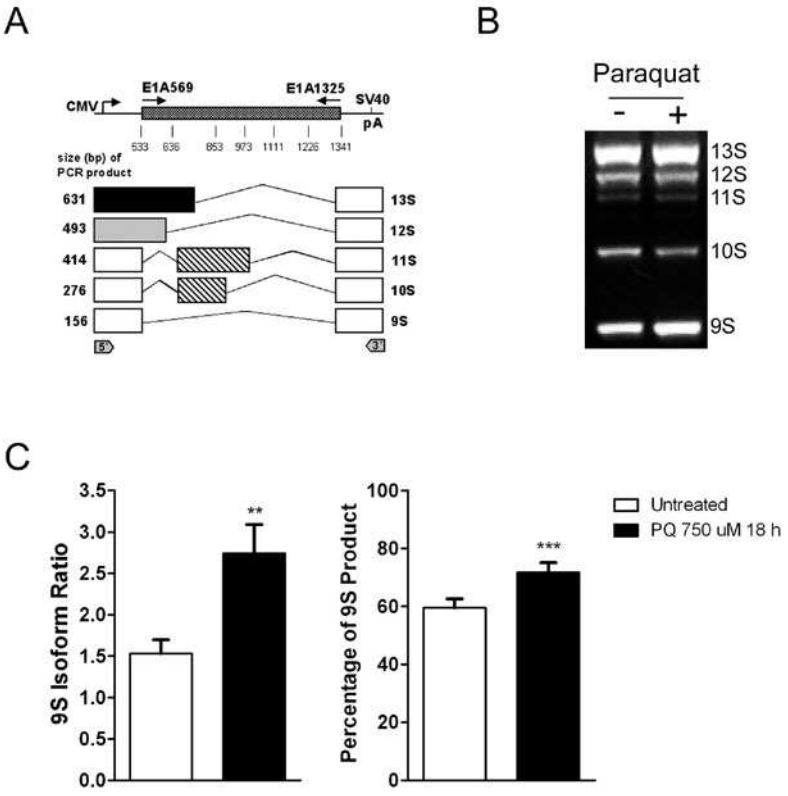
A
B
C
E1A569
E1A1325
SV40
CMV
pA
533
636
853
973
1111
1226
1341
size (bp) of PCR product
631
493
414
276
156
13S
12S
11S
10S
9S
5'
3'
Paraquat
-
+
13S
12S
11S
10S
9S
9S Isoform Ratio
3.5
3.0
2.5
2.0
1.5
1.0
0.5
0.0
**
Percentage of 9S Product
100
80
60
40
20
0
***
Untreated
PQ 750 uM 18 h

Figure 4

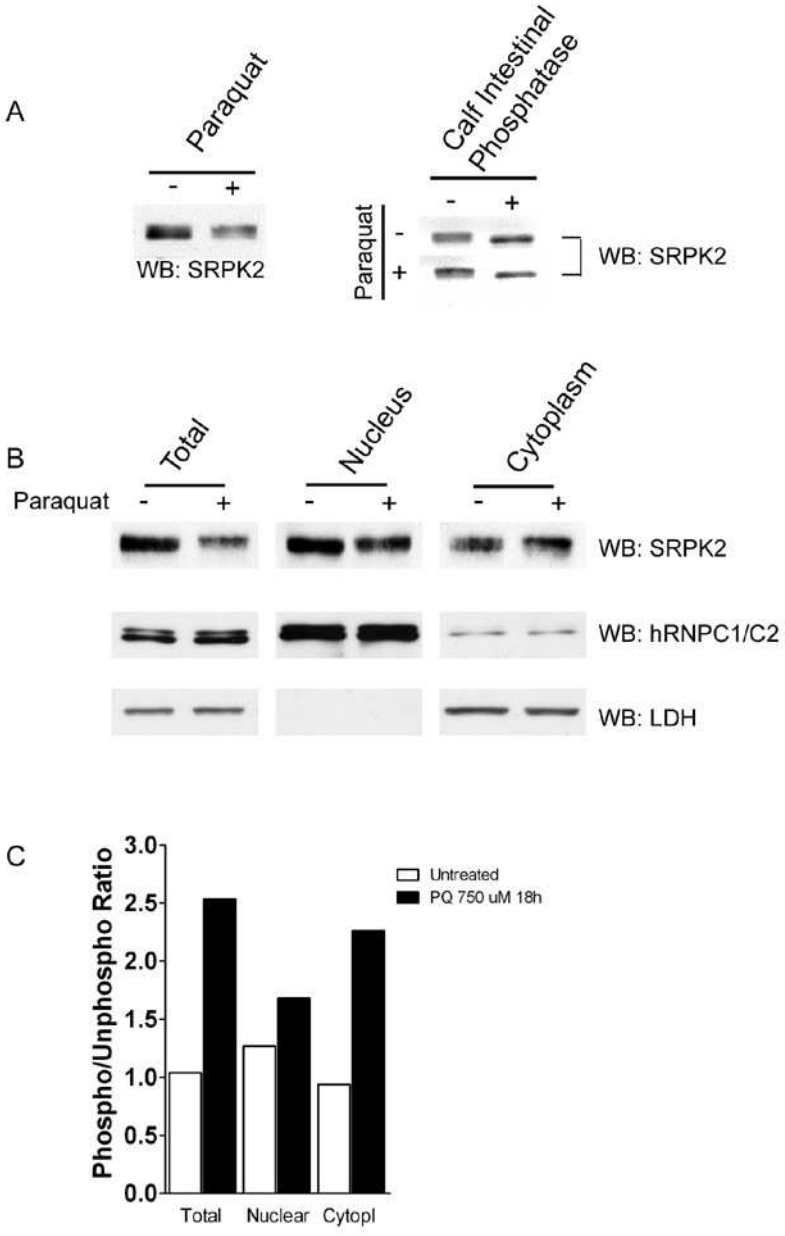
A
Paraquat
- +
WB: SRPK2
Calf Intestinal Phosphatase
- +
Paraquat
- +
WB: SRPK2
B
Total
Nucleus
Cytoplasm
Paraquat
- + - + - +
WB: SRPK2
WB: hRNPC1/C2
WB: LDH
C
Phospho/Unphospho Ratio
3.0
2.5
2.0
1.5
1.0
0.5
0.0
Untreated
PQ 750 uM 18h
Total
Nuclear
Cytopl

Figure 5

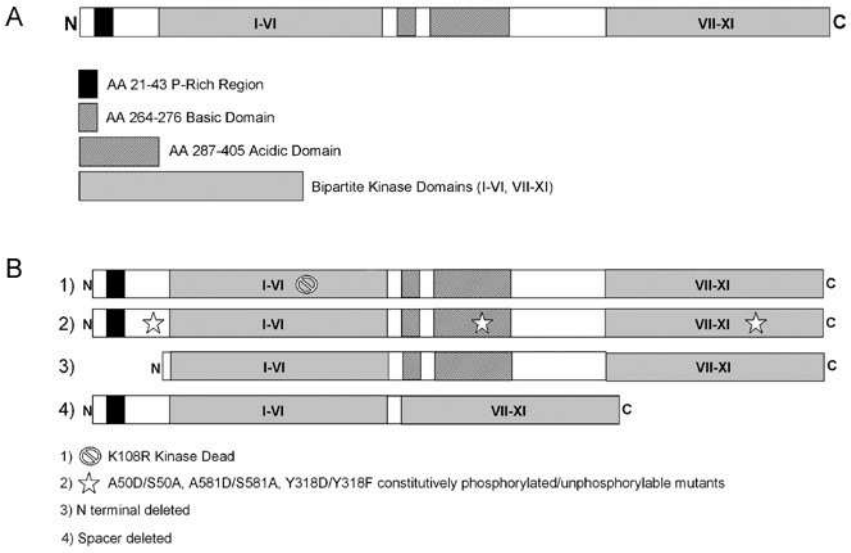
A
N
I-VI
VII-XI
C
AA 21-43 P-Rich Region
AA 264-276 Basic Domain
AA 287-405 Acidic Domain
Bipartite Kinase Domains (I-VI, VII-XI)
B
1) N
I-VI
VII-XI
C
2) N
I-VI
VII-XI
C
3)
N
I-VI
VII-XI
C
4) N
I-VI
VII-XI
C
1) K108R Kinase Dead
2) A50D/S50A, A581D/S581A, Y318D/Y318F constitutively phosphorylated/unphosphorylable mutants
3) N terminal deleted
4) Spacer deleted

Figure 6

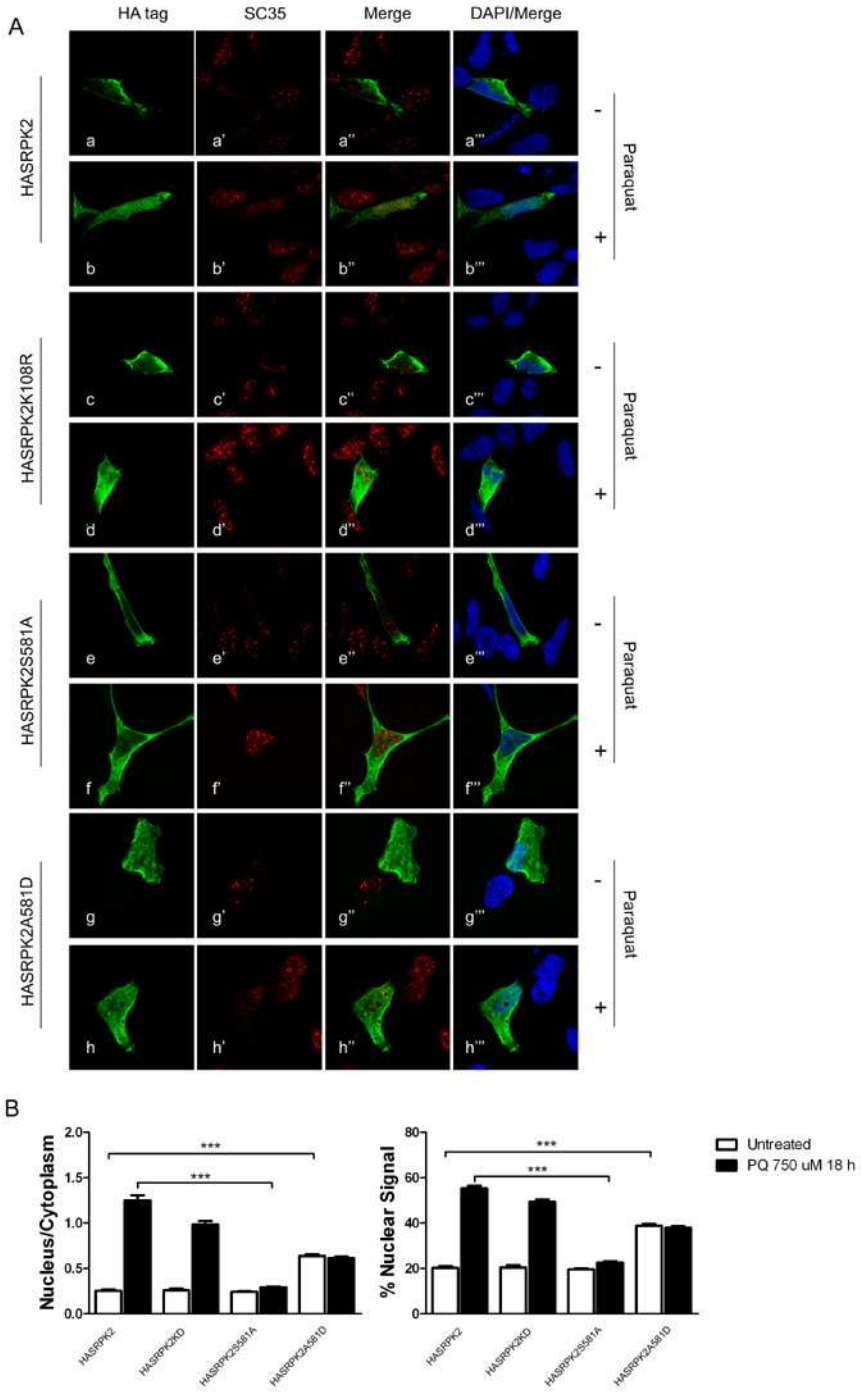
A
HA tag
SC35
Merge
DAPI/Merge
HASRPK2
HASRPK2K108R
HASRPK2S581A
HASRPK2A581D
Paraquat
-
+
B
Nucleus/Cytoplasm
% Nuclear Signal
***
Untreated
PQ 750 uM 18 h
HASRPK2
HASRPK2KD
HASRPK2S581A
HASRPK2A581D

Figure 7

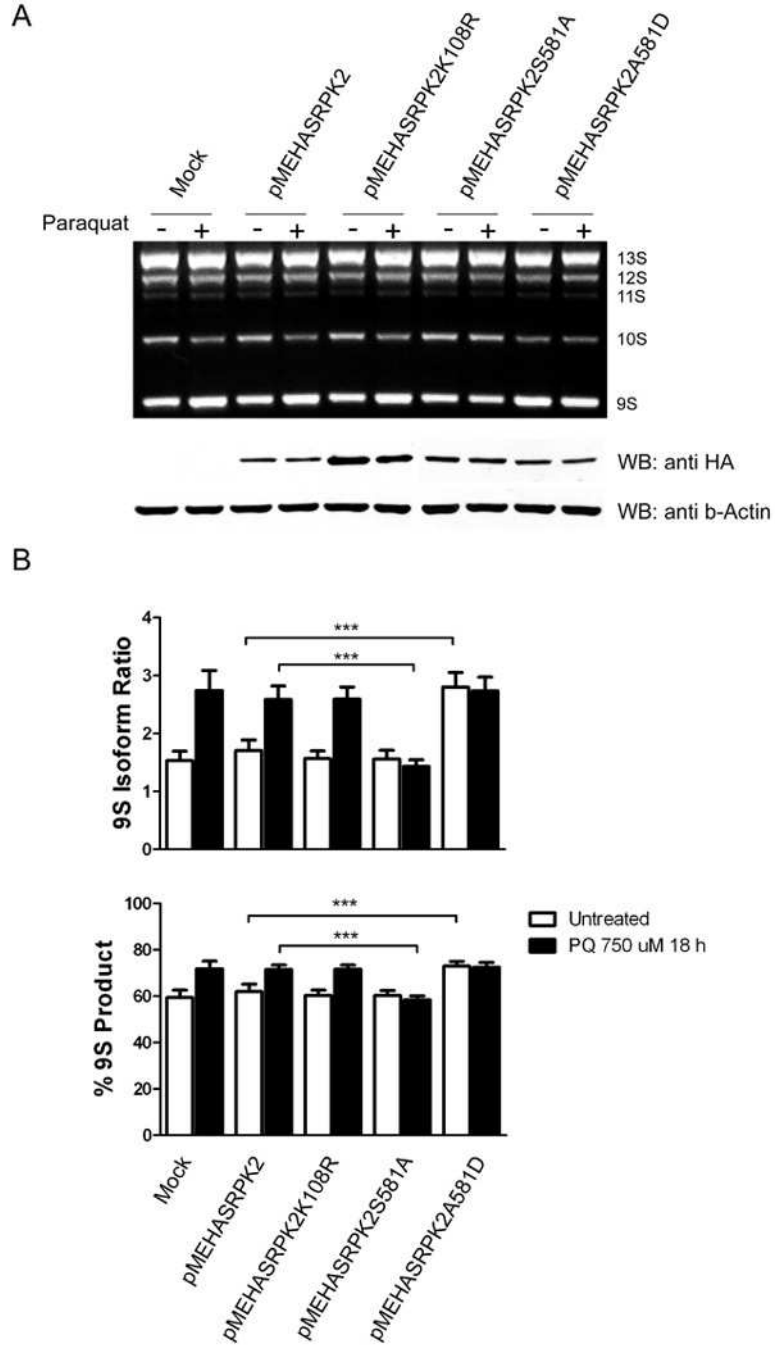
A
Mock
pMEHASRPK2
pMEHASRPK2K108R
pMEHASRPK2S581A
pMEHASRPK2A581D
Paraquat
- + - + - + - + - +
13S
12S
11S
10S
9S
WB: anti HA
WB: anti b-Actin
B
9S Isoform Ratio
% 9S Product
***
***
Untreated
PQ 750 uM 18 h
Mock
pMEHASRPK2
pMEHASRPK2K108R
pMEHASRPK2S581A
pMEHASRPK2A581D

Figure 8

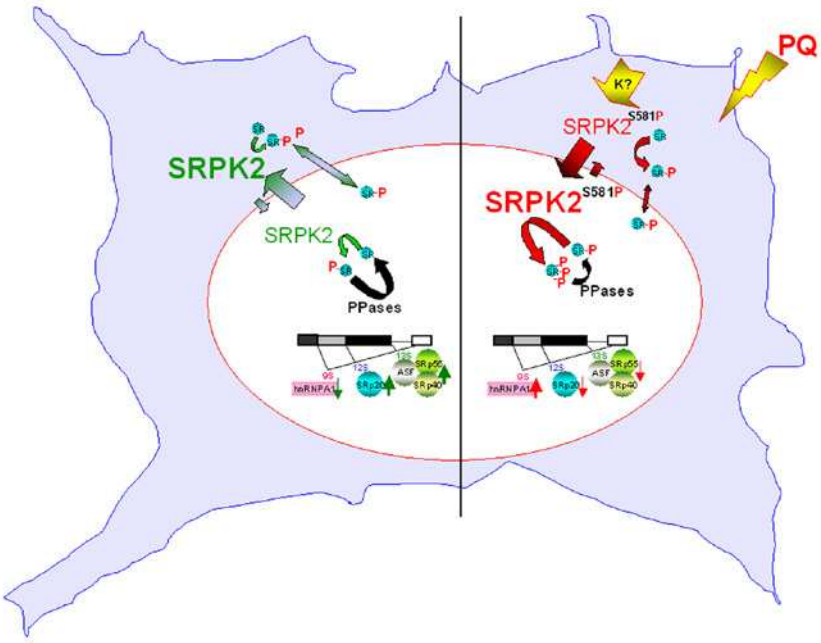

Table 1

Classical SR proteins	peptides
SFRS1, ASF/SF2	12
SFRS7, 9G8	7 + 5
SFRS5, SRp40	7
TRA2B	4

SR-related proteins	peptides
U2AF2, U2AF65	12
U1A	9
SNRNP70, U1-70K	7
ACIN1	7
CROP	5

Splicing factors	peptides
SNRPB	3
PRPF19	2
PRPF31	8
DDX50	2 + 6
DDX5	17
DDX17	7
DHX15	2 + 2

hnRNP proteins	peptides
HNRNPK	5
HNRNPF	5
HNRNPH1	5
HNRNPAB	13 + 10
HNRNPA3	7
HNRNPM	3
SYNCRIP	13
HNRNPR	7
HNRNPD	3

RNA binding proteins	peptides
IGF2BP1	15
IGF2BP3	7
FUS	3
RBM39	5
ILF3	13

Transcription/Replication	peptides
YBX-1	8
RFC4	3
THOC4	4

Ribosomal proteins and translation-related proteins	peptides
RPL4 60S	18 + 8
RPL7	21
RPS4X	20
RPL7A 60S	10 + 10
RPS3A 40S	19
RPS3 40S	18
RPL8 60S	11 + 6
RPS2 40S	15
MRPS22 28S	7
RPL10A	9
RPL13	5
EEF1A2	4

Heat shock proteins	peptides
HSP90AB1	7
HSP90AA1	5
HSPA8	23
HSPA1B	17
HSPD1	16 + 16

Proteins involved in DNA repair	peptides
XRCC5	14 + 11
XRCC6	19
PRPF19	3
YBX1	5 + 3
CROP	5 + 4
FUS	3

Figure S1

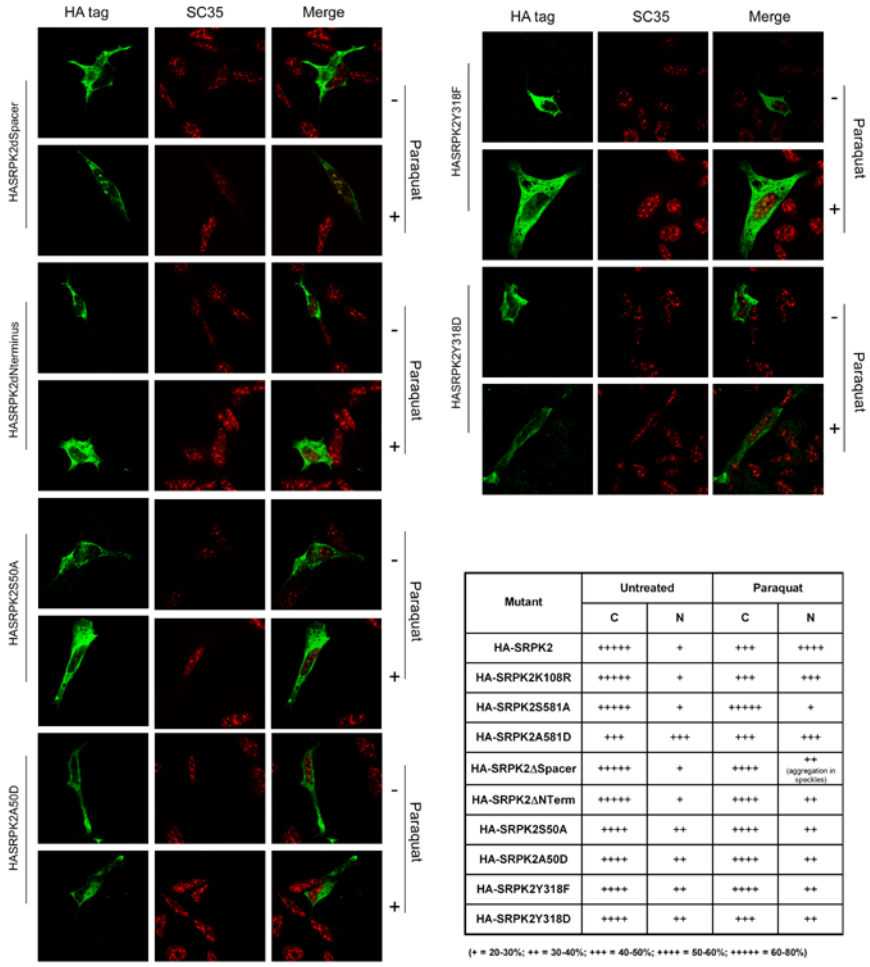

Mutant	Untreated		Paraquat	
	C	N	C	N
HA-SRPK2	+++++	+	+++	++++
HA-SRPK2K108R	+++++	+	+++	+++
HA-SRPK2S581A	+++++	+	+++++	+
HA-SRPK2A581D	+++	+++	+++	+++
HA-SRPK2ΔSpacer	+++++	+	++++	++ (aggregation in speckles)
HA-SRPK2ΔNTerm	+++++	+	++++	++
HA-SRPK2S50A	++++	++	++++	++
HA-SRPK2A50D	++++	++	++++	++
HA-SRPK2Y318F	++++	++	++++	++
HA-SRPK2Y318D	++++	++	+++	++

(+ = 20-30%; ++ = 30-40%; +++ = 40-50%; ++++ = 50-60%; +++++ = 60-80%)

Supplementary Table 1

Mutation	Primer Name	Primer sequence from 5' to 3' (Underlined is the degenerated nucleotide)
N term deleted	Nterm-FW	GTCGACGCGGCCGCGGAGATTCTGGGGTCAGATG
	HindIII-REV	CGGAAGCTTCTGCAGAGGT
K108R	S50-FW	GTCGACGCGGCCGCGATGTCAGTTAACTCTGAGAAGT
	HindIII-REV	CGGAAGCTTCTGCAGAGGT
	MutK108R-FW	GATTTGTTGCAATGAGAGTTGTAAAAAGTGCC
	MutK108R-REV	GGCACTTTTTACAACTCTCATTGCAACAAATC
S50A	S50-FW	GTCGACGCGGCCGCGATGTCAGTTAACTCTGAGAAGT
	HindIII-REV	CGGAAGCTTCTGCAGAGGT
	MutS50A-FW	GAGATTCTGGGGGGCAGATGATGAGGAGC
	MutS50A-REV	GTCCCTCATCATCTGCCCCCAGAATCTC
S581A	SacI-FW	TGGCATTTGAGCTCGCCAC
	SacII-REV	GGCCGCGGGAATTCGATTA
	MutS581A-FW	GTTCGAACCGCATGCTGGGGAAGACTATTC
	MutS581A-REV	GAATAGTCTTCCCCAGCATGCGGTTCGAAC
Y318F	Y318-FW	AGTTGCTGGAGAAACGCCTA
	Y318-REV	ACAAGCATTTCCCAGGTCAG
	MutY318F-FW	CAGGATGGAGAGTTCCAGCCGGAGGTGAC
	MutY318F-REV	CACCTCCGGCTGGACTCTCCATCCTGCCTC
Y318D	Y318-FW	AGTTGCTGGAGAAACGCCTA
	Y318-REV	ACAAGCATTTCCCAGGTCAG
	MutY318D-FW	CAGGATGGAGAGTGCCAGCCGGAGGTGAC
	MutY318D-REV	CACCTCCGGCTGGCCTCTCCATCCTGCTC
A50D	S50-FW	GTCGACGCGGCCGCGATGTCAGTTAACTCTGAGAAGT
	HindIII-REV	CGGAAGCTTCTGCAGAGGT
	MutA50D-FW	GAGATTCTGGGGGACGATGATGAGGAGCA
	MutA50D-REV	GCTCCTCATCATCGTCCCCCAGAATCTC
A581D	S50-FW	GTCGACGCGGCCGCGATGTCAGTTAACTCTGAGAAGT
	HindIII-REV	CGGAAGCTTCTGCAGAGGT
	MutA581D-FW	GTTCGAACCGCATGATGGGGAAGACTATTC

	MutA581D-REV	GAATAGTCTTCCCCATCATGCGGTTCGAAC

Supplementary Table 2

Mutation	PCR conditions
N term deleted	95℃ 5 min, (95℃ 30 sec, 57℃ 30 sec, 72℃ 1min) x 25 cycles, 72℃ 5 min
K108R	95℃ 5 min, (95℃ 30 sec, 54℃ 30 sec, 72℃ 1min) x 25 cycles, 72℃ 2 min
S50A	95℃ 5 min, (95℃ 30 sec, 54℃ 30 sec, 72℃ 1min) x 25 cycles, 72℃ 2 min
S581A	95℃ 5 min, (95℃ 30 sec, 56℃ 30 sec, 72℃ 30 sec) x 25 cycles, 72℃ 2 min
Y318F	95℃ 5 min, (95℃ 30 sec, 54℃ 30 sec, 72℃ 30 sec) x 25 cycles, 72℃ 2 min
Y318D	95℃ 5 min, (95℃ 30 sec, 54℃ 30 sec, 72℃ 30 sec) x 25 cycles, 72℃ 2 min
A50D	95℃ 5 min, (95℃ 30 sec, 54℃ 30 sec, 72℃ 1 min) x 25 cycles, 72℃ 2 min
A581D	95℃ 5 min, (95℃ 30 sec, 54℃ 30 sec, 72℃ 1 min) x 25 cycles, 72℃ 2 min

REFERENCES

1. Gallo, J.M., et al., *The role of RNA and RNA processing in neurodegeneration.* J Neurosci, 2005. **25**(45): p. 10372-5.
2. Melchiorri, D., et al., *Paraquat toxicity and oxidative damage. Reduction by melatonin.* Biochem Pharmacol, 1996. **51**(8): p. 1095-9.
3. Bonneh-Barkay, D., et al., *Redox cycling of the herbicide paraquat in microglial cultures.* Brain Res Mol Brain Res, 2005. **134**(1): p. 52-6.
4. Bishop, A.L., et al., *Phenotypic heterogeneity can enhance rare-cell survival in 'stress-sensitive' yeast populations.* Mol Microbiol, 2007. **63**(2): p. 507-20.
5. Bonilla, E., et al., *Paraquat-induced oxidative stress in drosophila melanogaster: effects of melatonin, glutathione, serotonin, minocycline, lipoic acid and ascorbic acid.* Neurochem Res, 2006. **31**(12): p. 1425-32.
6. Cicchetti, F., et al., *Systemic exposure to paraquat and maneb models early Parkinson's disease in young adult rats.* Neurobiol Dis, 2005. **20**(2): p. 360-71.
7. Maracchioni, A., et al., *Mitochondrial damage modulates alternative splicing in neuronal cells: implications for neurodegeneration.* J Neurochem, 2007. **100**(1): p. 142-53.

8. Senator, A., et al., *Prion protein protects against DNA damage induced by paraquat in cultured cells.* Free Radic Biol Med, 2004. **37**(8): p. 1224-30.
9. Dupiereux, I., et al., *Protective effect of prion protein via the N-terminal region in mediating a protective effect on paraquat-induced oxidative injury in neuronal cells.* J Neurosci Res, 2008. **86**(3): p. 653-9.
10. Gonzalez-Polo, R.A., et al., *Inhibition of paraquat-induced autophagy accelerates the apoptotic cell death in neuroblastoma SH-SY5Y cells.* Toxicol Sci, 2007. **97**(2): p. 448-58.
11. Moran, J.M., et al., *Identification of genes associated with paraquat-induced toxicity in SH-SY5Y cells by PCR array focused on apoptotic pathways.* J Toxicol Environ Health A, 2008. **71**(22): p. 1457-67.
12. Ortiz-Ortiz, M.A., et al., *Nitric oxide-mediated toxicity in paraquat-exposed SH-SY5Y cells: a protective role of 7-nitroindazole.* Neurotox Res, 2009. **16**(2): p. 160-73.
13. Yang, W. and E. Tiffany-Castiglioni, *Paraquat-induced apoptosis in human neuroblastoma SH-SY5Y cells: involvement of p53 and mitochondria.* J Toxicol Environ Health A, 2008. **71**(4): p. 289-99.
14. Yang, W., et al., *Paraquat activates the IRE1/ASK1/JNK cascade associated with apoptosis in human neuroblastoma SH-SY5Y cells.* Toxicol Lett, 2009. **191**(2-3): p. 203-10.

15. Lin, S. and X.D. Fu, *SR proteins and related factors in alternative splicing.* Adv Exp Med Biol, 2007. **623**: p. 107-22.
16. Fu, X.D., *The superfamily of arginine/serine-rich splicing factors.* RNA, 1995. **1**(7): p. 663-80.
17. Horowitz, D.S. and A.R. Krainer, *Mechanisms for selecting 5' splice sites in mammalian pre-mRNA splicing.* Trends Genet, 1994. **10**(3): p. 100-6.
18. Loomis, R.J., et al., *Chromatin binding of SRp20 and ASF/SF2 and dissociation from mitotic chromosomes is modulated by histone H3 serine 10 phosphorylation.* Mol Cell, 2009. **33**(4): p. 450-61.
19. Li, X. and J.L. Manley, *Inactivation of the SR protein splicing factor ASF/SF2 results in genomic instability.* Cell, 2005. **122**(3): p. 365-78.
20. Li, X. and J.L. Manley, *Cotranscriptional processes and their influence on genome stability.* Genes Dev, 2006. **20**(14): p. 1838-47.
21. Li, X., J. Wang, and J.L. Manley, *Loss of splicing factor ASF/SF2 induces G2 cell cycle arrest and apoptosis, but inhibits internucleosomal DNA fragmentation.* Genes Dev, 2005. **19**(22): p. 2705-14.
22. Zhong, X.Y., et al., *SR proteins in vertical integration of gene expression from transcription to RNA processing to translation.* Mol Cell, 2009. **35**(1): p. 1-10.

23. Xiao, R., et al., *Splicing regulator SC35 is essential for genomic stability and cell proliferation during mammalian organogenesis.* Mol Cell Biol, 2007. **27**(15): p. 5393-402.
24. Wang, J., Y. Takagaki, and J.L. Manley, *Targeted disruption of an essential vertebrate gene: ASF/SF2 is required for cell viability.* Genes Dev, 1996. **10**(20): p. 2588-99.
25. Lin, S., et al., *Dephosphorylation-dependent sorting of SR splicing factors during mRNP maturation.* Mol Cell, 2005. **20**(3): p. 413-25.
26. Ghigna, C., et al., *Altered expression of heterogenous nuclear ribonucleoproteins and SR factors in human colon adenocarcinomas.* Cancer Res, 1998. **58**(24): p. 5818-24.
27. Karni, R., et al., *The gene encoding the splicing factor SF2/ASF is a proto-oncogene.* Nat Struct Mol Biol, 2007. **14**(3): p. 185-93.
28. Pind, M.T. and P.H. Watson, *SR protein expression and CD44 splicing pattern in human breast tumours.* Breast Cancer Res Treat, 2003. **79**(1): p. 75-82.
29. Stickeler, E., et al., *Stage-specific changes in SR splicing factors and alternative splicing in mammary tumorigenesis.* Oncogene, 1999. **18**(24): p. 3574-82.
30. Sanford, J.R. and J.P. Bruzik, *Developmental regulation of SR protein phosphorylation and activity.* Genes Dev, 1999. **13**(12): p. 1513-8.

31. Lareau, L.F., et al., *Unproductive splicing of SR genes associated with highly conserved and ultraconserved DNA elements.* Nature, 2007. **446**(7138): p. 926-9.
32. Lai, M.C., R.I. Lin, and W.Y. Tarn, *Transportin-SR2 mediates nuclear import of phosphorylated SR proteins.* Proc Natl Acad Sci U S A, 2001. **98**(18): p. 10154-9.
33. Xiao, S.H. and J.L. Manley, *Phosphorylation of the ASF/SF2 RS domain affects both protein-protein and protein-RNA interactions and is necessary for splicing.* Genes Dev, 1997. **11**(3): p. 334-44.
34. Mermoud, J.E., P.T. Cohen, and A.I. Lamond, *Regulation of mammalian spliceosome assembly by a protein phosphorylation mechanism.* EMBO J, 1994. **13**(23): p. 5679-88.
35. Huang, Y., T.A. Yario, and J.A. Steitz, *A molecular link between SR protein dephosphorylation and mRNA export.* Proc Natl Acad Sci U S A, 2004. **101**(26): p. 9666-70.
36. Prasad, J., et al., *The protein kinase Clk/Sty directly modulates SR protein activity: both hyper- and hypophosphorylation inhibit splicing.* Mol Cell Biol, 1999. **19**(10): p. 6991-7000.
37. Mathew, R., et al., *Phosphorylation of human PRP28 by SRPK2 is required for integration of the U4/U6-U5 tri-snRNP into the spliceosome.* Nat Struct Mol Biol, 2008. **15**(5): p. 435-43.

38. Ding, J.H., et al., *Regulated cellular partitioning of SR protein-specific kinases in mammalian cells.* Mol Biol Cell, 2006. **17**(2): p. 876-85.
39. Wang, H.Y., et al., *SRPK2: a differentially expressed SR protein-specific kinase involved in mediating the interaction and localization of pre-mRNA splicing factors in mammalian cells.* J Cell Biol, 1998. **140**(4): p. 737-50.
40. Zhong, X.Y., et al., *Regulation of SR protein phosphorylation and alternative splicing by modulating kinetic interactions of SRPK1 with molecular chaperones.* Genes Dev, 2009. **23**(4): p. 482-95.
41. Jang, S.W., et al., *Interaction of Akt-phosphorylated SRPK2 with 14-3-3 mediates cell cycle and cell death in neurons.* J Biol Chem, 2009. **284**(36): p. 24512-25.
42. Bedford, M.T., D.C. Chan, and P. Leder, *FBP WW domains and the Abl SH3 domain bind to a specific class of proline-rich ligands.* EMBO J, 1997. **16**(9): p. 2376-83.
43. Chan, D.C., M.T. Bedford, and P. Leder, *Formin binding proteins bear WWP/WW domains that bind proline-rich peptides and functionally resemble SH3 domains.* EMBO J, 1996. **15**(5): p. 1045-54.
44. Sudol, M., *Structure and function of the WW domain.* Prog Biophys Mol Biol, 1996. **65**(1-2): p. 113-32.
45. Kuroyanagi, N., et al., *Novel SR-protein-specific kinase, SRPK2, disassembles nuclear speckles.* Biochem Biophys Res Commun, 1998. **242**(2): p. 357-64.

46. Roth, M.B., A.M. Zahler, and J.A. Stolk, *A conserved family of nuclear phosphoproteins localized to sites of polymerase II transcription.* J Cell Biol, 1991. **115**(3): p. 587-96.
47. Shevchenko, A.K., *[Blood-sucking diptera (Diptera, Nematocera) of the left-bank Polesie in the Ukraine].* Med Parazitol (Mosk), 1966. **35**(1): p. 28-32.
48. Zhang, W. and B.T. Chait, *ProFound: an expert system for protein identification using mass spectrometric peptide mapping information.* Anal Chem, 2000. **72**(11): p. 2482-9.
49. Takeuchi, M. and M. Yanagida, *A mitotic role for a novel fission yeast protein kinase dsk1 with cell cycle stage dependent phosphorylation and localization.* Mol Biol Cell, 1993. **4**(3): p. 247-60.
50. Gui, J.F., W.S. Lane, and X.D. Fu, *A serine kinase regulates intracellular localization of splicing factors in the cell cycle.* Nature, 1994. **369**(6482): p. 678-82.
51. Fu, X.D., et al., *General splicing factors SF2 and SC35 have equivalent activities in vitro, and both affect alternative 5' and 3' splice site selection.* Proc Natl Acad Sci U S A, 1992. **89**(23): p. 11224-8.
52. Guil, S., J.C. Long, and J.F. Caceres, *hnRNP A1 relocalization to the stress granules reflects a role in the stress response.* Mol Cell Biol, 2006. **26**(15): p. 5744-58.

53. Zahler, A.M., et al., *SR proteins: a conserved family of pre-mRNA splicing factors.* Genes Dev, 1992. **6**(5): p. 837-47.
54. Stoss, O., et al., *The in vivo minigene approach to analyze tissue-specific splicing.* Brain Res Brain Res Protoc, 1999. **4**(3): p. 383-94.
55. van der Houven van Oordt, W., et al., *The MKK(3/6)-p38-signaling cascade alters the subcellular distribution of hnRNP A1 and modulates alternative splicing regulation.* J Cell Biol, 2000. **149**(2): p. 307-16.
56. Amanchy, R., et al., *A curated compendium of phosphorylation motifs.* Nat Biotechnol, 2007. **25**(3): p. 285-6.
57. Mylonis, I. and T. Giannakouros, *Protein kinase CK2 phosphorylates and activates the SR protein-specific kinase 1.* Biochem Biophys Res Commun, 2003. **301**(3): p. 650-6.
58. Yomoda, J., et al., *Combination of Clk family kinase and SRp75 modulates alternative splicing of Adenovirus E1A.* Genes Cells, 2008. **13**(3): p. 233-44.
59. Cao, W., S.F. Jamison, and M.A. Garcia-Blanco, *Both phosphorylation and dephosphorylation of ASF/SF2 are required for pre-mRNA splicing in vitro.* RNA, 1997. **3**(12): p. 1456-67.
60. Shi, Y. and J.L. Manley, *A complex signaling pathway regulates SRp38 phosphorylation and pre-mRNA*

splicing in response to heat shock. Mol Cell, 2007. **28**(1): p. 79-90.

61. Lamond, A.I. and D.L. Spector, *Nuclear speckles: a model for nuclear organelles.* Nat Rev Mol Cell Biol, 2003. **4**(8): p. 605-12.
62. Huang, S. and D.L. Spector, *Dynamic organization of pre-mRNA splicing factors.* J Cell Biochem, 1996. **62**(2): p. 191-7.

Chapter 3

Mol Biol Cell 20(24): 5211-23, 2009

Mammalian pre-mRNA 3' end processing factor CF I_m68 functions in mRNA export

Marc-David Ruepp[2#], Chiara Aringhieri[1#], Silvia Vivarelli[1], Stefano Cardinale[1,3], Simona Paro[14], Daniel Schümperli[2], and Silvia M.L. Barabino[1*]

[1]Department of Biotechnology and Biosciences, University of Milano-Bicocca, Piazza della Scienza, 2, I-20126 Milano, Italy

[2]Institute of Cell Biology, University of Bern, CH-3012 Bern, Switzerland

[3]Present address: Lawrence Berkeley National Laboratory, 1 Cyclotron Road, Mailstop Stanley 922, Berkeley, CA 94720.

[4]Present address: Medical Research Council Human Genetics Unit, Western General Hospital, Edinburgh EH4 2XU, Scotland, UK

#Both authors contributed equally to the work.

*Correspondence to: Silvia M.L. Barabino, Department of Biotechnology and Biosciences, University of Milano-Bicocca, Piazza della Scienza, 2; I-20126 Milano, Italy; Phone: +39-02-6448 3352; Fax: +39-02-6448 3569; Email: silvia.barabino@unimib.it

ABSTRACT

Export of mRNA from the nucleus is linked to proper processing and packaging into ribonucleoprotein complexes. Although several observations indicate a coupling between mRNA 3' end formation and export, it is not known how these two processes are mechanistically connected. Here, we show that a subunit of the mammalian pre-mRNA 3' end processing complex, CF I_m68, stimulates mRNA export. CF I_m68 shuttles between the nucleus and the cytoplasm in a transcription-dependent manner and interacts with the mRNA export receptor NXF1/TAP. Consistent with the idea that CF I_m68 may act as a novel adaptor for NXF1/TAP, we show that CF I_m68 promotes the export of a reporter mRNA as well as of endogenous mRNAs while silencing by RNAi results in the accumulation of mRNAs in the nucleus. Moreover, CF I_m68 associates with 80S ribosomes but not polysomes, suggesting that it is part of the mRNP that is remodelled in the cytoplasm during the initial stages of translation. These results reveal a novel function for the pre-mRNA 3' end processing factor CF I_m68 in mRNA export.

INTRODUCTION

The removal of introns by splicing as well as cleavage and polyadenylation at the 3' end of RNA polymerase II primary transcripts (pre-mRNAs) are usually required before they can be exported from the nucleus as mature mRNAs (Erkmann and Kutay, 2004). This observation has suggested that transport factors interact with the RNA during pre-mRNA processing. Indeed, recent discoveries have lent support to this hypothesis. The splicing reaction deposits on the mRNA a specific subset of proteins called the Exon Junction Complex (EJC, for review see Tange et al., 2004). REF, a component of the EJC, facilitates mRNA export by interacting with the mRNA export factor NXF1 (also called TAP, for review, see Reed and Hurt, 2002). NXF1 was originally identified as the export receptor for type D retroviral RNAs that associate with NXF1 through a sequence-specific interaction with the constitutive transport element (CTE). However, NXF1 recruitment on cellular mRNAs requires adaptor proteins such as Aly/REF (hereafter named REF). In yeast Mex67 (the homolog of NXF1) is recruited by Yra1 (homolog of REF), which is also essential for the export of poly(A) RNA in *S. cerevisiae*. In contrast in metazoans, REF is dispensable for bulk mRNA export. This raises the possibility that multiple and partially redundant adaptor proteins may be responsible for the recruitment of NXF1. Indeed, spliceosomal proteins, including U2AF35 (Zolotukhin et al., 2002) and some members of the SR family of splicing factors, were shown to

interact with NXF1 and act as adaptors for NXF1-dependent export of poly(A) mRNAs (Huang and Steitz, 2001; Huang *et al.*, 2003; Lai and Tarn, 2004; Hargous *et al.*, 2006; Tintaru *et al.*, 2007).

Several observations have linked 3' end cleavage and polyadenylation to mRNA export (for review see, Zhao et al., 1999). For example, RNA polymerase II reporter transcripts lacking a polyadenylation signal are retained in the nucleus of yeast cells. Positioning a transcribed poly(A) tract at the end of an mRNA by ribozyme cleavage does not result in efficient nuclear export, indicating that the 3' end processing reaction itself, and not simply the presence of the poly(A) tail, is required for nuclear export (Huang and Carmichael, 1996). Moreover, the NS1A protein of influenza A virus specifically inhibits export of cellular but not viral mRNAs by targeting two essential components of the pre-mRNA 3' end processing machinery (Nemeroff et al., 1998). Although three yeast polyadenylation factors, Hrp1/Nab4, Nab2, and Pab1 (Kessler *et al.*, 1997; Hector *et al.*, 2002; Brune *et al.*, 2005), and the mammalian nuclear poly(A) tail binding protein (PABPN1, Calado et al., 2000), are nucleocytoplasmic shuttling proteins, to date there is no evidence for a direct role of 3' end processing factors in mRNA export.

The mature 3' ends of most eukaryotic mRNAs are generated by endonucleolytic cleavage of the primary transcript followed by the addition of a poly(A) tail to the upstream cleavage product (for reviews see Zhao *et al.*, 1999; Gilmartin,

2005). Cleavage Factor I_m (CF I_m) is a component of the 3' end processing complex that participates in the cleavage reaction. CFI_m is a heterodimer comprised of a small subunit of 25 kDa and a large subunit of 59, 68, or 72 kDa (Rüegsegger et al., 1998). The 25 and 68 kDa subunits have been shown to be sufficient to reconstitute CFI_m activity for poly(A) site cleavage *in vitro* upon addition to partially purified 3' processing factors (Rüegsegger et al., 1998). Both subunits contact the RNA substrate, as demonstrated by UV cross-linking studies (Rügsegger et al., 1996). The structure of the CFI_m 68 kDa subunit is strikingly similar to that of the SR family of proteins that play an essential role in basal and regulated pre-mRNA splicing (reviewed by Graveley, 2000). The 68 kDa protein possesses an N-terminal RNP-type RNA recognition motif (RRM) and an RS-like C-terminal region enriched in RS/D/E dipeptides that is reminiscent of the RS domain of SR proteins. The RS-like domain of CF I_m 68 kDa subunit is sufficient for the localization in nuclear speckles (and in the nucleoplasm) and mediates the interaction in vitro with a subset of shuttling SR proteins (Dettwiler *et al.*, 2004; Cardinale *et al.*, 2007).

Here, we demonstrate that CF I_m68 is a nucleocytoplasmic shuttling protein that can stimulate mRNA export. First, we show that CF I_m68 is associated with components of the EJC. Second, we establish that CF I_m68 interacts with the mRNA export factor NXF1. Finally, we demonstrate that CF I_m68 is directly involved in mRNA export. While CF I_m68 can stimulate export when tethered to a

luciferase reporter mRNA and its overexpression results in an increase of endogenous mRNAs in the cytoplasmic fraction, RNAi-mediated silencing leads to the retention of polyadenylated transcripts in the nucleus. Furthermore, we show by sucrose gradient centrifugation that CF I_m68 cosediments with the 80S ribosome particle. CF I_m68 is a well-established component of the pre-mRNA 3' end processing complex. Our data showing that CF I_m68 is part of the mature mRNP particles and contributes to their export to the cytoplasm, highlight a novel function for CF I_m68 and provide a link between pre-mRNA 3' end formation and mRNA export.

MATERIALS AND METODS

Oligonucleotides , Plasmids, Antibodies

Sequences for real-time RT–PCR probes, description of plasmids and antibodies are presented in Supplemental Material.

Cell Culture and Heterokaryon Assay

HeLa and HEK293 cells were cultured in DMEM supplemented with 10% FBS and transfected using Effectene Transfection Reagent (Qiagen) or Escort V (Sigma) according to the manufacturer's instructions. Drug treatments were carried as follows: Actinomycin D treatment (5 µg/ml, Sigma) B for 2 hr or Leptomycin (25 µg/ml, Sigma) for 1h in DMEM, followed by fixation and fluorescence microscopy.

For heterokaryon nucleocytoplasmic shuttling assays, HeLa cells were transiently transfected with different vectors as described. 24 hours post transfection, an equal number of HeLa cells were seeded onto the same coverslip as NIH3T3 cells. The cells were incubated for 3 h in the presence of 50 µg/ml cycloheximide and for 30 min in the presence of 100 µg/ml cycloheximide before fusion. Cell fusions were done as described (Pinol-Roma and Dreyfuss, 1992). Heterokaryons were incubated further for 2 hr in media containing 100 µg/ml cycloheximide before fixation.

Immunoprecipitations

After transfection, HEK293 cells were washed and harvested. For the immunoprecipitations of Flag-hUpf3b complexes, 8 x

100 mm dishes of transfected cells were used for each assay. The pellets were quickly frozen in liquid nitrogen, thawed, and resuspended in lysis buffer (50 mM Tris HCl pH 8; 150 mM NaCl; 1% NP40; 1X protease inhibitor cocktail (PIC, Roche) and then incubated on ice for 1 h with occasional shaking. For the coimmunoprecipitation of HA-CF I_m68 with either Flag-CF I_m25 or Flag-NXF1, cells were lysed in high salt lysis buffer (50 mM Tris-HCl pH 8,0, 250 mM NaCl, 1% NP40). The samples were then centrifuged at 15.000 rcf for 15 min at 4°C and the supernatants collected. RNase A digestion (200 ug/ml, Roche) was performed for 30 min at 30°C.

Flag-tagged proteins were immunoprecipitated from the precleared, RNase A treated-cell lysate with M2 anti-Flag agarose (Sigma) at 4° C for 2 hr on a rotator wheel in IP150 buffer (10mM $MgCl_2$; 10% NP40; 150 mM NaCl). Then samples were centrifuged at 10'600 g for 10 min at 4°C and washed five times with 500 µl of IP150 or IP250 buffer. Precipitated proteins were eluted either with SDS-sample buffer or M2 peptide and analyzed by Western blotting. Detection was performed with an ECL detection kit (Amersham).

GST-fusion protein purification and GST-Pull Down Assays

To study protein–protein interactions in vitro, GST fusion proteins were expressed in *E. coli* BL21(DE3)LysS or BL21(DE3) RIPL transformed with pGEX-derived plasmids encoding GST (negative control) or GST-fusions with CFI_m25, NXF1, or NXF1-202. After purification over Glutathione Sepharose 4B beads (GE Healthcare), GST-CFI_m25 and GST-

NXF1 were further purified by gel filtration over a Superdex 75 column (GE Healthcare).

GST pull-down assays with hexahistidine-tagged CF I_m68 were performed as follows:

The purified GST-fusions were coupled to glutathione sepharose 4B beads, by using equimolar amounts of either GST-CF I_m25 or GST-NXF1 (1.5 µg and 3 µg respectively) and 3 µg of GST as negative control. The beads and proteins were incubated in phosphate-buffered saline (PBS, 137 mM NaCl, 2.7 mM KCl, 10 mM Na_2HPO_4, 2 mM KH_2PO_4) supplemented with 0.1% NP-40 (PBS/NP-40) at 4°C for 1.5 h with gentle agitation on a wheel, followed by the addition of 400 ng histidine-tagged CF I_m68 and incubation for 1.5 hours at 4°C. Subsequently, the beads were washed with PBS/NP-40 and the bound material was analysed by SDS–PAGE and subsequent western blotting. As input 1/5th of the added recombinant CF I_m68 was loaded on the gel. His-CF I_m68 was detected by incubation of the blot with a mouse monoclonal anti-His antibody (HIS1, Sigma) and a species-specific Horse-Raddish Peroxidase coupled antibody (Promega) and developped by the enhanced chemilumenescence method (ECL-Plus, GE Healthcare). To visualise the boud recombinant GST-fusions the membrane was stained with Coomassie Brilliant Blue R-250.

GST-Pull down assays with *in vitro* translated proteins were performed as follows: The purified GST-fusions were coupled to glutathione sepharose 4B beads (GE Healthcare) in PBS/NP-40

for one hour and subsequently incubated with RNAse treated [^{35}S]-methionine labelled proteins obtained by coupled *in vitro* transcription/translation in rabbit reticulocyte lysate (TNT T7 kit, Promega). For non-radioactive *in vitro* translation, methionine was added to a final concentration of 20-30 µM. The samples were incubated in PBS supplemented with 0.1% NP-40 at 4°C for 2 hours with gentle agitation. Subsequently beads were washed with PBS/NP-40 (NP-40 concentration increased to 1%) and input and bound fraction were analysed by SDS-PAGE and detected on a storm 820 Phosphorimager (Amersham).

Tethered mRNA export assay

Assays were carried out as described in (Hargous et al., 2006; Tintaru et al., 2007) with the exception that *renilla* luciferase rather than ß-galactosidase was used for the normalization of transfection efficiency. For each transfection, 700 ng of each of the plasmids encoding the MS2-protein, 50 ng of luc-RRE firefly construct, and 5 ng of pRL-TK, a thymidine kinase renilla luciferase control vector, were co-transfected in 24-well plates. Detection of luciferase activity was performed with the Dual-luciferase Reporter Assay System (Promega) according to the manufacturer's instruction. Luminescence measurements were performed by using a Berthold luminometer. Four independent sets of transfections were carried out in triplicate with two different plasmids preparations. The average normalized luciferase activity in all the experiments was calculated and expressed as percentage of the activity measured for REF.

For analysis of the tethering experiments on the RNA-level, 1.4 x 10^6 HeLa cells were transfected with 10 µg MS2 fusion plasmid and 500 ng of pLucSalRRE-6MS2 using Dreamfect (OZ Biosciences). The cells were harvested 48 h after transfection. Nuclei were isolated as described below and RNA was prepared by using an "Absolutely RNA RT-PCR Miniprep Kit" (Stratagene). 1 µg RNA was reverse transcribed with random hexamers and StrataScript 6.0 reverse transcriptase (Stratagene) according to the manufacturer's protocol. Real-time RT-PCR was performed as described below.

FISH

For the visualisation of the luciferase reporter RNA, the FISH probes were 390 nt biotinylated antisense RNA molecules transcribed in vitro from pRRE-Luc linearized with *Eco*RV with the BioArray™ HighYield™ RNA Transcript Labeling Kit (Enzo Life Sciences). HeLa cells were transiently transfected with pLUCRRE6MS2 reporter alone or cotransfected with pCNMS2CFI$_m$68GFP, pCNMS2GFP, pCNMS2TAP, pCNMS2REF, or pCNMS2REFmut, respectively. After 30 h, the cells were fixed and FISH was performed according to standard protocols. Briefly, cells were incubated in pre-hybridization buffer (2 x SSC, 20% Formamide, 0.2% BSA 1µg/µl tRNA) for 30 min at 37°C, and then in hybridization solution (2 x SSC, 20% Formamide, 0.2% BSA, 10% Dextran Sulphate, 1 µg/µl tRNA) in the presence of the biotinylated RNA probe (50ng/slide) for 3 h at 37°C. Stringent washes were performed in order to wash out unlabelled probe (twice with 2 x SSC +

20% Formamide, twice with 2 x SSC, once with 1 x SSC for 15 min at 45°C, once with 0.5 x SSC for 15 min at 45°C, once with 0.5 x SSC + 0.3% NP-40 for 2 min at 72°C, once with 2 x SSC + 0.1%NP-40 for 1 min at RT, and once with 2 x SSC for 10 min at RT,). After a pre-incubation wash with 4 x SSC + 0.1% Triton X-100 for 5 min at RT, the FISH probe was revealed with 3 µg/mL of Streptavidin-APC conjugate (BD Bioscience) diluted in 4 x SSC, 1%BSA for 1 h at RT. Finally, cells were stained with DAPI and mounted with FluorSave reagent (Calbiochem). Images were collected with a Leica TCS SP2 AOBS confocal microscope and by using LSC software. 12-bit images were acquired by using the same setting parameters for all the samples (gain, offset); for each field, five different xy sections along the z axis were acquired. FISH quantification was carried out with the same LCS software. Measurements of the FISH probe were obtained for the nuclear fluorescence (Sn), the total cell fluorescence (Sc), the area of the nucleus (An), and area of the cell (Ac). The cytoplasmic (C') amount of mRNA was calculated as: C'=1 - [(An Sn)/(Ac Sc)]. C/N ratios were calculated as C/N=C'/(1 – C') (for reference see Valencia et al., 2008).

For the visualisation of poly(A)+ RNA, HeLa cells were grown in 6-well plates on coverslips and transfected with the different plasmids, as indicated. Seven days past transfection, the cells were washed two times in phosphate buffered saline (PBS, 137 mM NaCl, 2.7 mM KCl, 10 mM Na_2HPO_4, 2 mM KH_2PO_4) before they were fixed for 10 minutes at room temperature in

3.7% paraformaldehyde (PFA). After a wash in PBS for 5 min, the cells were permeabilized for 10 min with 100% methanol, followed by a 10 min incubation in 70% ethanol, and a 5 min incubation in 1M Tris pH 8.0. The cells were then blocked for 30 min at 40°C in pre-warmed prehybridisation solution (2 x SSC, 20% formamide, 0.2% BSA, 1µg/µl tRNA in DEPC-H_2O). Pre-warmed hybridisation solution (2 x SSC, 20% formamide, 10% dextran sulfate, 0.2% BSA, 1µg/µl tRNA, 1ng/µl Cy3-labelled oligo-$(dT)_{50}$ in DEPC-H_2O) was added to the coverslips and incubated at 37°C for two h. Next, the cells were washed twice with pre-warmed 2 x SSC and 20% formamide in PBS, twice with pre-warmed 2 x SSC in PBS for 5 min each at 42°C and once in 1 x SSC in PBS for 5 min at RT. Before the coverslips were mounted (Mowiol 4-88, Calbiochem, containing 0.25 ug DAPI/ml), they were washed three times for 5 min in PBS.

RNA interference

HeLa cells stably transfected transfected with pcDNA3-ßglobin cDNA were transfected either with two siRNAs against CF I_m68 or NXF1 (Silencer® Select Pre-Designed & Validated siRNA, Applied Byosystems) at 25 nM concentration each or a non-targeting siRNA control at 50 nM concentration, by using Lullaby reagent (OZ Biosciences) according to the manufacturer's instructions. After splitting, cells were subjected to a second round of transfection with 50% of the amount of siRNAs indicated above. Cells depleted from CF I_m68 were harvested four days after the first transfection for analysis,

whereas cells depleted from NXF1 were harvested 48 hours post transfection.

Real-time PCR analysis

For the analysis of the nuclear and cytoplasmic distribution of mRNAs, HeLa cells were cotransfected with pSUPuro constructs or pcDNA3-HA-derived plasmids containing a puromycin selection marker by using Dreamfect (Oz Biosciences). Culturing the cells in the presence of 1.5 µg/ml puromycin eliminated untransfected cells. Three days after transfection cells were harvested.

Nuclear-cytoplasmic fractionations of HeLa cells were performed as described elsewhere (Carneiro and Schibler, 1984), except that RNase A treatment was omitted. From each fraction, 20 µl aliquots were taken for Western blot analysis. Subsequently RNA was isolated by using TRI-Reagent (Molecular Research Center), and DNA contamination was removed by using Turbo DNA-free (Ambion). 2 µg of total RNA from each fraction was reverse transcribed with Stratascript reverse transcriptase (Stratagene) according to the manufacturer's instruction. cDNA corresponding to 40 ng RNA was amplified with specific primers and TaqMan probes in an ABI SDS7000 Sequence Detection System. The relative mRNA levels of the cytoplasmic and nuclear fractions were normalized to 18S rRNA levels. The RT-PCR for X-ist and MIC 2a was performed in 50 µl 1x Fast Start Master Mix (Roche) supplemented with 400 nM f.c. of each primer pair, and 38 cycles were performed.

Polysome profile

Sucrose gradient fractionation was performed as described in (Sanford et al., 2004). Briefly, HEK293 cells were cotransfected with plasmids expressing HA-CF I_m68 and T7-ASF. After 24 h cells were washed and collected by short centrifugation at 4.000 rpm at 4°C and resuspended cold lysis buffer (100 mM NaCl; 10 mM $MgCl_2$; 30 mM Tris HCl pH 7,5; 1mM DTT; 0,05% Triton-X100) containing 100 µg/ml cycloheximide, RNase and protease inhibitors. After 5 minutes on ice, the extract was centrifuged for 4 min at 12.000 g at 4°C to pellet nuclei and debris. For negative controls, extracts were treated prior to sucrose gradient analysis either with 30 mM EDTA for 10 min at 4°C on a rotator wheel, followed by the addition of 2□g RNase A (Roche) and further incubation for 30' at 30°C, or with 20 mM puromycin for 1 hour at 4°C on a rotator wheel. Supernatants were resolved on 15-50% sucrose gradients prepared in (100 mM NaCl; 10 mM $MgCl_2$; 10 mM Tris HCl pH 7.5). The gradient was centrifuged at 4°C at 38,000 rpm in a Beckman SW41 rotor for 3 h. Following centrifugation, fractions were collected from the bottom, precipitated with TCA and analysed by immunoblotting.

Online supplemental material

Supplemental File 1: Legends to Supplemental Figures S1 to S8.

Supplemental File 2: Supplemental methods.

Supplemental Figure S1: CF I_m is imported into the nucleus as a heterodimer.

Supplemental Figure S2: Nucleocytoplasmic shuttling is an active process.

Supplemental Figure S3: Western blot analysis of HEK293 cell extracts used in the mRNA export assay.

Supplemental Figure S4: Western blot assessing the purity of the nuclear fractions used in the experiments shown in Figure 6D and 7E.

Supplemental Figure S5: NXF1 depletion increases nuclear levels of ß-globin mRNA.

Supplemental Figure S6: Sucrose gradient fractionation of puromycin-treated extracts.

Supplemental Figure S7: colour version of Figure 1.

Supplemental Figure S8: colour version of Figure 2.

RESULTS

CF I_m large subunits are nucleocytoplasmic shuttling proteins

We reported previously that the 68 kDa subunit of CF I_m interacts with a subset of SR proteins that were shown to shuttle continuously between the nucleus and the cytoplasm (Dettwiler et al., 2004). In addition, the 25 kDa subunit interacts with PABPN1, which is a nucleocytoplasmic shuttling protein (Calado et al., 2000). On the base of these observations we wished to test whether also the CF I_m subunits shuttle between the nucleus and the cytoplasm. We analyzed their migration in an interspecies heterokaryon fusion assay. HeLa cells expressing HA-tagged CF I_m68 were fused to mouse NIH3T3 cells in the presence of cycloheximide to produce heterokaryons. Shuttling of HA-CF I_m68 would lead to its equilibration into the nuclei of fused NIH3T3 cells. As a control, HeLa cells were cotransfected with a plasmid expressing GFP-hnRNP A1, a well-known shuttling protein, or GFP-hnRNP C, a protein that is always restricted to the nucleus (Pinol-Roma et al., 1988). In a representative heterokaryon, two hours after fusion, HA-CF I_m68 and GFP-hnRNP A1 were present both in the two HeLa cell nuclei and in the mouse cell nucleus (Figure 1A, upper row). In contrast, GFP–hnRNP C was restricted, as expected, to the HeLa cell nucleus (Figure 1A, bottom row). Quantitative analysis showed that NIH3T3 nuclei were positive for HA-CF I_m68 in all of the 51 heterokaryons examined. Thus,

although CF I_m68 is nuclear at steady state, it is continuously traversing the nuclear envelope. A similar assay was performed with HeLa cells expressing either GFP-CF I_m59 or GFP-CF I_m25. As shown in Figure 1B, while CF I_m59 can efficiently migrate into the mouse nucleus (Figure 1B, upper row), shuttling of CF I_m25 is less efficient (Figure 1B, lower row). A possible explanation for the observed, inefficient migration of CF I_m25 into the mouse nucleus could be that this subunit is not able to shuttle on its own and may be imported into the nucleus only in association with one of the endogenous larger polypeptides. Therefore, if GFP-CF I_m25 is overexpressed but the endogenous large subunits are limiting, this may result in poor nuclear import of GFP-CF I_m25. Cotransfection experiments with CFP-CF I_m68 and YFP-CF I_m25 constructs in which both ORFs are expressed under the same strong promoter (so that the two CF I_m subunits should be present in the cell in almost equimolar amounts and could therefore efficiently dimerize) demonstrated that, under these conditions, the CF I_m 25 kDa subunit is imported into nucleus more efficiently, in agreement with the explanation proposed above (Supplemental Figure S1).

In order to identify the region involved in the export of CF I_m68, we analyzed the shuttling behaviour of various domain deletion mutants fused to GFP (68ΔN, 68ΔRS, 68RS, 68RRM/RS, depicted in Supplemental Figure S2, (Dettwiler et al., 2004) at 37°C or, in addition, at 4°C to check for passive diffusion. The rationale for this assay is that, at 4°C, both

receptor-mediated nuclear import and export are blocked, whereas passive diffusion continues to occur. Temperature shift experiments were performed as described in (Michael et al., 1995). As shown in Supplemental Figure S2, all the mutants were able to shuttle at 37°C but were restricted to the HeLa cell nucleus at 4°C.

Nuclear export of CF I_m68 is CRM1-independent and requires active transcription

The most common mechanism for the nuclear export of proteins in eukaryotic cells is based on CRM1-dependent systems. CRM1-mediated export is specifically blocked in the presence of the fungal metabolite leptomycin B (LMB), which inhibits the formation of the ternary complex between CRM1, Ran-GTP, and the cargo protein. To check whether CRM1 is responsible for CF I_m68 nuclear export, heterokaryon assays were thus performed the presence of LMB. HeLa cells treated in this way were transfected with plasmids expressing HA-CF I_m68 in combination with GFP-. HMGB1, a protein that requires CRM1 for export (Figure 2A). Treatment with LMB specifically restricted HMGB1 to the HeLa cell nucleus. while CF I_m68 could still be efficiently exported thus indicating that its export does not require CRM1.

Previous studies have shown that CF I_m is an RNA-binding factor (Rüegsegger et al., 1996). CF I_m68 contacts the RNA mainly via the charged C-terminal domain while the RRM is primarily involved in protein interactions with the small subunit

(Dettwiler et al., 2004). Therefore, it is possible that CF I_m68 is leaving the nucleus by "piggy-backing" on RNA molecules being exported by other factors, either in association with the 25 kDa subunit or because of a direct interaction via the C-terminal domain. To determine whether shuttling of CF I_m68 depends on mRNA synthesis, we performed heterokaryon assays in the presence of actinomycin D. As shown in Figure 2B, GFP-CF I_m68 shuttling is blocked in presence of the transcription inhibitor, while relocalization of the protein in cap-like structures around the nucleoli of the human cell can be observed, as previously described (Cardinale et al., 2007), Figure 2B, panel b'). Although we can not formally rule out the possibility that actinomycin D could affect the synthesis of a short-lived protein required for export, the most likely conclusion of these experiments is that CF I_m68 shuttling is dependent on mRNA synthesis and possibly export. Therefore, based on this observation, we began to investigate a possible involvement of CF I_m68 in mRNA export.

CF I_m68 interacts with the mRNA export factor NXF1

The EJC, which is deposited on the mRNA by the splicing reaction, consists of four core components (Y14, Magoh, MLN51, and eIFAIII) and several more peripherally associated proteins (for review see Tange et al., 2004). Complexed proteins include the splicing factors SRm160, RNPS1, Acinus, SAP18 and Pinin, the mRNA export factors UAP56, Aly/REF, and NXF1 and the NMD factor Upf3b. To determine if CF I_m68

may be present in post-splicing complexes, Upf3b-containing mRNPs were immunopurified from extracts of HEK293 cells transiently transfected with Flag–tagged hUpf3b and analyzed by Western blotting with antibodies against EJC proteins, hnRNP proteins, and with anti-CF I_m68 antiserum (Figure 3A). Since several of these factors, including CF I_m, can bind RNA, extracts were treated with RNase A before immunoprecipitation to test for true protein:protein interactions. RNase treatment was shown to be effective by the disappearance of ß-actin mRNA as revealed by RT-PCR (Figure 3A, left panel). Consistent with previous reports, CBP80, NXF1, REF and Magoh coimmunopurified with Flag-hUpf3b (Figure 3A, right panel, Kim et al., 2001; Lejeune et al., 2002; Singh et al., 2007). In addition to these proteins, CF I_m68 can also be detected in Upf3b-containing mRNPs even in the presence of RNaseA, suggesting that it must interact with at least one of the non-RNA components of the complex. As expected, hnRNPA1, which is an abundant component of heterogeneous nuclear RNP (hnRNP) complexes but not of post-splicing complexes (Kim et al., 2001), is not present in the pellet of the coimmunoprecipitation.

Since export of CF I_m68 is not mediated by CRM1 but instead requires mRNA transcription, we asked whether NXF1 might be the export receptor for CF I_m68. Control Flag–tagged CF I_m25, -NXF1, -Upf1, -Upf3b, or the empty Flag vector alone were transiently coexpressed with HA-tagged CF I_m68 in HEK293 cells. Interaction with CF I_m68 was analyzed by

immunoprecipitation of the cell lysates with anti-Flag antibodies in the presence of RNase A followed by Western blotting with anti–CF I_m68 antiserum. The expression level of Flag-NXF1 was significantly lower than that of the other Flag-tagged proteins, and especially of Flag-Upf1 (Figure 3B, input, compare lanes 4 and 5). Nevertheless, the amount of CF I_m68 associated with Flag-NXF1 was far greater than that obtained with either Flag-Upf3b or Flag alone, and equivalent to the amount coprecipitated with Flag-Upf1 (pellet, compare lanes 8 to 11). These results suggest that CF I_m68 interacts specifically with NXF1 *in vivo*, and possibly also with Upf1. Thus, to determine if the interaction between CF I_m68 and NXF1 is a direct one, we performed GST-pull down experiments with purified recombinant proteins. *E. coli*–expressed GST, control GST-CF I_m25 or GST-NXF1 were incubated with purified baculovirus-expressed, histidine-tagged CF I_m68. Bound proteins were analyzed by Western blotting using anti-histidine (Figure 3C). Since GST–NXF1 coprecipitated equivalent amount of CF I_m68 to that coprecipitated by CF I_m25 (compare lanes 2 and 3), we conclude that CF I_m68 interacts specifically with the mRNA export factor NXF1.

We next aimed to identify the region in CF I_m68 responsible for the interaction with NXF1. We tested the interaction by coimmunoprecipitation of Flag-tagged NXF1 with GFP-fusions of wild type and mutant CF I_m68 that were co-expressed in HEK293 cells (Figure 4B). Tested mutants included a deletion of the N-terminal portion of CFI_m68, a region that contains the

RRM and was shown to bind the 25 kDa subunit (68ΔN), a deletion of the entire RS-like region at the C-terminus (68ΔRS), the RS-like domain alone (68RS), and a fusion of the RRM and the RS domains (68RRM/RS). As shown in Figure 4B Flag-NXF1 precipitated the fragments 68RRM/RS and 68ΔRS. Deletion of the N-terminal portion impaired the interaction with NXF1 while the RS-like domain appeared to interact with NXF1 albeit very inefficiently. Similar results were obtained in GST pull down experiments in which recombinant GST-CF I_m68 truncations were incubated with Flag-NXF1 expressed in HEK293 cells (data not shown).

To confirm the requirement of the N-terminal region of CF I_m68 for the direct interaction with NXF1, in vitro binding assays were performed. Glutathione beads pre-bound with GST or GST-NXF1 were incubated with [^{35}S]-labeled CF I_m68 or 68ΔN. Bound fractions were resolved and visualized by autoradiography. As shown in Figure 4C, only the full length protein, but not the N-terminally deleted one, bound NXF1, indicating that the NXF1 interaction region lies within the first 213 amino acids of CF I_m68.

NXF1 can be functionally divided into three domains (Figure 5A, Izaurralde, 2002): the N-terminal half (aa 1–372) interacts with REF (Stutz et al., 2000); the region between aa 371-551 binds the essential export cofactor p15 (Katahira *et al.*, 1999; Guzik *et al.*, 2001; Izaurralde, 2002); the C-terminal domain interacts with components of the NPC (Bachi et al., 2000). Shuttling SR proteins interact with the same domain of NXF1 that binds REF

(Huang et al., 2003). To determine if CF I_m68 and SR proteins bind the same domain of NXF1, glutathione beads loaded with GST or GST-NXF1 were individually incubated with in vitro translated, [^{35}S]-labelled HA-tagged CF I_m68 or 68ΔN. As shown in Figure 5B only full-length NXF1, but not the first 202 aa, which bind shuttling SR proteins (Huang et al., 2003 and data not shown), interacts with CF I_m68.

We previously demonstrated that the C-terminal charged domain of CF I_m68 interacts with shuttling SR proteins (Dettwiler et al., 2004). Thus, we tested whether the C-terminal region of CF I_m68 may mediate the formation of a ternary complex between SR proteins and NXF1. In the presence of the SR protein hTra2ß, GST-NXF1 can indeed efficiently select [^{35}S]-labeled 68ΔN, which on its own did not bind NXF1 (compare Figures 4C and 5C).

CF I_m68 stimulates mRNA export

To test if CF I_m68 may contribute to general mRNA export through the interaction with the receptor protein NXF1 (as is the case for REF and some SR proteins), we used a recently described, tethered mRNA export assay (Hargous et al., 2006). In this assay, an mRNA export factor is expressed as a fusion protein with a bacteriophage MS2 coat protein tag and then artificially tethered to a reporter RNA, containing the luciferase ORF and six MS2 coat protein binding sites within an inefficiently spliced intron (Figure 6A). The binding of the export factor leads to the nuclear export of the unspliced RNA that

would otherwise be retained in the nucleus, resulting in the expression of luciferase activity. We therefore checked whether tethering CF I_m68 protein in this way would promote export of the reporter RNA. Vectors expressing the different MS2 fusion proteins were transfected into HEK293 cells together with the luciferase reporter construct. Cotransfection of a third vector encoding *renilla* luciferase was used to control the transfection efficiency. As controls, MS2 fusions of GFP, NXF1, REF and REF-RRM (aa71-155, Hargous et al., 2006) were tested in the same experiments. As seen in Figure 6B, direct tethering of NXF1 resulted in a very strong luciferase activity. Importantly, tethering of CF I_m68 led to a luciferase expression that was about 10 times lower than that elicited by NXF1, but still higher than that of REF. As expected, REF-RRM did not stimulate export of the RNA Control experiments revealed that all the MS2 fusion proteins were expressed (Western blot; Supplemental Figure S3) and correctly localized to the cell nucleus (immunofluorescence microscopy, data not shown).

Mutant CF I_m68 proteins were also tested by this assay. Deletion of the N-terminal domain (68ΔN) that is necessary for the direct interaction with NXF1 in vitro did not significantly affect mRNA export, most likely because the protein can still interact with NXF1 via SR protein(s) bound to the C-terminus (see above). In contrast, the deletion of 2/3 of the C-terminal RS motif (68ΔC) strongly reduced luciferase expression. However, because this fragment is known to be imported into the nucleus inefficiently (Dettwiler et al., 2004) this result must

be interpreted with caution. In further control experiments, the 30 kDa and the 73 kDa subunits of the cleavage and polyadenylation specificity factor CPSF had no effect when tethered to the reporter RNA (Figure 6B and data not shown, respectively).

The assay described above relies on the measurement of luciferase enzymatic activity and thus requires mRNA translation. To rule out that CF I_m68 might affect the translation efficiency rather than RNA export, we sought to measure directly nuclear and cytoplasmic mRNA levels in the presence of varying amounts of CF I_m68. First, steady state pRRE-Luc mRNA levels were visualized by fluorescent in situ hybridization (FISH; Figure 6C). Quantitation of FISH images for individual cells revealed that the cytoplasmic to nuclear (C/N) ratio of the FISH signal was ~1 for the GFP control, 2,28 for GFP-CF I_m68 and 3,54 for NXF1 (Figure 6D). Additionally, we carried out quantitative reverse-transcription PCR (qPCR) analysis of the relative amount of luciferase mRNA in the nuclear fractions of cells transfected with different MS2-fusion constructs (Figure 6E). Quantitation of the relative nuclear luciferase RNA levels showed that tethering of MS2-CF I_m68 decreased the amount of transcript in the nucleus by approximately 2.5 fold compared to MS2-REF while the two CF I_m68 deletion mutants (68ΔN and 68ΔC) were less effective in promoting mRNA export. The nuclear fractions were devoid of cytoplasmic contaminations as shown by Western blot analyses for lamin A/C (nuclear) and tyrosine tubulin (cytoplasmic; Supplemental Figure S4). Taken

together, these experiments indicate that tethering of CF I_m68 can promote mRNA export.

To further characterize this new function of CF I_m68, we investigated the effect of its overexpression on the export of endogenous mRNAs. HeLa cells were transfected with a selectable plasmid driving CF I_m68 expression under the CMV promoter, and the nucleo-cytoplasmic distribution of polyadenylated RNAs was examined by FISH with a Cy3-labelled oligo(dT) probe (Figure 7A). In cells overexpressing CF I_m68, a slight but appreciable reduction of the amount of nuclear polyadenylated RNA could be observed. In order to analyse the effect of CF I_m68 overexpression on the nucleocytoplasmic transport of specific mRNAs, nuclear and cytoplasmic fractions were prepared, and RNA was isolated from these extracts. Reverse-transcription PCR for the nuclear X-inactivation specific (X-ist) mRNA revealed that no nuclear RNA had leaked into the cytoplasmic fractions (Figure 7B). The amounts of four different mRNAs were then measured by qPCR. They are shown in Figure 7C as relative values normalised to the amounts of the same transcripts measured in cells overexpressing HA-EGFP. Importantly, the nuclear concentration of each of these transcripts was reduced two to three fold, whereas cytoplasmic levels were increased for three of them, with the exception of ß-actin. Nevertheless, even for ß-actin mRNA, the cytoplasmic to nuclear ratio increased approximately 2.2 fold compared to the control, indicating that

CF I_m68 overexpression stimulates mRNA export also in this case.

We also determined the effect of CF I_m68 depletion on mRNA export. Silencing experiments were performed in HeLa cells stably transfected with the ß-globin gene lacking natural introns and therefore expressing cDNA transcripts that do not undergo splicing (Valencia et al., 2008). The assay was validated by depleting NXF1. Two days after transfection of specific siRNAs or of a control siRNA, mRNA levels were analyzed by real-time reverse transcription PCR. NXF1 mRNA was reduced by ≈ 92% compared to control siRNA-treated cells, and, as a consequencce, the level of the nuclear ß-globin mRNA was increased ~2.5 times (Supplemental Figure S5). In the case of CF I_m68, four days after transfection of two specific siRNAs, CF I_m68 mRNA was reduced by ≈ 93% compared to control siRNA-treated cells, whereas the level of the mRNA of the closely related 59 kDa subunit remained unchanged (data not shown). Western blot analysis (Figure 7D) confirmed that the level of the remaining CF I_m68 protein was below detection. Importantly, this silencing of CF I_m68 resulted in a small but statistically significant increase in the nuclear level of ß–globin mRNA (Figure 7E). As above, the purity of these nuclear fractions was assessed by Western blot analyses for lamin A/C and tyrosine tubulin (Supplemental Figure S4). This result supports the idea that CF I_m68 may act in mRNA export, similarly to SR proteins and/or REF, by contributing to the recruitment of NXF1 to the mRNA.

Another variable that could potentially affect the nucleocytoplasmic distribution of mRNAs is inefficient 3' end processing that would lead to nuclear retention of the unprocessed transcript. However, CF I_m68 depletion did not significantly affect the 3' end processing efficiency of neither endogenous ß-actin pre-mRNA (Figure 7F) nor of the ß-globin cDNA transcript, which has the strong polyadenylation signal of bovine growth hormone (BGH, data not shown).

In summary, the above experiments indicate a relevant biological role for CF I_m68 in the export of mRNAs.

CF I_m68 cosediments with ribosomal particles

Some of the components of the EJC, including REF and NXF1, dissociate from the mRNA upon entry into the cytoplasm (Le Hir et al., 2001). Therefore, it is possible that CF I_m68 is present in the mRNPs in the nucleus but may then dissociate during or shortly after mRNA export. To gain insight into the remodelling of CF I_m68–containing mRNPs after export, cytoplasmic fractions of HEK293 cells were fractionated across 15%-50% sucrose gradients, and the distribution of CF I_m68 was determined by Western blotting. Figure 8A shows that most of the cytoplasmic CF I_m68 was found in lighter complexes at the top of the gradient. However, CF I_m68 could also be detected in the 80S (monosome) region, although to a lesser extent than ASF/SF2. CF I_m68 distribution correlated with that of the nuclear cap-binding complex component CBP80 (Figure 8B). Treatment of cytoplasmic extracts with RNaseA, which induces

dissociation of mono- and polyribosomes into ribosomal subunits, led to a redistribution of CF I_m68, SF2/ASF and rpS6 to the top of the gradient (Figure 8C). Likewise, we found that cosedimentation of CF I_m68 with 80S particles was sensitive to EDTA (data not shown). In contrast, treatment with puromycin, which causes premature termination and thus the disassembly of translating heavy polysomes and an increase of the 80S peak (Sabatini et al., 1971), did not affect CF I_m68 distribution (Supplemental Figure S6). We conclude that CF I_m68 is not associated with translating ribosomes but, like CBP80 and PABP2, is part of the mRNP particle that is remodelled in the cytoplasm during the initial stages of translation when nuclear proteins are replaced by their cytoplasmic counterparts (Ishigaki *et al.*, 2001; Dostie and Dreyfuss, 2002).

DISCUSSION

Although stimulation of mRNA export by polyadenylation has long been observed, so far little is known about the possible mechanism. In this report we provide first evidence that the 68 kDa subunit of CF I_m, a pre-mRNA 3' end processing factor, interacts with the mRNA export receptor NXF1 and stimulates mRNA export. Based on our observations and on previous data showing that CF I_m68 is associated with BrU-labelled nascent transcripts (Cardinale et al., 2007), we propose that CF I_m68 is loaded onto the pre-mRNA during cleavage and polyadenylation of the 3' end of the transcript and remains bound to the mRNA all the way to the cytoplasm where it is removed by the translation machinery. CF I_m68 may thus act as a mark of correct 3' end maturation and contribute to efficient mRNA export via NXF1 recruitment.

Role of RNA-binding shuttling proteins in mRNA export

Several RNA binding proteins exhibit shuttling activity including the splicing factor U2AF, the polyadenylation factor PABPN1 and members of the hnRNP and SR protein families (for review see Gama-Carvalho and Carmo-Fonseca, 2001). While U2AF, PABPN1, and the hnRNP proteins were shown to shuttle actively and independently of mRNA traffic, shuttling SR proteins are exported bound to the mRNA. Similar to SR proteins, CF I_m shuttling activity depends on active transcription suggesting that it leaves the nucleus in association with the mRNA. Consistent with this observation both CF I_m subunits

contact the RNA substrate, as demonstrated by UV cross-linking studies (Rüegsegger et al., 1996).

What is the role of shuttling proteins in mRNA export? Shuttling RNA-binding proteins may contribute to the assembly of an export competent mRNP by recruiting mRNA export factors. Consistent with this view U2AF 35 kDa subunit (Zolotukhin et al., 2002), several shuttling SR proteins (Huang et al., 2003; Lai and Tarn, 2004), and now CF I_m have been shown to interact with the mRNA export receptor NXF1. In addition, shuttling RNA binding proteins may fulfil different roles in the nucleus and in the cytoplasm. This is the case for instance for the shuttling SR protein ASF/SF2 that, besides its well-characterized role in basal and regulated splicing, is involved in mRNA surveillance and in translation (Sanford et al., 2004; Zhang and Krainer, 2004).

Mechanisms for the recruitment of the mRNA export receptor NXF1

In S. cerevisiae where only 5% of the genes contain introns, export factor recruitment is coupled to transcription and 3' end formation rather than to intron splicing. The interaction between the mRNA and the heterodimeric export receptor Mex67/Mtr2 (NXF1/p15 in metazoa) is provided by the RNA-binding protein Yra1 (REF). Yra1 interacts with the transcription elongation complex (THO complex, Strasser *et al.*, 2002; Abruzzi *et al.*, 2004) and requires 3' end formation to be recruited cotranscriptionally to mRNAs (Lei and Silver, 2002). How the

yeast pre–mRNA 3' end processing complex participates in the recruitment of mRNA export factors is, however, still unknown.
In metazoans, the current model for the recruitment of export factors on the mRNA proposes that adaptor proteins such as REF and the export receptor NXF1 are "deposited" after splicing as components of the EJC (for review see Stutz and Izaurralde, 2003). REF is recruited by UAP56 that binds cotranscriptionally. Before export, NXF1/p15 would bind to REF and thereby release UAP56. However, only NXF1, p15, and UAP56 have been shown so far to be essential for this process (Tan *et al.*, 2000; Herold *et al.*, 2001; Wilkie *et al.*, 2001; Gatfield and Izaurralde, 2002; Wiegand *et al.*, 2002). Recently, an EJC-independent mechanism was proposed for the recruitment of REF based on the observation that UAP56 and REF bind at the 5' end of the mRNA and interact with the cap-binding complex. In this new model recruitment occurs via an interaction between REF and the cap-binding protein CBP80 (Cheng et al., 2006). The observation that depletion of REF in *Drosophila* cells does not lead to accumulation of poly(A)RNA in the nucleus (Gatfield and Izaurralde, 2002) suggests that alternative mechanisms must exist for the recruitment of NXF1 on mature mRNAs. Consistent with this idea, the shuttling SR proteins SRp20, 9G8 and ASF/SF2 that can bind to the pre-mRNA independently of the EJC, were shown to act as NXF1-adaptor proteins. Here, we have demonstrated that CF I_m68 interacts with NXF1 and contributes to mRNA export most likely in conjunction with SR proteins. The presence of CF I_m68 may

signal that the mRNA has been properly cleaved and polyadenylated (Figure 9) and may be packaged into an export-competent mRNA ribonucleoprotein particle (mRNP) that can recruit the export receptor. This novel observation provides for the first time a molecular connection between 3' end formation and mRNA export.

In contrast to NXF1, CF I_m68 does not appear to dissociate from the mRNA upon entry into the cytoplasm. Instead, sucrose gradient centrifugation shows that CF I_m68 cosediments with the 80S ribosome. According to current models, the first passage of the 80S ribosome on an mRNA (called 'pioneer round' of translation) leads to a major rearrangement of the mRNP composition whereby the remaining nuclear mRNP components are removed and replaced by cytoplasmic factors (for review see Maquat, 2004; Moore, 2005). Thus, our findings that CFI_m68 is released from the mRNP at this stage may have interesting implications not only for mRNA export and translation initiation but also for mRNA quality control mechanisms. For example, the presence of CF I_m bound downstream of a stop codon may contribute to the definition of the proper termination codon in metazoa. Further studies on the role of the factors that bind the 3' end of the mRNA should provide new important insight into the mechanism that defines premature stop codons and leads to NMD.

Acknowledgements

We gratefully acknowledge M. Bianchi, J. Lykke-Andersen, W.Y. Tarn, R. Reed and S. Wilson for plasmids, F. Loreni for antibodies, E. Izuarralde for plasmids and antibodies, W. Keller for histidine-tagged CF I_m subunits and S. Stamm for Sf9 cells expressing His-Tra2□. We also thank A.I. Lamond, J. Sanford and J. Caceres for help with some of the experiments and O. Mühlemann for valuable suggestions and proofreading of the manuscript. We appreciate the technical help of N. Kleinschmidt, Lukas Stalder, Sandro Waltersperger, and K. Schranz. This study was partially supported by a MIUR-PRIN 2006 grant and by the Cariplo Foundation. S.C. was supported by a short term EMBO fellowship. M-D.R. and D.S. were supported by the Swiss National Science Foundation (grants 3100A0-105547 and -120064) and the Canton Bern.

FIGURES

Figure 1. The two large CF I_m subunits migrate between nuclei in interspecies heterokaryons.

A. CF I_m68 is a shuttling protein. Left: merge of DAPI staining of HeLa and NIH3T3 nuclei (indicated by broken arrows) and phase contrast microscopy view. Middle: localization of GFP–hnRNP A1 or GFP-hnRNP C. Right: localization of HA-CF I_m68.

B. CF I_m59 but not the 25 kDa subunit shuttles between the nucleus and the cytoplasm. Representative heterokaryons of HeLa cells, transfected with either GFP-CF I_m59 or GFP-CF I_m25. Broken arrows indicate the mouse nuclei.

A full-colour version of this figure is available as Supplementary Figure S7 at *Molecular Biology of the Cell* Online.

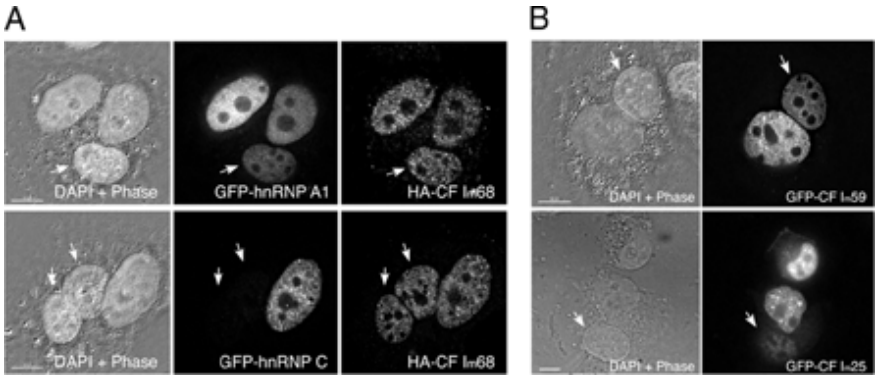

Figure 2. Export of CF I_m68 depends on mRNA traffic.

A. Inhibition of the CRM1-mediated nuclear export pathway does not affect CF I_m68 shuttling activity. HeLa cells were cotransfected with expression constructs for HA-CF I_m68 and

GFP–HMGB1. Two hours prior to fusion with NHI3T3 cells and throughout the experiment, cells were incubated in the absence (not shown) or in the presence of LMB as described in Materials and methods. HA-CF I_m68 was detected by immunofluorescence.

B. HeLa cells transfected with GFP-CF I_m68 and mouse NIH3T3 cells were treated with actinomycin D and then fused as described in Materials and methods. Left: merge of DAPI staining of HeLa and NIH3T3 nuclei (indicated by broken arrows) and phase contrast microscopy view.

A full-colour version of this figure is available as Supplementary Figure S8 at *Molecular Biology of the Cell*.

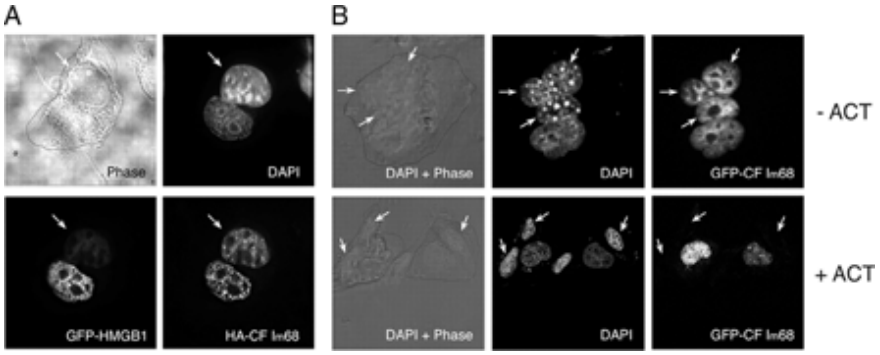

Figure 3. CF I_m68 and NXF1 interact in HEK293 cells and in vitro.

A. CF I_m68 associates with hUpf3b-containing protein complexes.

Left panel: RT-PCR quantitation of the level of ß-actin mRNA before or after RNase treatment. Extracts were treated with increasing amounts of RNaseA. Lane 1: untreated extract; lane 2: 1 µg/ml; lane 3: 3 µg/ml; lane 4: 15 µg/ml.

Right panel: Coimmunoprecipitation experiment of RNase A-treated extracts of HEK293 cells transfected with Flag-Upf3b by using anti-Flag antibodies (lanes 3, and 5). For mock transfection, the same amount of Flag-pCMVTag2 was used as negative control (lanes 2, and 4). Coimmunoprecipitated proteins were visualized by Western blotting with the indicated antibodies. Lane 1: total extract from untransfected cells.

B. CF I_m68 interacts with NXF1 in HEK293 cell extract. Coimmunoprecipitations with anti–Flag antibody of RNase A-treated extracts of HEK293 cells transfected with Flag-tagged CF I_m25 (positive control, lanes 3 and 8), NXF1 (lanes 4 and 9), hUpf1 (lanes 5 and 10), or hUpf3b (lanes 6 and 11) and HA-tagged CF I_m68, as indicated. For mock transfections (lanes 2 and 7), the same amount of Flag-pCMVTag2 was used. Bound proteins (Pellet) were detected by Western blotting with anti-CF I_m68 antiserum (upper panel). To control for equal loading, the membrane was sequentially probed without stripping with anti–Flag and anti–actin antibodies (lower panel). An asterisk indicates residual signal of the anti-CF I_m68 antibody. Lane 1: total extract from untransfected cells.

C. Recombinant CF I_m68 interacts with NXF1 in vitro.

Left panel: Coomassie-stained SDS-PAGE of the purified recombinant proteins used in the pull-down assay.

Right panel: GST (lane 2), GST-tagged CF I_m25 (lane 3) and NXF1 (lane 4) were tested for interaction with histidine-tagged CF I_m68. Eluted proteins were analyzed by Western blotting with anti-histidine antibody.

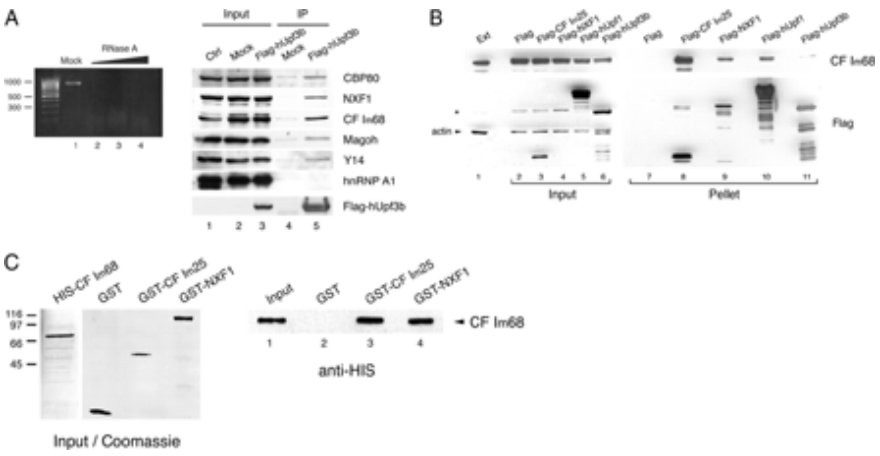

Figure 4. CF I_m68 interacts with NXF1 via its N Terminus.

A. Schematic representation of the domain structure of CF I_m68. The open and solid boxes indicate the regions of the protein present in each mutant relative to the 552 amino acid wild type protein shown at the top. The connecting line indicates missing residues (222–419) in the RRM/RS protein.

B. HEK293 cells were transfected either with pCMVTag2-Flag or with pFlag–NXF1 and plasmids expressing GFP-tagged full length CF I_m68 (lanes 2-4), or the domain deletion mutant proteins 68□N (lanes 5-7), 68RRM/RS (lanes 8-10), 68RS (lanes 11-13) and 68□RS (lanes 14-16). Total extracts were immunoprecipitated with anti-Flag antibody and analysed by Western blotting. Lane 1: extract from untransfected cells.

C. E. coli-expressed GST or GST-NXF1 prebound to beads were individually incubated with in vitro translated, [^{35}S]-labelled HA-tagged CF I_m68 or 68ΔN. Bound fractions (lanes 2, 3, 5, and 6) were subjected to SDS-PAGE and analyzed by autoradiography.

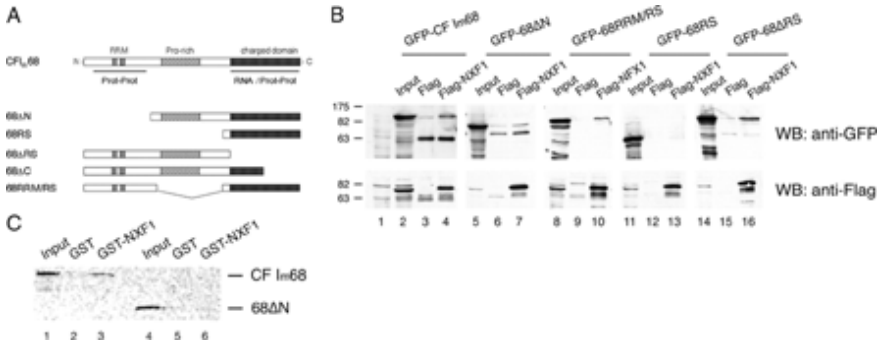

Figure 5. CF I_m68 and SR proteins do not bind the same region of NXF1.

A. NXF1 domain organization with the 202 aa fragment depicted below. The regions interacting with SR proteins, REF, p15, and the NPC are indicated.

B. SR proteins and CF I_m68 do not bind to the same NXF1 region. Left: *E. coli*-expressed GST, GST-NXF1or GST-NXF1 202 were incubated with in vitro translated, [^{35}S]-labelled CF I_m68. Bound fractions were analyzed by autoradiography. Left: Coomassie-stained gel of the purified recombinant proteins.

C. SR proteins can bridge the interaction between NXF1 and CF I_m68. *E. coli*-expressed GST, or GST-NXF1 were incubated with in vitro translated, [^{35}S]-labelled CF I_m68ΔN in the presence of recombinant, histidine-tagged hTra2ß as described in Materials and Methods. Bound fractions were analyzed by autoradiography.

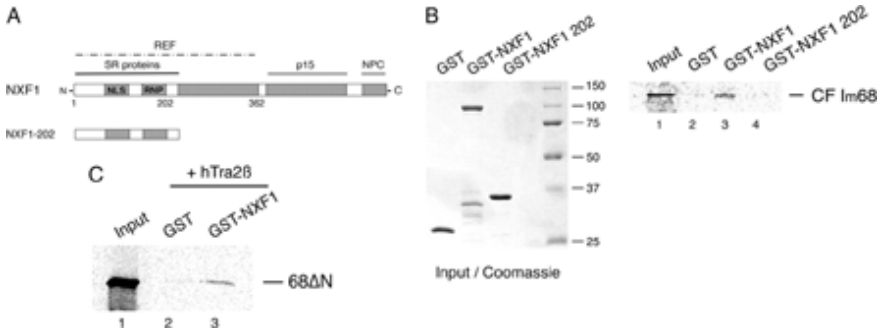

Figure 6. Tethering of CFI$_m$68 leads to mRNA export.

A. Schematic of pRRE-Luc construct. The position of the FISH probe is indicated.

B. Normalized firefly/*renilla* luciferase activity generated by the MS2 fusion proteins in the tethered mRNA export assay. Error bars represent standard deviations from four independent sets of assays. The averaged activity of each MS2-fusion protein was expressed as a percentage of the average activity measured for MS2-REF calculated as described in Materials and methods. RRE, transfection with pRRE-Luc without MS2 fusion protein.

C. Fluorescent in situ hybridization of HeLa cells cotransfected with pRRE-Luc and double-tagged GFP/MS2 (a-a"), GFP/MS2–CF I$_m$68 (b-b"), or Myc/MS2-NXF1 (c, c'). DAPI staining was used to identify the cell nucleus (a-c), localization of RRE-Luc mRNA in representative cells was visualized by FISH (a'-c'), GFP fluorescence was used to identify cells expressing the exogenous protein (a", b").

D. The average cytoplasmic to nuclear (C/N) ratio for the RRE-Luc mRNA was determined by quantitative analysis of

FISH experiments as shown in panel C for the indicated number of cells per construct. Error bars indicate standard deviations.

E. Real-time PCR analysis of the relative amount of RRE-Luc mRNA in the nuclear fractions of cells transfected with the indicated MS2-fusions constructs as determined by real-time reverse transcription PCR. Three experiments were performed and average values are shown.

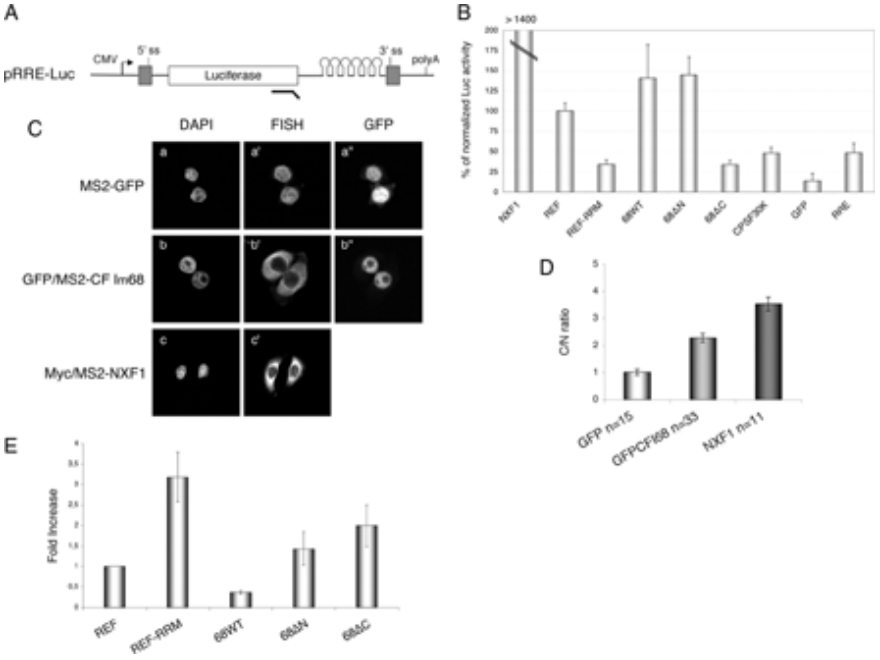

Figure 7. CF I_m68 promotes export of mRNAs.

A. Hela cells growing on coverslips, overexpressing HA-tagged CFI_m68 and a puromycin resistance as well as control cells expressing only the puromycin resistance were fixed with formaldehyde and permeabilised with methanol. Polyadenylated mRNA was visualised by hybridisation of a

Cy3-labelled oligo(dT)50 probe, whereas the nuclei were stained with DAPI. The panels are projections of Z-stacks from top to bottom of the nuclei. Images were collected on a Leica TCS SP2 AOBS laser scanning confocal microscope equipped with a HCX PL APOlbd.BL 63.0x 1.2W objective (Leica Microsystems Inc., Exton, PA).

B. PCR analysis of nuclear and cytoplasmic RNAs of the nuclear X-ist mRNA (top) and the X-encoded Mic 2A transcript (bottom).

C. Overxpression of CF I_m68 stimulates mRNA export. Real-time PCR analysis of the relative amount of ß-actin, Gapdh, Upf2 and Smg7 mRNA levels in the cytoplasmic (upper histogram) and nuclear (lower histogram) fraction of cells expressing HA-tagged EGFP (white bars) or HA-tagged CFI_m68 (grey bars). The values were normalized to 18S rRNA levels and then divided by the values obtained in cells expressing the EGFP control. Three independent experiments were performed and average values of three real-time PCR runs with cDNAs from one representative experiment are shown.

D. HeLa cells stably expressing ß-globin mRNA were transfected with a control siRNA or with siRNAs against CFI_m68. Total extract was prepared and analyzed by Western blotting with anti-CFI_m68 and with anti-SmB/B' antibodies. Three different experiments are shown.

E. CFI_m68 depletion increases nuclear levels of ß-globin mRNA. Real-time RT-PCR analysis of the relative amount of ß-globin mRNA in the nuclear fraction of HeLa cells transfected

with a control siRNA or cells depleted of CFI_m68. The indicated values are normalized to 18S rRNA levels. Three experiments were performed and average values are shown.

F. CFI_m68 depletion does not affect pre-mRNA 3' end processing. Real-time RT-PCR of ß-actin mRNA was performed with probes spanning the 5'UTR or the cleavage site to measure total and unprocessed mRNA, respectively. The ratio of precursor to total mRNA (pre/tot) was calculated to assess the efficiency of 3' end processing. The processing activity of cells transfected with the control siRNA was set to 1.

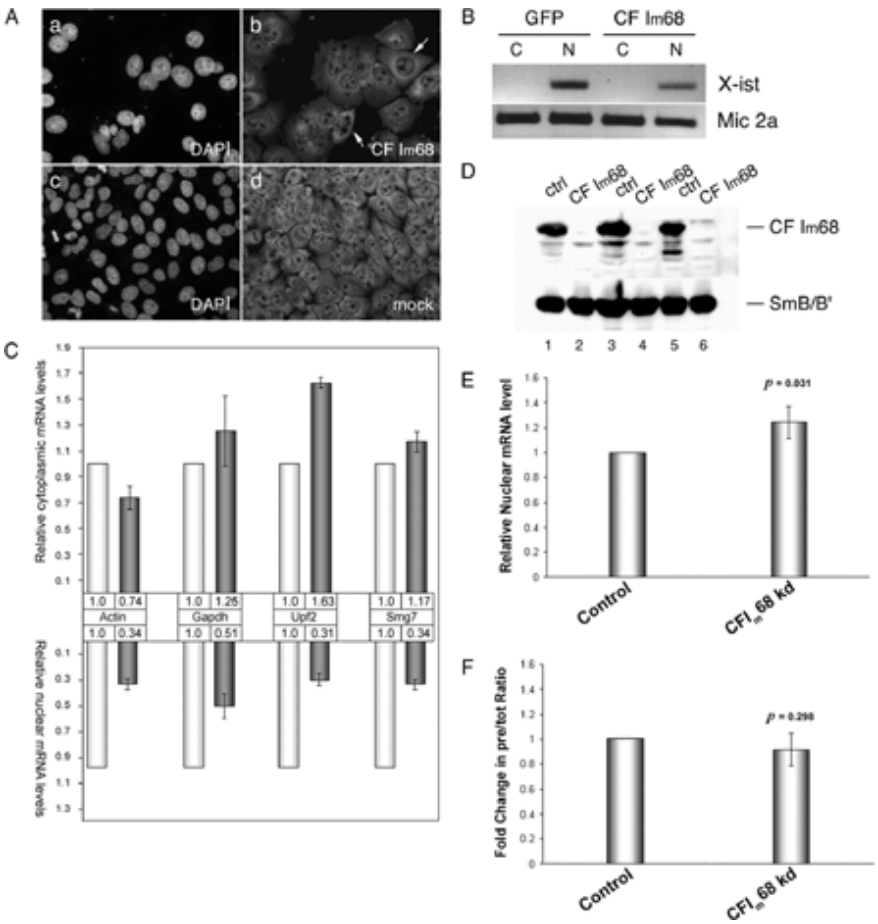

Figure 8. CF I_m68 cosediments with the translation machinery.

A. HEK293 cell cytoplasmic extracts were fractionated across 15%-50% sucrose gradients and analysed by immunoblotting with ASF/SF2, CF I_m68, and rpS6. (Top) UV absorbance (254 nm) profile of cytosolic ribonucleoprotein complexes.

B. Fractions were additionally analysed by immunoblotting with ASF/SF2, CF I_m68, and in addition CBP80 and PABPC1.

C. Sucrose gradient analysis of RNase A-treated cytoplasmic extracts. CF I_m68, SF2/ASF and rpS6 concentrate very narrowly across the gradient of HEK293 cytoplasmic extracts treated with RNase A, which induces dissociation of ribosomal subunits. (Top) UV absorbance (254 nm) profile of cytosolic ribonucleoprotein complexes.

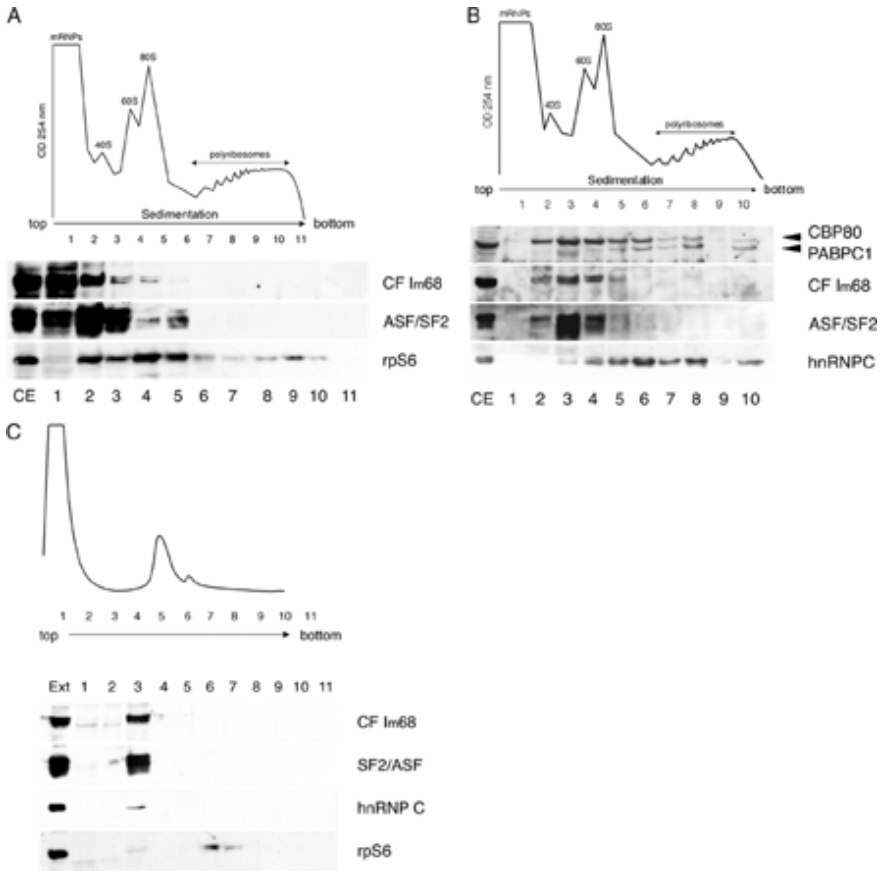

Figure 9. Model of potential role of CF I_m68 in assembly and export of mRNPs.

a) CF I_m is recruited to the pre-mRNA as part of the cleavage and polyadenylation complex.

b) Once correct 3' end processing has occurred, CF I_m68 remains associated with the mRNA, and

c) in conjunction with SR proteins contributes to the recruitment of the export receptor NXF1.

d) In the cytoplasm, the translating ribosomes remove the nuclear proteins that are reimported into the nucleus.

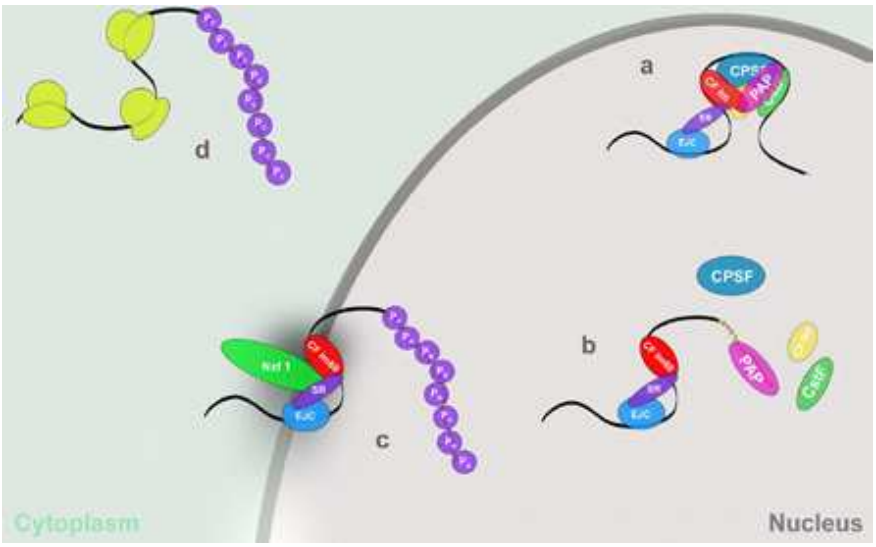
a
CPSF
PAP
EJC
b
CPSF
PAP
CstF
EJC
c
Rrd1
EJC
d
Cytoplasm
Nucleus

SUPPLEMENTAL MATERIALS

Supplemental Figure S1. CF Im is imported into the nucleus as a heterodimer.

A. Confocal microscope sections of HeLa cells transiently transfected with pEYFP (a), pEYFP-CF Im25 (b), pECFP-CF Im68 (c), pECFP-CF Im68 and pEYFP (d), pEYFP-CF Im25 and pECFP–CF Im68 (e), pEYFP-CF Im25 and pECFP-68RNP2 (f), respectively. Panels a-f are images of the yellow fluorescence of YFP while the insets d', e', and f' are images of the blue fluorescence of CFP.

While the endogenous 25 kDa protein is exclusively localized to the nucleus, YFP-CF Im25, although predominantly nuclear, could also be observed in the cytoplasm (panel b) suggesting that it is not efficiently imported into the nucleus. However, when YFP-CF Im25 was coexpressed with the large subunit, the cytoplasmic signal disappeared (Figure 2A, panel e). In contrast, when YFP-CF Im25 was coexpressed with CFP-CF Im68 carrying a mutation in the RNP2 motif that impairs the interaction with the 25 kDa subunit in vitro (68RNP2, Dettwiler et al., 2004), import into the nucleus was less efficient (panel f).

B. Immunoprecipitation experiments with anti-Flag antibody were carried out on total extracts from HEK293 cells transfected with Flag-tagged CF Im25 and wild-type or mutant GFP-CF Im68. Western blots were then probed simultaneously with anti-GFP and anti-Flag antibodies. These coimmunoprecipitation

experiments confirmed that the CF Im68 RNP2 mutation destabilizes the interaction between the two subunits.
Lanes 1-4: input 3% of the amount used for the immunoprecipitation. Lanes 5-8: immunoprecipitated proteins.

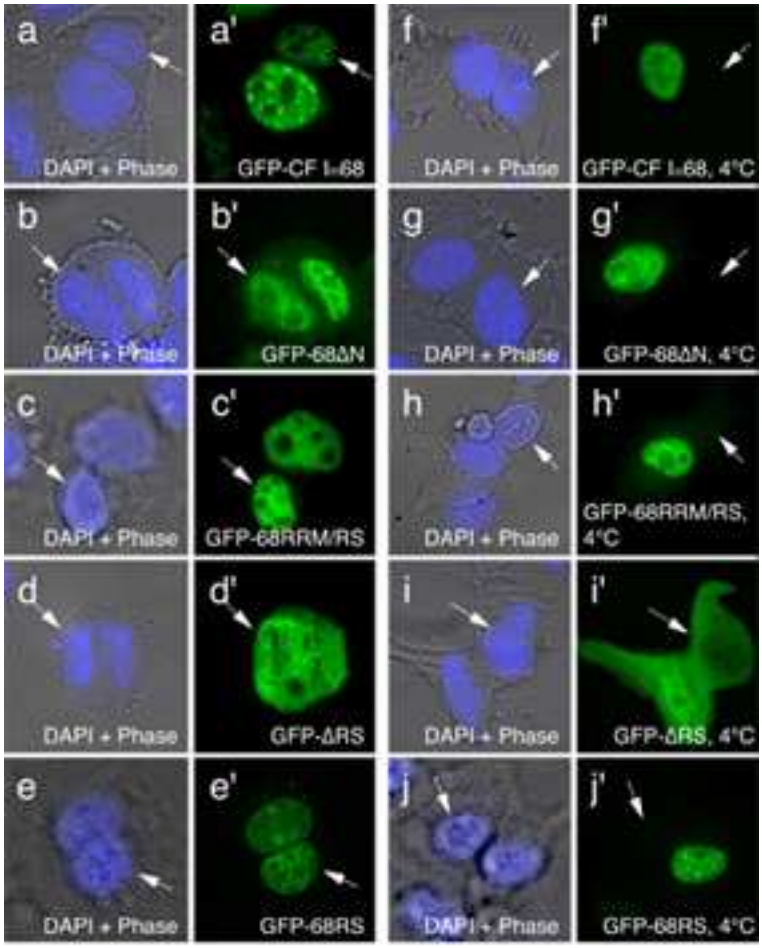

Supplemental Figure S2. Nucleocytoplasmic shuttling behaviour of various CF Im68 mutants and demonstration that shuttling is an active process.

Interspecies heterokaryon assays performed at 37℃ (a-e') or at 4℃ (f-j') with HeLa cells transfected with the indicated GFP-fusion constructs and mouse NIH3T3 cells.

a-j: merge of DAPI staining of nuclei and phase contrast microscopy view; a'-j': fluorescence image of GFP signal. Broken arrows indicate the NIH3T3 nuclei.

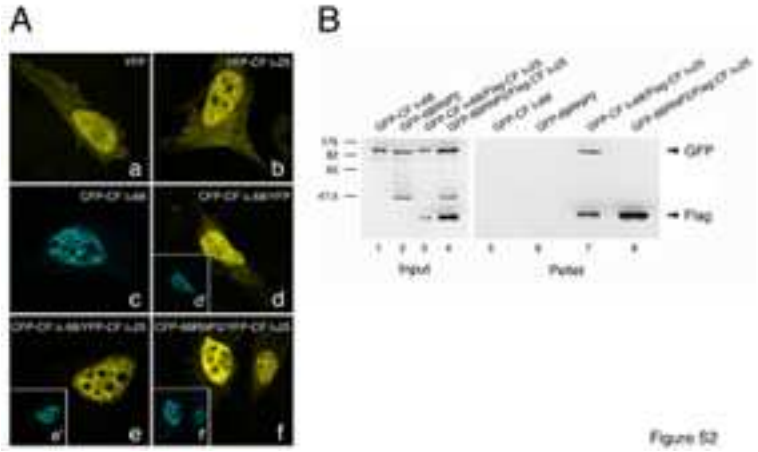

Supplemental Figure S3. Western blot analysis of HEK293 cell extracts used in the mRNA export assay.

HEK293 cells were transfected with the firefly luciferase reporter construct and the indicated plasmids expressing the following proteins with dual Myc/MS2 tags: NXF1, REF, REF-RRM, GFP, or Flag/MS2–tagged CF Im68, 68ΔN, and 68ΔC. Blots were probed with anti-Myc and anti-Flag antibodies.

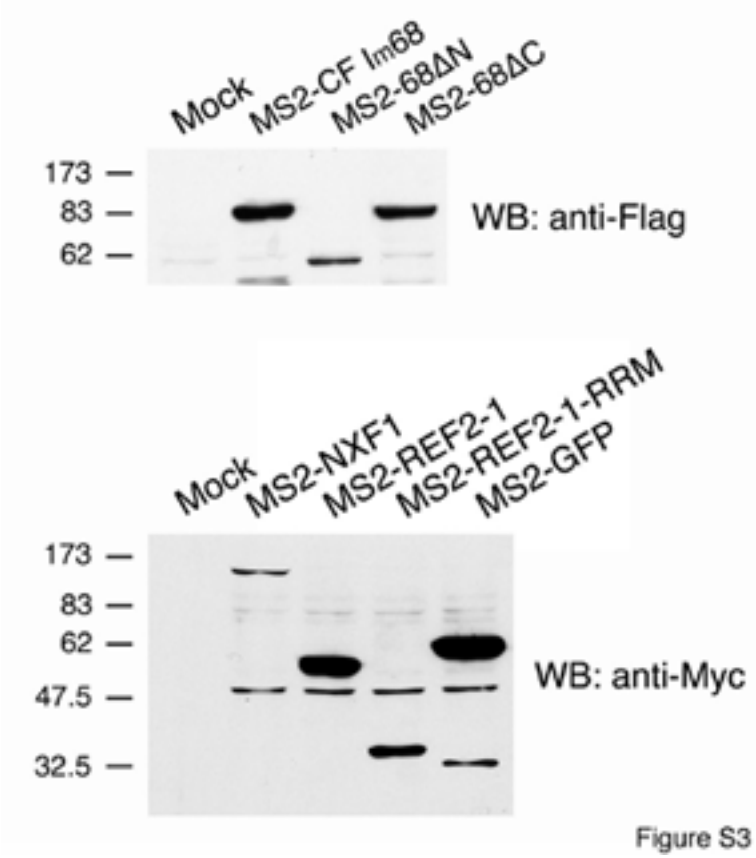

Supplemental Figure S4. Western blot assessing the purity of the nuclear fractions used in the experiments shown in Figure 7E and 7F.

10% of the nuclear extracts used for RNA isolation were subjected to SDS-PAGE followed by immunoblotting for lamin A/C and tyrosine tubulin as nuclear and cytoplasmic markers, respectively. Lanes 1-5 show the nuclear fractions from the MS2-tethering assay (Figure 6E), lane 6 is a cytoplasmic fraction shown as control for tyrosine tubulin, while lanes 7 and

8 are nuclear fractions from cells transfected with a control siRNA or CFIm68, respectively (expt shown in Figure 7E).

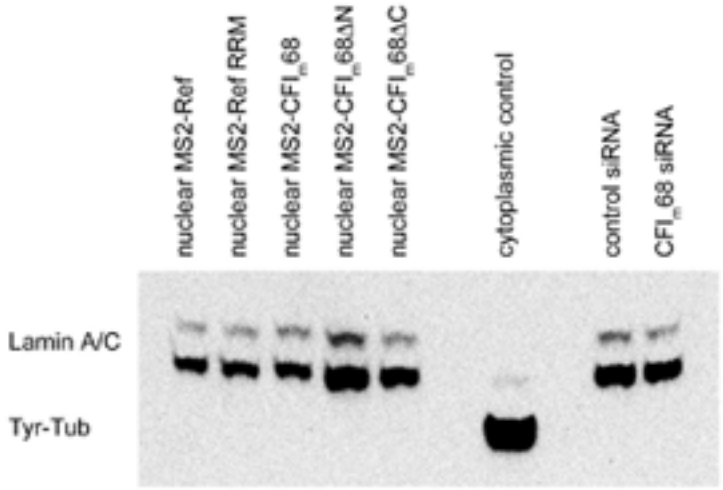

Figure S4

Supplemental Figure S5. NXF1 depletion increases nuclear levels of ß-globin mRNA.

HeLa cells stably expressing ß-globin mRNA were transfected with a control siRNA or with siRNAs against NXF1 and the relative amount of ß-globin mRNA in the nuclear fraction of HeLa cells was measured by qRT-PCR. The indicated values are normalized to 18S rRNA levels. Three experiments were performed 48 hours post transfection and average values are shown. A. NXF1 mRNA was reduced to 8.6% (50% of the cells were dead). B. Nuclear ß-globin RNA was increased ~2.5 times.

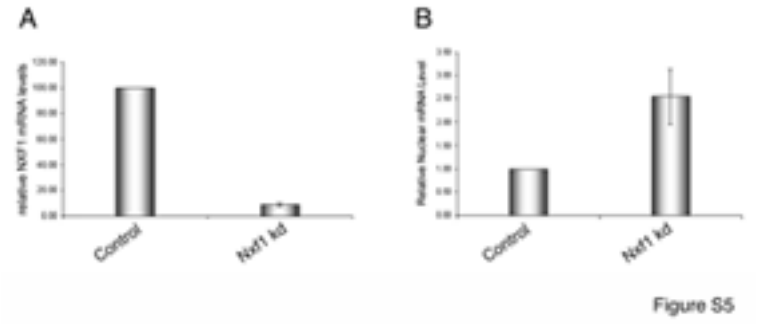

Supplemental Figure S6. Sucrose gradient analysis of puromycin-treated cytoplasmic extracts.

Left: Untreated cytoplasmic extracts were resolved by 15%-50% sucrose gradients and analyzed by immunoblotting for CF Im68, ASF/SF2 and rpS19. Right: Across the gradient prepared from cytoplasmic extracts treated with puromycin, which induces dissociation of polysomes, ribosomal protein S19 concentrates more narrowly across the gradient. Likewise, CF Im68 and ASF/SF2 shift to lighter fractions mostly corresponding to 80 S ribosome monomers and 60 S large subunits. (Top) UV absorbance (254 nm) profile of cytosolic ribonucleoprotein complexes.

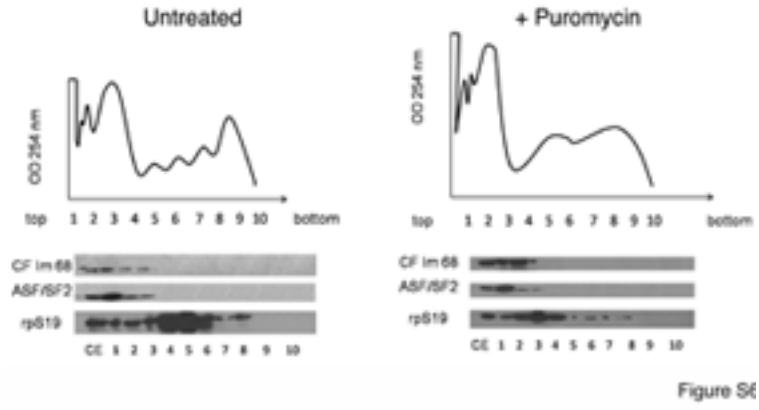

Supplemental Figure S7. Color version of Figure 1.

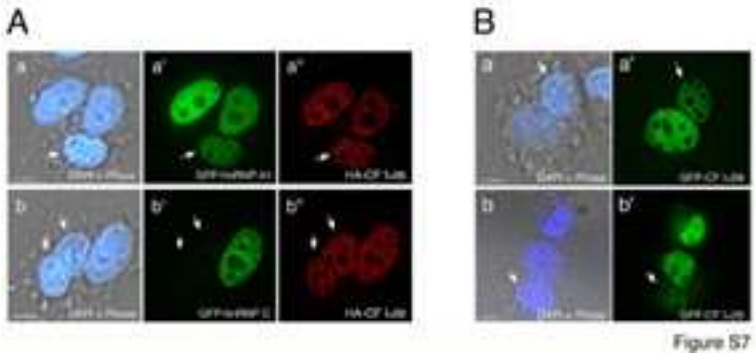

Figure S7

Supplemental Figure S8. Color version of Figure 2.

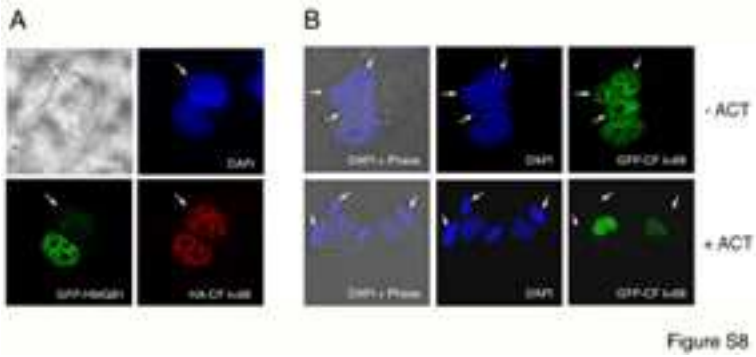

Figure S8

Supplemental Methods and References

Oligonucleotide Probes

FISH antisense probe transcribed in vitro from pRRE:

GAGACCCAAGCTTCGAGGCCTCGGAGGATTACAATAGCTA

AGAATTTCGTCATCGCTGAATACAGTTACATTTTACAATTTG

GACTTTCCGCCCTTCTTGGCCTTTATGAGGATCTCTCTGAT

TTTTCTTGCGTCGAGTTTTCCGGTAAGACCTTTCGGTACTT

CGTCCACAAACACAACTCCTCCGCGCAACTTTTTCGCGGT

TGTTACTTGACTGGCGACGTAATCCACGATCTCTTTTTCCG

TCATCGTCTTTCCGTGCTCCAAAACAACAACGGCGGCGGG

AAGTTCACCGGCGTCATCGTCGGGAAGACCTGCCACGCC
CGCGTCGAAGATGTTGGGGTGTTGTAACAATATCGATTCC
AATTCAGCGGGGGCCACCTGATATC.

The primer sequences of the nuclear X inactive specific transcript (XIST) and of the X-encoded MIC2 transcript are described elsewhere (Das et al., 2001).

Antibodies

Flag-fusion proteins were detected with an anti Flag-M2 monoclonal antibody (Sigma). The anti-histidine and anti-GST tag antibodies were from Qiagen and Amersham, respectively. The anti-ASF and anti-SRp20 monoclonal antibodies were from Zymed. The anti-hnRNP A1 and hnRNP C monoclonal antibodies were from Sigma. The anti-rpS6 antibody was from Cell Signalling while the anti-rpS19 antibody was a kind gift of F. Loreni (Orru et al., 2007). The anti-CF Im68 rabbit polyclonal antibody was as described in (Rüegsegger et al., 1998). Monoclonal mouse antibodies from Santacruz and Sigma were used to detect Lamin A/C and Tyrosin- Tubulin respectively. Anti-CBP80, anti-NXF1, anti–Magoh, and anti-Y14 were kindly provided by Dr. E. Izuarralde.

Plasmids Constructs

Plasmids GST-CF Im25, pEGFP-CF Im68, pEGFP-CF Im59, pEGFP-CF Im25 and the domain deletion mutants were described elsewhere (Dettwiler et al., 2004). CFPCF Im68 and YFP-CF Im25 were cloned by PCR into pECFP-C1 and pEYFP-C1. CFP-68RNP2 was obtained by digesting pBS68RNP2 (Dettwiler et al., 2004) with BamHI and SalI and inserting the

two fragments that are generated into pCFP-C1 linearized with BglII and SalI. pCMV-FlagCFIm25 was generated by cloning the CF Im25 fragment into the BamHI and SalI sites of pCMV-Tag4 (Stratagene). The GFPhnRNP A1 and GFP-hnRNP C plasmids were a gift from W.Y. Tarn. The plasmid for for GFP-HMGB1 was a gift from M. Bianchi. GST-NXF1 was a gift from E. Izuarralde. The luciferase reporter plucRRE, and the pCINEOMycMS2 constructs expressing NXF1, REF1, REFRRM, and GFP were a gift from S. Wilson. Plasmids expressing N-terminal MS2-Flag protein fusions were obtained by subcloning the respective DNA fragment into the BamHI and the XhoI sites of a modified pcNMS2 (Lykke-Andersen et al., 2000) in which the Flag epitope was introduced downstream of the MS2 fragment. pcNMS2Flag-68ΔC was prepared by deletion of the C-terminal SalI fragment.

Fluorescence microscopy

Indirect immunofluorescence study was conducted as described previously (Cardinale et al., 2007; Dettwiler et al., 2004). Immunofluorescence staining and slide preparation was carried out according to standard techniques. Fluorescence microscopy was carried out either with a Zeiss DeltaVision Restoration microscope (Applied Precision, Inc.) or with a Leica DM IRE2 confocal microscope.

References

Cardinale, S., Cisterna, B., Bonetti, P., Aringhieri, C., Biggiogera, M. and Barabino, S.M. (2007) Subnuclear localization and dynamics of the Pre-mRNA 3' end processing

factor mammalian cleavage factor I 68-kDa subunit. Mol Biol Cell, 18, 1282-1292.

Das, M., Harvey, I., Chu, L.L., Sinha, M. and Pelletier, J. (2001) Full-length cDNAs: more than just reaching the ends. Physiol Genomics, 6, 57-80.

Dettwiler, S., Aringhieri, C., Cardinale, S., Keller, W. and Barabino, S.M. (2004) Distinct sequence motifs within the 68-kDa subunit of cleavage factor Im mediate RNA binding, protein-protein interactions, and subcellular localization. J. Biol. Chem., 279, 35788-35797.

Lykke-Andersen, J., Shu, M.D. and Steitz, J.A. (2000) Human Upf proteins target an mRNA for nonsense-mediated decay when bound downstream of a termination codon. Cell, 103, 1121-1131.

Orru, S., Aspesi, A., Armiraglio, M., Caterino, M., Loreni, F., Ruoppolo, M., Santoro, C. and Dianzani, I. (2007) Analysis of the ribosomal protein S19 interactome. Mol Cell Proteomics, 6, 382-393.

Rüegsegger, U., Blank, D. and Keller, W. (1998) Human pre-mRNA cleavage factor Im is related to spliceosomal SR proteins and can be reconstituted in vitro from recombinant subunits. Mol. Cell, 1, 243-253.

REFERENCES

Abruzzi, K.C., Lacadie, S., and Rosbash, M. (2004). Biochemical analysis of TREX complex recruitment to intronless and intron-containing yeast genes. Embo J *23*, 2620-2631.

Boisvert, F.M., Cote, J., Boulanger, M.C., and Richard, S. (2003). A proteomic analysis of arginine-methylated protein complexes. Mol Cell Proteomics *2*, 1319-1330.

Brune, C., Munchel, S.E., Fischer, N., Podtelejnikov, A.V., and Weis, K. (2005). Yeast poly(A)-binding protein Pab1 shuttles between the nucleus and the cytoplasm and functions in mRNA export. RNA *11*, 517-531.

Calado, A., Kutay, U., Kuhn, U., Wahle, E., and Carmo-Fonseca, M. (2000). Deciphering the cellular pathway for transport of poly(A)-binding protein II. RNA *6*, 245-256.

Cardinale, S., Cisterna, B., Bonetti, P., Aringhieri, C., Biggiogera, M., and Barabino, S.M. (2007). Subnuclear localization and dynamics of the Pre-mRNA 3' end processing factor mammalian cleavage factor I 68-kDa subunit. Mol Biol Cell *18*, 1282-1292.

Carneiro, M., and Schibler, U. (1984). Accumulation of rare and moderately abundant mRNAs in mouse L-cells is mainly post-transcriptionally regulated. J Mol Biol *178*, 869-880.

Cheng, H., Dufu, K., Lee, C.S., Hsu, J.L., Dias, A., and Reed, R. (2006). Human mRNA export machinery recruited to the 5' end of mRNA. Cell *127*, 1389-1400.

Dettwiler, S., Aringhieri, C., Cardinale, S., Keller, W., and Barabino, S.M. (2004). Distinct sequence motifs within the 68-kDa subunit of cleavage factor Im mediate RNA binding, protein-protein interactions, and subcellular localization. J. Biol. Chem. *279*, 35788-35797.

Dostie, J., and Dreyfuss, G. (2002). Translation is required to remove Y14 from mRNAs in the cytoplasm. Curr Biol *12*, 1060-1067.

Erkmann, J.A., and Kutay, U. (2004). Nuclear export of mRNA: from the site of transcription to the cytoplasm. Exp Cell Res *296*, 12-20.

Gama-Carvalho, M., and Carmo-Fonseca, M. (2001). The rules and roles of nucleocytoplasmic shuttling proteins. FEBS Lett *498*, 157-163.

Gatfield, D., and Izaurralde, E. (2002). REF1/Aly and the additional exon junction complex proteins are dispensable for nuclear mRNA export. J Cell Biol *159*, 579-588.

Gilmartin, G.M. (2005). Eukaryotic mRNA 3' processing: a common means to different ends. Genes Dev *19*, 2517-2521.

Godin, K.S., and Varani, G. (2007). How arginine-rich domains coordinate mRNA maturation events. RNA Biol *4*, 69-75.

Graveley, B.R. (2000). Sorting out the complexity of SR protein functions. Rna *6*, 1197-1211.

Guzik, B.W., Levesque, L., Prasad, S., Bor, Y.C., Black, B.E., Paschal, B.M., Rekosh, D., and Hammarskjold, M.L. (2001). NXT1 (p15) is a crucial cellular cofactor in TAP-dependent

export of intron-containing RNA in mammalian cells. Mol Cell Biol *21*, 2545-2554.

Hargous, Y., Hautbergue, G.M., Tintaru, A.M., Skrisovska, L., Golovanov, A.P., Stevenin, J., Lian, L.Y., Wilson, S.A., and Allain, F.H. (2006). Molecular basis of RNA recognition and TAP binding by the SR proteins SRp20 and 9G8. Embo J *25*, 5126-5137.

Hector, R.E., Nykamp, K.R., Dheur, S., Anderson, J.T., Non, P.J., Urbinati, C.R., Wilson, S.M., Minvielle-Sebastia, L., and Swanson, M.S. (2002). Dual requirement for yeast hnRNP Nab2p in mRNA poly(A) tail length control and nuclear export. Embo J *21*, 1800-1810.

Herold, A., Klymenko, T., and Izaurralde, E. (2001). NXF1/p15 heterodimers are essential for mRNA nuclear export in Drosophila. RNA *7*, 1768-1780.

Huang, Y., and Carmichael, G.G. (1996). Role of polyadenylation in nucleocytoplasmic transport of mRNA. Mol Cell Biol *16*, 1534-1542.

Huang, Y., Gattoni, R., Stevenin, J., and Steitz, J.A. (2003). SR splicing factors serve as adapter proteins for TAP-dependent mRNA export. Mol Cell *11*, 837-843.

Huang, Y., and Steitz, J.A. (2001). Splicing factors SRp20 and 9G8 promote the nucleocytoplasmic export of mRNA. Mol Cell *7*, 899-905.

Ishigaki, Y., Li, X., Serin, G., and Maquat, L.E. (2001). Evidence for a pioneer round of mRNA translation: mRNAs subject to

nonsense-mediated decay in mammalian cells are bound by CBP80 and CBP20. Cell *106*, 607-617.

Izaurralde, E. (2002). A novel family of nuclear transport receptors mediates the export of messenger RNA to the cytoplasm. Eur J Cell Biol *81*, 577-584.

Katahira, J., Strasser, K., Podtelejnikov, A., Mann, M., Jung, J.U., and Hurt, E. (1999). The Mex67p-mediated nuclear mRNA export pathway is conserved from yeast to human. Embo J *18*, 2593-2609.

Kessler, M.M., Henry, M.F., Shen, E., Zhao, J., Gross, S., Silver, P.A., and Moore, C.L. (1997). Hrp1, a sequence-specific RNA-binding protein that shuttles between the nucleus and the cytoplasm, is required for mRNA 3'-end formation in yeast. Genes Dev. *11*, 2545-2556.

Kim, V.N., Kataoka, N., and Dreyfuss, G. (2001). Role of the nonsense-mediated decay factor hUpf3 in the splicing-dependent exon-exon junction complex. Science *293*, 1832-1836.

Lai, M.C., and Tarn, W.Y. (2004). Hypophosphorylated ASF/SF2 binds TAP and is present in messenger ribonucleoproteins. J Biol Chem *279*, 31745-31749.

Le Hir, H., Gatfield, D., Izaurralde, E., and Moore, M.J. (2001). The exon-exon junction complex provides a binding platform for factors involved in mRNA export and nonsense-mediated mRNA decay. Embo J *20*, 4987-4997.

Lei, E.P., and Silver, P.A. (2002). Intron status and 3'-end formation control cotranscriptional export of mRNA. Genes Dev *16*, 2761-2766.

Lejeune, F., Ishigaki, Y., Li, X., and Maquat, L.E. (2002). The exon junction complex is detected on CBP80-bound but not eIF4E-bound mRNA in mammalian cells: dynamics of mRNP remodeling. Embo J *21*, 3536-3545.

Maquat, L.E. (2004). Nonsense-mediated mRNA decay: splicing, translation and mRNP dynamics. Nat Rev Mol Cell Biol *5*, 89-99.

Michael, W.M., Choi, M., and Dreyfuss, G. (1995). A nuclear export signal in hnRNP A1: a signal-mediated, temperature-dependent nuclear protein export pathway. Cell *83*, 415-422.

Moore, M.J. (2005). From birth to death: the complex lives of eukaryotic mRNAs. Science *309*, 1514-1518.

Nemeroff, M.E., Barabino, S.M., Li, Y., Keller, W., and Krug, R.M. (1998). Influenza virus NS1 protein interacts with the cellular 30 kDa subunit of CPSF and inhibits 3'end formation of cellular pre-mRNAs. Mol. Cell *1*, 991-1000.

Pinol-Roma, S., Choi, Y.D., Matunis, M.J., and Dreyfuss, G. (1988). Immunopurification of heterogeneous nuclear ribonucleoprotein particles reveals an assortment of RNA-binding proteins. Genes Dev *2*, 215-227.

Pinol-Roma, S., and Dreyfuss, G. (1992). Shuttling of pre-mRNA binding proteins between nucleus and cytoplasm. Nature *355*, 730-732.

Reed, R., and Hurt, E. (2002). A conserved mRNA export machinery coupled to pre-mRNA splicing. Cell *108*, 523-531.

Rüegsegger, U., Beyer, K., and Keller, W. (1996). Purification and characterization of human cleavage factor Im involved in 3' end processing of messenger RNA precursors. J. Biol. Chem. *271*, 6107-6113.

Rüegsegger, U., Blank, D., and Keller, W. (1998). Human pre-mRNA cleavage factor Im is related to spliceosomal SR proteins and can be reconstituted in vitro from recombinant subunits. Mol. Cell *1*, 243-253.

Sabatini, D.D., Blobel, G., Nonomura, Y., and Adelman, M.R. (1971). Ribosome-membrane interaction: Structural aspects and functional implications. Adv Cytopharmacol *1*, 119-129.

Sanford, J.R., Gray, N.K., Beckmann, K., and Caceres, J.F. (2004). A novel role for shuttling SR proteins in mRNA translation. Genes Dev *18*, 755-768.

Singh, G., Jakob, S., Kleedehn, M.G., and Lykke-Andersen, J. (2007). Communication with the exon-junction complex and activation of nonsense-mediated decay by human Upf proteins occur in the cytoplasm. Mol Cell *27*, 780-792.

Strasser, K., Masuda, S., Mason, P., Pfannstiel, J., Oppizzi, M., Rodriguez-Navarro, S., Rondon, A.G., Aguilera, A., Struhl, K., Reed, R., and Hurt, E. (2002). TREX is a conserved complex coupling transcription with messenger RNA export. Nature *417*, 304-308.

Stutz, F., and Izaurralde, E. (2003). The interplay of nuclear mRNP assembly, mRNA surveillance and export. Trends Cell Biol *13*, 319-327.

Tan, W., Zolotukhin, A.S., Bear, J., Patenaude, D.J., and Felber, B.K. (2000). The mRNA export in Caenorhabditis elegans is mediated by Ce-NXF-1, an ortholog of human TAP/NXF and Saccharomyces cerevisiae Mex67p. Rna *6*, 1762-1772.

Tange, T.O., Nott, A., and Moore, M.J. (2004). The ever-increasing complexities of the exon junction complex. Curr Opin Cell Biol *16*, 279-284.

Tintaru, A.M., Hautbergue, G.M., Hounslow, A.M., Hung, M.L., Lian, L.Y., Craven, C.J., and Wilson, S.A. (2007). Structural and functional analysis of RNA and TAP binding to SF2/ASF. EMBO Rep *8*, 756-762.

Valencia, P., Dias, A.P., and Reed, R. (2008). Splicing promotes rapid and efficient mRNA export in mammalian cells. Proc Natl Acad Sci U S A *105*, 3386-3391.

Wiegand, H.L., Coburn, G.A., Zeng, Y., Kang, Y., Bogerd, H.P., and Cullen, B.R. (2002). Formation of Tap/NXT1 heterodimers activates Tap-dependent nuclear mRNA export by enhancing recruitment to nuclear pore complexes. Mol Cell Biol *22*, 245-256.

Wilkie, G.S., Zimyanin, V., Kirby, R., Korey, C., Francis-Lang, H., Van Vactor, D., and Davis, I. (2001). Small bristles, the Drosophila ortholog of NXF-1, is essential for mRNA export throughout development. Rna *7*, 1781-1792.

Zhang, Z., and Krainer, A.R. (2004). Involvement of SR proteins in mRNA surveillance. Mol Cell *16*, 597-607.

Zhao, J., Hyman, L., and Moore, C. (1999). Formation of mRNA 3' ends in eukaryotes: mechanism, regulation, and interrelationships with other steps in mRNA synthesis. Microbiol. Mol. Biol. Rev. *63*, 405-445.

Zolotukhin, A.S., Tan, W., Bear, J., Smulevitch, S., and Felber, B.K. (2002). U2AF participates in the binding of TAP (NXF1) to mRNA. J Biol Chem *277*, 3935-3942.

Chapter 4

Nucleic Acid Research, Submitted

Association of the 68 kDa subunit of mammalian cleavage factor I with the U7 small nuclear ribonucleoprotein: possible role in 3' end processing of animal histone mRNAs

Marc-David Ruepp[1], Ramesh S. Pillai[1,3], Nicole Kleinschmidt[1], Teldja N. Azzouz[1,4], Silvia Vivarelli[2], Silvia M.L. Barabino[2] and Daniel Schümperli[1]*

[1] Institute of Cell Biology, University of Bern, CH-3012 Bern, Switzerland; and [2] Department of Biotechnology and Biosciences, University of Milano-Bicocca, I-20126 Milan, Italy; [3] European Molecular Biology Laboratory, Grenoble Outstation, B.P. 181, F-38042 Grenoble Cedex 9, France; and [4] VIFOR Pharma SA, route de Moncor 10, 1752 Villars-sur-Glâne, Switzerland

*Correspondence to: Daniel Schümperli, University of Bern; Institute of Cell Biology; Baltzerstrasse 4; CH-3012 Bern; Switzerland; Tel.: +41.31.631.4675; Fax: +41.31.631.4616; Email: daniel.schuemperli@izb.unibe.ch

ABSTRACT

Transcripts from metazoan replication-dependent histone genes undergo a unique 3' cleavage reaction which does not result in polyadenylation of the mRNA. Although the cleavage site is defined by histone-specific factors (hairpin binding protein, a 100 kDa zinc finger protein and the U7 snRNP), a large complex consisting of cleavage/polyadenylation specificity factor, two subunits of cleavage stimulatory factor and symplekin acts as the effector of RNA cleavage. Here we report that yet another protein involved in cleavage/polyadenylation, mammalian cleavage factor I 68 kDa subunit (CF I_m68), participates in histone RNA 3' end processing. CF I_m68 was found in a highly purified U7 snRNP preparation. Its interaction with the U7 snRNP depends on the N-terminus of Lsm11 as we could show *in vitro* by GST-pulldown with the N-terminus of Lsm11, in extract by co-immunoprecipitation with anti-Lsm11 and anti-Lsm10 antibodies and *in vivo* by the bimolecular fluorescence complementation (BiFC) technique. Interestingly these interactions are abolished in a processing-deficient Lsm11 mutant. *In vivo*, both depletion and overexpression of CF I_m68 cause significant decreases in processing efficiency, whereas addition of CF I_m68 to *in vitro* processing reactions can stimulate 3' end formation. Finally, immunoprecipitation of CF I_m68 results in a strong enrichment of histone pre-mRNAs.

INTRODUCTION

Pre-messenger RNAs undergo a series of processing reactions, such as capping, splicing and 3' cleavage before they are exported from the nucleus and serve as templates for translation. For most mRNAs, 3' cleavage is immediately followed by polyadenylation (reviewed in (1). Only the metazoan replication-dependent histone mRNAs are generated by a different processing reaction and do not acquire a poly(A) tail (2).

The pre-mRNAs undergoing cleavage/polyadenylation contain cis-acting elements that direct the required factors to the cleavage site. Cleavage and polyadenylation specificity factor (CPSF) recognises the highly conserved AAUAAA hexamer located 10-30 nucleotides upstream of the cleavage site (3). Cleavage stimulatory factor (CStF) binds to a G/U rich sequence element downstream of the cleavage site (4). In addition, symplekin, cleavage factors I and II, poly(A) polymerase and nuclear poly(A) binding protein (PABN1) are required (1).

Different from the other mRNAs, the transcripts of replication-dependent histone genes in metazoans lack introns and poly(A) tails (2). Instead of the poly(A) tail, their mRNAs end in a conserved 26 nucleotide long sequence, 16 nucleotides of which form a hairpin-structure. The processing at the 3' end requires only one endonucleolytic cut that usually occurs five nucleotides after the hairpin. This cleavage reaction

is mediated by several trans-acting factors, among them the U7 small nuclear ribonucleoprotein (snRNP) which binds by RNA:RNA base pairing to a conserved histone downstream element (HDE) located a few nucleotides after the processing site. The U7 snRNP exhibits a unique ring-shaped protein complex composed of five Sm proteins and two U7-specific Sm-like proteins, termed Lsm10 and Lsm11 (5;6). Other important processing factors are the hairpin binding protein (HBP; also termed stem-loop binding protein, SLBP; (7;8), a 100 kDa zinc finger protein (ZFP100; (9) that connects HBP bound to the upstream hairpin with the U7 snRNP bound to the HDE, as well as an essential heat-labile protein complex (10;11).

Thus, in the past, the two types of processing reactions seemed to be very different, except, perhaps, for the chemistry of the ends produced and the preference for certain nucleotides at the cleavage sites (12-14). However, in 2005, the endonuclease executing the cleavage after the hairpin was identified as the 73 kDa subunit of CPSF (CPSF-73) (15) and the heat-labile factor (HLF) was identified as a complex consisting of all five subunits of CPSF, two subunits of CstF as well as symplekin (16). In addition, the U2 snRNP was found to bind to an RNA element in the coding region of replication-dependent histone mRNAs and thereby to stimulate the U7-snRNP-dependent 3'-end formation (17), similarly to interactions that occur between the last 3' splice site and CPSF bound to the polyadenylation site during cleavage and polyadenylation (18).

However, certain components of the cleavage polyadenylation machinery, including mammalian cleavage factor I (CF I_m), were not detected in the heat-labile complex. CF I_m is a heterodimer consisting of a small 25 kDa subunit and one of three different larger subunits of 59, 68 and 72 kDa, respectively (19). All three large polypeptides can be UV crosslinked to a cleavage and polyadenylation substrate. In addition, analysis of the kinetics of the cleavage reaction indicated that interaction of CF I_m with the RNA is one of the earliest steps in the assembly of the 3' end processing complex. It facilitates the recruitment of other processing factors and stabilises the binding of CPSF (20). The 68 kDa subunit has a domain organisation that is reminiscent of spliceosomal SR proteins with an N-terminal RNA recognition motif (RRM) and a C-terminal RS-like domain. The RRM does not bind strongly to RNA, but seems to function in the interaction with the small subunit CF I_m25 (21). The RS-like domain of CF I_m68 is sufficient for the localisation in nuclear speckles (and in the nucleoplasm) and mediates the interaction *in vitro* with a subset of shuttling SR proteins (21;22).

Surprisingly, we have identified CF I_m68 in our most highly purified U7 snRNP preparations (5;6). We could validate this association which appears to depend on the N-terminus of Lsm11 *in vitro and in vivo*. In addition CF I_m68 co-precipitates histone mRNA precursors (as well as some mature histone mRNA), and the efficiency of histone RNA 3' processing seems to depend on the presence of CF I_m68.

MATERIALS AND METHODS

Plasmids

Complementary DNA clones of mouse Lsm11 or its MPL>AAA mutant in the pcDNA3-HA vector as well as pGex-4T-derived plasmids containing the first 156 amino acid codons of Lsm11 or the MPL mutant as well as the first 202 amino acids of NXF1 have been described (6;23)(Ruepp, Aringhieri et al. 2009). pcDNA3-Flag-Lsm11 was constructed by replacing the HA-tag of the pcDNA3-HA-Lsm11 vector (5) with a linker encoding the Flag epitope. The cDNA for CF I_m68, kindly provided by Walter Keller (Biozentrum, University of Basel), was subcloned into pcDNA3-HA and pGex-4T1 (Amersham Biosciences). pMal-Tev-HA-CF I_m25 was constructed by inserting the CF I_m25 open reading frame together with a linker encoding the TEV protease cleavage site and the HA epitope into pMal-c (New England Bioloabs). pCMV-Flag- CF I_m25 is described elsewhere (Ruepp, Aringhieri et al. 2009).

To produce plasmids encoding HA-VC155-CF I_m68, HA-VC155-CF I_m25, Flag-VN173-Lsm11 and Flag-VN173-Lsm11/MPL, the open reading frames of CF I_m68, CF I_m25, Lsm11 and Lsm11/MPL were amplified by PCR from plasmids described above and subcloned in the Venus vectors pHA-VC155 and pFlag-VN173 (24).

Sequences coding for short hairpin RNAs (shRNAs) were inserted as double-stranded oligos into pSUPERpuro between the *Bgl*II and *Hin*dIII sites as described (25;26). Two different

target sequences were used for Lsm11 (5'-GGTATTCACTCGACACATA-3' and 5'-GTATTCACTCGACACATAA-3') and for Tcβ (5'-TAACCATGACTATATGTAC-3' and 5'-GGCTGATCCATTACTCATA-3').

In each construct, the sense and antisense sequences are separated by a 9-nucleotide spacer (TTCAAGAGA) that allows the formation of a hairpin loop. These vectors are referred to as pSUPuro-Lsm11-1 and -2 as well as pSUPuro-Tcr□-1 and -2. To obtain a puromycin-selectable HA-CFIm68 expression plasmid (HA-CFIm68-SUPuro), a fragment of pcDNA3-HA-CFIm68 containing CMV promoter, HA-CFIm68 cDNA and bovine growth hormone polyadenylation signal was inserted into pSUPERpuro (thereby replacing the shRNA expression cassette). All clones were verified by DNA sequencing. Details of the constructs are available on request.

Antibodies

An antibody to GST-CF I_m68 was raised in rabbits and affinity-purified by binding to the recombinant protein immobilised on nitrocellulose filters. On western blots, this antibody was detected with anti-rabbit antibody coupled to HRP (Promega). It revealed a single ~68 kDa protein in whole cell extract from human 293-T cells (data not shown). Other previously described antibodies were directed against Lsm10 and Lsm11 (5;6) and CF I_m25 (19) and SmB/B' (46). Flag-tagged proteins were detected by anti-Flag M2 monoclonal antibody (Sigma) coupled to horse radish peroxydase (HRP).

HA-tagged proteins were detected either directly with anti-HA antibody (12CA5, Roche) coupled to HRP or indirectly with a species-specific antibody coupled to HRP (Promega). Hexahistidine-tagged proteins were detected using an anti-His antibody (HIS1, Sigma).

For immunofluorescence, we used anti HA-tag (6E2, mouse monoclonal antibody, Cell Signaling) or anti Flag M2 (mouse monoclonal antibody, SIGMA) as primary antibodies and goat-anti-mouse Alexa fluor 488 and 633 (Molecular Probes) as secondary antibodies.

U7 snRNP purification and peptide sequencing

The purification of U7 snRNPs and peptide microsequencing (performed at the Harvard Microchemistry Facility) have been described (5).

Cell culture and transfection

Human HeLa and 293-T cells were grown in Dulbecco's modified Eagle's medium (Invitrogen, AG, Basel, Switzerland) supplemented with 10% fetal calf serum (BioConcept, Allschwil, Switzerland), 100 U/ml penicillin and 100 µg/ml streptomycin (Invitrogen, AG, Basel, Switzerland) at 37 °C in a wet atmosphere containing 5% CO_2. For plasmid transfection, they were grown to 60-70% confluency in 10 cm dishes and transfected with 10 µg of the appropriate plasmids complexed with Dreamfect (OZ Biosciences); cells were usually harvested 48 h post transfection.

For the fluorescence experiments of Figure 3, HeLa cells were grown on glass coverslips in Dulbecco's modified Eagle's

Medium High Glucose (Euroclone) supplemented with 10% fetal bovine serum (Euroclone), L-glutamine 2 mM (Euroclone) and 100 U/ml penicillin/streptomycin (Euroclone) at 37°C, 5% CO_2. Plasmid transfections were performed after cells had reached 80% confluency by using Escort V transfection reagent (Sigma) as recommended by the manufacturer.

CF I_m68 and Lsm11 depletion and CF I_m68 overexpression

Hela cells were transfected with either two siRNAs against CF I_m68 at 25 nM concentration each or a non-targeting siRNA control (Ambion) at 50 nM concentration by using Lullaby reagent (OZ Biosciences) according to the manufacturer's instructions. The cells were split 1:1 at 24 hours post transfection. After another 24 hours, a second round of transfection with half the initial amount of siRNAs was performed. Cells were then harvested 4 days after the primary transfection for RNA isolation and Western blot analysis of CF I_m68.

For depletion of Lsm11, the cells were transfected in 6-well plates with a mixture of 0.5 µg each of pSUPuro-Lsm11-1 and -2 or, as control, a similar mixture of pSUPuro-Tcr□-1 and -2. For the overexpression of CF I_m68, the cells were transfected with HA-CFIm68-SUPuro in 10 cm dishes by using the standard Dreamfect protocol described above. Control cells were either transfected with an empty pSUPERpuro or with a pSUPERpuro derivate expressing an HA-tagged EGFP. Both controls yielded similar results, indicating that the strong expression from the CMV promoter has no effect on its own. Culturing the cells in

the presence of 1.5 µg/ml puromycin eliminated untransfected cells. Three to five days after transfection cells were harvested for RNA isolation and Western blot analysis of CF I_m68.

To assess the depletion of Lsm11, cDNA corresponding to 100 ng reverse transcribed RNA was subjected to a Lsm11-specific PCR. The PCR was performed in a volume of 25 µl containing 12.5 µl 2x FastStart PCR Mastermix (Roche) supplemented with a primer pair specific for Lsm11 at a final concentration of 200 nM each, and 35 cycles were performed (for primer sequences see Supplementary Table S1).

Interaction studies by co-immunoprecipitation

The preparation of small-scale nuclear extracts and immunoprecipitations were performed as described (5). The extract from one 10 cm dish (100 µl) was incubated with 100 µg of RNase A (Sigma) for 20 min at 30°C prior to immunoprecipitation. Proteins were resolved on 12% high-TEMED SDS–polyacrylamide gels (27), analysed by western blots with appropriate antibodies (see below) and developed by the enhanced chemiluminescence method (Amersham).

Interaction studies by GST pull-down assays

To study protein-protein interactions *in vitro*, recombinant GST (negative control) GST fusion proteins were expressed in *Escherichia coli* BL21 Gold or BL21(DE3)LysS transformed with pGex-4T-derived plasmids encoding GST-fusions with the N-terminus of Lsm11, the N-terminus of Lsm11-MPL/AAA mutant or the first 202 amino acids of Nxf1. MBP- CF I_m25 and MBP-TEV-HA-CF I_m25 was expressed in BL21(DE3)LysS and

purified over Amylose (New England Biolabs) followed by the removal of the MBP-tag from MBP-TEV-HA-CF I_m25 by digestion of the fusion protein with ProTev protease (Promega). The purified GST-fusions were coupled to glutathione sepharose 4B beads (Amersham Biosciences) and incubated with hexahistidine-tagged CF I_m68 or HA-tagged CF I_m25. The beads and proteins were incubated in IIP150-NP40 (10 mM Tris·HCl, pH 8.0, 150 mM NaCl, 0.1% Nonidet P-40) at 4°C for 2 h with gentle agitation on a wheel. Subsequently, the beads were washed with IIP150-NP40 and the bound and input materials were resolved on 12% high-TEMED SDS–polyacrylamide gels (27), analysed by western blots with appropriate antibodies (see below) and developed by the enhanced chemiluminescence method (Amersham).

*BiF**C** detection*

HeLa cells that had been incubated for 24 hours after transfection were washed with PBS (130 mM NaCl, 20 mM potassium phosphate, pH 7.4), fixed for 10 min with PBS containing 4% (w/v) paraformaldehyde and mounted in Fluorsave Reagent (Calbiochem).

For measurement of Venus Fluorescent Protein fluorescence after complementation, the YFP beam-path was used as described (28). Complementation of the C-terminal YFP fragment VC155 with the N-terminal YFP fragment VN173 generates a fluorophore with an excitation maximum at 515 nm and an emission maximum at 528 nm. Therefore, the fluorescence resulting from complementation was recorded

through the Leica laser scanning acquisition system by using the argon laser line of excitation.

For immunofluorescence, cells fixed as described above were washed with PBS, permeabilised in CKS solution (Hepes 20 mM, Sucrose 300 mM, NaCl 50 mM, $MgCl_2$ 3 mM, Triton-X100 0,2%) for 5 minutes at 4°C, blocked in PBS containing 10% fetal bovine serum for 1 hour at room temperature, and incubated with the primary antibodies diluted in PBS containing 0.2% bovine serum albumin (BSA) for 1 hour at 37°C. Subsequently, cells were washed with PBS (3 times 5 min) and incubated with the secondary antibody diluted in PBS/0.2% BSA for 45 min at room temperature. The cells were again washed with PBS (3 times 5 min) and mounted in Fluorsave Reagent (Calbiochem).

Images were collected with a confocal microscope Leica TCS SP2 AOBS, by using LSC software. Fluorophores were excited by using standard laser lines.

RNA Immunoprecipitation

RNA immunoprecipitation was performed essentially as described (29). Briefly, $2.5x10^7$ cells were fixed in 1% formaldehyde for 30 min at room temperature, lysed in FA lysis buffer (50 mM HEPES-KOH [pH 7.5], 150 mM NaCl, 1 mM EDTA, 1% Triton X-100, 0.1% sodium deoxycholate, protease inhibitors) containing RNase inhibitor (RNAsin [Promega]; 80 U/500 µl buffer), and then nucleic acids were fragmented by sonication. Before immunoprecipitation, the extract was treated with DNase (400–500 units RNase-free DNase I [Sigma] per

500 µl extract) in 25 mM $MgCl_2$, 5 mM $CaCl_2$, 3 µl RNAsin for 10 min at 37°C. Nuclease digestion was stopped by the addition of EDTA to 20 mM. Reactions were cleared by centrifugation at 16'100 x g in a microcentrifuge for 15 min. For input RNA, all following steps up to Proteinase K digestion were omitted. Immunoprecipitation was performed by adding 30 µg anti-CF I_m68 or 30 µg BSA to the DNase-treated extract and incubating head over tail at 4°C overnight. Then 67 µl of protein G slurry (equilibrated in FA lysis buffer containing RNasein) were added to each tube and incubated for 2 hours at 4°C. All subsequent precipitate washes and the final elution were performed as described in (29). To the eluate fractions, NaCl was added to a final concentration of 200mM before addition of 80 µg proteinase K and incubation at 42°C for 1 hr. Crosslinks were reversed by heating at 65°C for 5 hours. The reactions were extracted with an equal volume of acid-equilibrated (pH 4.8) phenol:chloroform 5:1. For 1 to 2 hr, 1/10 volume of 3 M sodium acetate (pH 5.5), 20 µg glycogen, and 2.5 volumes of ice-cold absolute ethanol were added to the aqueous layer before precipitation at -80°C. The reaction was centrifuged at maximum speed in a microcentrifuge for 15 min and the precipitate washed twice with ice-cold 70% ethanol. To remove contaminating DNA, RNA was treated with Turbo DNase (Ambion) according to the manufacturer's protocol.

Quantitative reverse transcription PCR

Usually 400-1000 ng RNA were reverse transcribed in 50 µl Stratascript 6.0 RT buffer in the presence of 4 mM of all four

desoxy nucleotide triphosphates, 300 ng random hexamers, 40 U RNasIn (Promega), and 1 µl Stratascript 6.0 reverse transcriptase (Stratagene). For real-time PCR, reverse-transcribed material corresponding to 40 ng RNA was amplified in 25 µl Universal PCR Master Mix, No AmpErase UNG (Applied Biosystems) with specific primers, and TaqMan probes by using the ABI SDS7000 Sequence Detection System. The TaqMan assays for endogenous histone H3 RNA are specific for histone H3C, and use probes spanning the start codon and the 3' cleavage site to measure total RNA and pre-mRNA, respectively. Primer and probe sequences for these assays are shown in Supplementary Table S1.

In vitro histone 3' end processing

The standard reaction was carried out with 24 ul of HeLa nuclear extract and 10'000 cpm (1-3 fmol) 12/12 RNA template [2] in a total volume of 40 ul. To the processing reactions different amounts of either BSA or hexahistidine-tagged CF I_m68 in Buffer D (20 mM HEPES [pH 7.9], 20% glycerol, 100 mM KCl, 0.2 mM EDTA, and 0.5 mM DTT) were added. After incubation at 30°C, 1 ml TRI reagent was added followed by subsequent purification of the RNA. The samples were resolved by 8% denaturing polyacrylamide gel electrophoresis (7M Urea). The gel was dried and revealed on a Storm820 Phosphoimager (Amersham). The quantification of the bands was performed using Aida software V3.11 (Raytest Isotopenmessgeräte GmbH, Straubenhardt).

RESULTS

Identification of CF I_m68 as an interaction partner of the U7 snRNP

We previously reported the purification of U7 snRNPs and the characterisation of some of the associated proteins (5). Apart from the subunits already described, in our most highly purified U7 snRNP preparation, two additional bands of ~70 and ~50 kDa, respectively, were present (marked with asterisks in Figure 1C of reference (5). Microsequencing of the 50 kDa band later led to the identification of Lsm11 (6). The other marked band of approx. 70 kDa was also subjected to microsequencing by nano-electrospray tandem mass spectrometry coupled to the Sequest database search algorithm (30). This analysis revealed several peptides from bovine serum albumin (theoretical, unmodified molecular mass: 69'293 Da) and human cytokeratin 10 (59511 Da) that we considered to be contaminants. Additionally, the peptides GFALVGVGSEASSK, AISSSAISR and GPPPTDPYGRPPPYDR were indicative of the 68 kDa subunit of cleavage factor I (CF I_m68; 59210 Da). The location of the peptides is indicated in figure 1 as bars below the schematic domain organisation of CF I_m68.

Because it was not clear whether this association with highly purified U7 snRNPs might be due to a contamination or may reflect a real interaction, we immunopreciptated U7 snRNPs from total cell extract of 293-T cells expressing HA-tagged CF

I_m68. Separate precipitations were carried out with antibodies specific for Lsm10 (5) or Lsm11 (6), and co-precipitation of CF I_m68 was analysed by Western blotting with anti-HA antibody. Indeed, HA-CF I_m68 was efficiently co-precipitated by both antibodies, but not by beads alone (Figure 2A). Since the extracts had been treated with RNAse A, the interaction of CF I_m68 with the U7 snRNP-specific proteins Lsm10 and Lsm11 was apparently not mediated by RNA but rather due to a protein-protein interaction.

In an inverse experiment, protein G sepharose beads coupled with anti-Actin (negative control) or anti-CF I_m68 were used. However, in this case, nuclear extract from cells expressing FLAG-tagged Lsm11 was used, as our anti-Lsm11 antibodies fail to recognize endogenous Lsm11 in western blots, probably due to the low abundance of this protein. Following immunoprecipitation with anti-CF I_m68, the samples were boiled in sample buffer and subjected to SDS-PAGE and Western blotting. The results indeed showed that the anti-CF I_m68 antibody can co-precipitate Flag -Lsm11 (Figure 2B).

As CF I_m68 is usually found in a complex with CF I_m25 (19), we tested whether the small 25 kDa subunit of CFI is also associated with Lsm11. However, we could not detect any interaction, by trying to precipitate either Flag-tagged Lsm11 with anti-CF I_m25 antibody or CF I_m25 with anti-Flag antibody from cells expressing Flag-Lsm11 (Supplementary Figure S1).

CF I_m68 interacts directly with the N-terminus of Lsm11

The N-terminus of the U7-specific Lsm11 protein and, more specifically, an evolutionarily conserved amino acid motif, NVLTRMPLH, are essential for histone RNA 3' end processing but not required for incorporation of Lsm11 into U7 snRNPs (6;23;32). To investigate if CF I_m68 directly interacts with this part of Lsm11, we coupled purified, recombinant, GST-tagged N-terminal fragment of Lsm11 to glutathione beads and used these to precipitate -hexahistidine-tagged CF I_m68. Indeed, CF I_m68 interacted with the wild-type N-terminus of Lsm11, but not with a mutant in which the three amino acids MPL of the mentioned motif had been replaced by alanines (23) (Figure 3A, lanes 3 and 4). Additionally, no binding was observed with beads loaded with a GST fusion of the first 202 amino acids of Nxf1 (Figure 3A, lane 2) (Ruepp, Aringhieri et al. 2009). These interaction data were confirmed by GST-Pulldowns using *in vitro* translated HA-tagged CF I_m68, and we also found that the GST-fusion of the N-terminus of Lsm11 could bind CF I_m68 from an extract of mammalian cells (data not shown).

CF I_m68 is normally in a complex with CF I_m25, but the small subunit was neither found in the U7 snRNP purification, nor in Lsm11 co-precipitations. However, we wondered whether at least *in vitro* assembled CF I_m and the N-terminus of Lsm11 can form a trimeric complex or whether CF I_m25 competes with Lsm11 for the binding to CF I_m68. To adress this question we repeated the GST pulldown experiments but this time adding recombinant HA-tagged CF I_m25 to the GST-N-terminal

fragment of Lsm11-CF I_m68 binding reaction. As can be seen in figure 3B CF I_m25 does not interact directly with Lsm11 (lane 4) but can form a trimeric complex *in vitro* by interaction with CF I_m68 (lanes 6-8). When higher molar ratios of CF I_m25 in respect to CF I_m68 are added to the binding reaction, the amount of precipitated CF I_m25 does not increase, showing that the co-precipitated amount of CF I_m25 depends on the precipitated amount of CF I_m68. This experiment was also performed using MBP-CF I_m25 yielding the same results (data not shown).

In vivo interaction of CF I_m68 with Lsm11 but not the MPL mutant

To analyse whether the interaction between CF I_m68 and the U7 snRNP or Lsm11 can be detected in unperturbed cells *in vivo*, we used the recently developed method of bimolecular fluorescence complementation (BiFC; (24;33). In this method fluorescent proteins are split into two non-fluorescent halves, which then tag the proteins under study. The affinity of the fragments for each other is very low and therefore fluorescence complementation increases considerably when an interaction between the respective fusion partners brings them into close proximity. BiFC detects stable interactions: for complementation to occur, the halves have to interact for several seconds (33).

Flag-tagged full length wild-type Lsm11, as well as its MPL mutant mentioned above, were fused to the N-terminal 173 amino acids of the YFP mutant Venus (Flag-Lsm-VN and Flag-MPL-VN), while HA-tagged CF I_m68 or HA-tagged CF I_m25 were fused to the C-terminal 155 residues. The use of Venus

allows for BiFC analysis under physiological conditions and increases the signal output and specificity (24). First, we characterised the intracellular distribution of the fusion proteins in transiently transfected HeLa cells. While HA-CF I_m68-VC, like endogenous CF I_m68, was concentrated in the nucleus, with exclusion of the nucleoli (21) (Figure 4A), HA-CF I_m25-VN, Flag-Lsm11-VN and Flag-MPL-VN were distributed both in the cytoplasm and in the nucleus (Figure 4 B-D). In immunofluorescence anlyses, we found endogenous Lsm11 to be similarly distributed as U7 snRNA detected by fluorescent *in situ* hybridisation (34) and Lsm10 (5), i.e. predominantly in Cajal bodies with some background nucleoplasmic staining (supplementary Figure 2). The observation that VN-Lsm11 showed a stronger cytoplasmic staining than the endogenous protein could be explained by the fact that, upon overexpression, some of the recombinant protein does not get assembled into U7 snRNPs and therefore remains in the cytoplasm. Cytoplasmic accumulation of the fusion protein does not appear to depend on the presence of the VN-tag since cells expressing HA-tagged Lsm11 also showed a strong cytoplasmic signal (data not shown). Similarly, HA-CF I_m25-VN was distributed both in nucleus and cytoplasm. In this case, we reported previously that nuclear localization of exogenous CF I_m25 is stongly increased by the concomitant expression of the 68 kDa subunit, showing that the nuclear import of the small subunit of CF I_m requires association with one of the larger subunits (ref.). Control Western blot analyses indicated that the

different Venus fusion proteins were expressed at similar levels in the cells (Supplementary figure 3).

For direct comparison, the same cells were stained with either an anti-HA antibody that detects HA-CF I_m68-VC, HA-CF I_m68-VC or an anti-Flag antibody that detects Flag-Lsm11-VN.

As shown in Figure 4 (A column 2, C columns 1 and 2), the complementation signal was predominantly nuclear with exclusion of the nucleoli and was characterised by a patchy appearance. While CF I_m25, CF I_m68, and Lsm11 can form a trimeric complex *in vitro*, *in vivo* there seems to be no interaction between the small subunit of CF I_m and Lsm11 in the nucleus, where these proteins normally reside (Figure 4B). The fluorescence complementation observed between Flag-Lsm11-VN and HA-CF I_m25-VC could be an artefact of the high cytoplasmic level of both proteins that are not efficiently imported into the nucleus.

Importantly, however, upon cotransfection of VN-Lsm11 and VC-CF I_m68, fluorescence complementation was observed in more than 90% of the cells. In contrast, no BiFC colocalisation was observed between the MPL mutant of Lsm11 and CF I_m68 (Figure 4 D).

These experiments clearly demonstrate that the tagged Lsm11 and CF I_m68 colocalise in the cell nucleus in a speckled pattern.

CF I_m68 is involved in histone RNA 3' end processing

Since we found CF I_m68 to interact with Lsm11, but not with the processing-defective MPL mutant, we wanted to investigate its importance of this association for histone pre-mRNA 3' end processing. For this purpose, we established an assay to study a possible dependence of the histone RNA processing reaction on CF I_m68 *in vivo*. The measurements are based on quantitative real-time reverse transcription PCR (qRT-PCR) for total RNA and pre-RNA from the histone H3A/C genes (*Homo sapiens* histone cluster 2, H3A and H3C, The sequences of the two transcripts are identical and are referred to as H3C from now on). To ensure that both primer-probe sets are specific for H3C, the one for the total mRNA spans the AUG initiation codon (Figure 5A), thereby excluding several non-allelic H3 genes which are very similar in the coding sequences but differ in the 5' untranslated region. The primer-probe set for the pre-mRNA spans the 3' end processing site.

HeLa cells were depleted of CF I_m68 by transfection of siRNAs. Depletion of Lsm11, which was expected to reduce 3' end processing of histone mRNA, was used as positive control. The knock-down was performed using two plasmids, each encoding a different Lsm11-specific short hairpin and a puromycin selection marker. For both proteins, the depletion was almost complete within 4 days, as detected by Western blot for CF I_m68 and by RT-PCR for Lsm11, since in this case the endogenous protein can not be detected by Western blot due to its very low abundance (Figure 5D). As reference for the

normalisation of qRT-PCR, we used HeLa cells similarly transfected with a control siRNA or with two control plasmids encoding shRNAs specific for human T-cell receptor □ subunit (TcR□) mRNA that is not expressed in this cell line. Please also note that, because of the toxicity of the Lsm11 depletion, the cells had sometimes to be harvested at different times, in order to have enough live cells for the analysis. In these control cells, H3C pre-mRNA constituted 0.5-2 % of total H3C mRNA (data not shown). As expected, the depletion of Lsm 11 affected the 3' processing of histone H3 RNA. Compared to TcR□-depleted cells, the apparent *in vivo* processing efficiency was reduced, as reflected by a 3.5-fold increase in the ratio of pre to tot RNA (Figure 5E, dark columns). Depletion of CF I_m68, reduced the level of total histone H3C RNA to 92%, and increased the level of histone H3 pre-mRNA to 174% in comparison to the control cells, resulting in an overall 2-fold decrease in the apparent *in vivo* processing efficiency (i.e. the ratio of pre to tot RNA).

The differences between the control siRNA and CF I_m68 siRNA as well as between control or HA-CF I_m68 transfected cells were highly significant as evaluated by Student's *t*-test (Figure 5E). Taken together, these experiments therefore indicate a significant quantitative contribution of CF I_m68 to histone mRNA 3' end processing *in vivo*.

Surprisingly, overexpression of HA-tagged CF I_m68 decreased total H3C RNA and increased H3C pre-RNA, resulting in an overall 3.1-fold decrease in the apparent *in vivo* processing activity (Figure 5E, light columns). This processing

deficiency is additionally reflected by a decrease of the cytoplasmic levels of Histone H3 and Histone H1 mRNAs by 2.5- and 3-fold, respectively (data not shown). A possible explanation for this unexpected observation might be that exogenous CF I_m68 sequesters other 3' end formation factors into free (not RNA associated) and therefore nonfunctional complexes.

To further clarify the role of CF I_m68 in histone processing we performed *in vitro* cleavage assays in the presence of recombinant protein. We first titrated different amounts of histidine-tagged CF I_m68 and analysed its effect on 3' end formation. Interestingly, the addition of an excess of CF I_m68 affects 3' end formation (Figure 6B) leading to a more than 15% decrease of the processing efficiency, whereas more physiological amounts stimulated 3' end formation. Since CF I_m was reported to enhance the kinetics of the 3' end formation reaction for polyadenylated mRNAs we performed an *in vitro* processing time course adding 600 ng or 30 ng of His-CF I_m68 to our processing reaction. Indeed, compared to the control, the addition of 30 ng CF I_m68 leads to a slightly faster accumulation of processed histone mRNA (Figures 6C and D), whereas an excess of His-CF I_m68 reduces the accumulation of processed substrate, probably by sequestering other 3'end formation factors (Figures 6E and F).

CF I_m68 is associated with both unprocessed and processed histone pre-mRNA

Because we could demonstrate an interaction between Lsm11 and CF I_m68 *in vitro* as well as *in vivo* and because both CF I_m68 depletion and overexpression significantly influenced the 3' processing events, we asked if an association of CF I_m68 with histone pre-mRNAs or total RNAs can be demonstrated *in vivo*. To adress this question, we performed RNA immunoprecipitations. If the interaction of CF I_m68 with the U7 snRNP is occurring during the snRNP's activity in 3' end processing, it should be possible to enrich unprocessed histone mRNAs due to the binding of the U7 snRNP to histone mRNAs in the processing reaction. Alternatively, an interaction of CF I_m68 with mature mRNAs could be interesting in the light of a recent study of our two groups that demonstrated a novel role of CF I_m68 in mRNA export from the nucleus to the cytoplasm (36).

For this analysis, HeLa cells were fixed with formaldehyde, and whole cell lysates, supplemented with either anti-CF I_m68 antibody or bovine serum albumin (as negative control), were subjected to immunoprecipitation. After washing, the formaldehyde fixation was reversed by incubation with proteinase K and heat treatment, RNA was isolated, reverse transcribed and subjected to real-time RT-PCR analysis. The results indicated that, in these experiments, the H3C pre-RNA represented 0.53 ± 0.11 % of the total H3C RNA. In the immunoprecipitated sample this proportion was increased to 7.

8 ± 8.0 %. Despite this high standard variation which resulted from a very high pre/tot ratio in one of the immunoprecipitates, the pre/tot ratios were at least 4-fold higher in the precipitates than in the controls in all experiments (Figure 7). These results clearly indicate an interaction of CF I_m68 with both unprocessed histone precursors and mature histone RNA, but they also show that the immunoprecipitation enriched the histone pre-mRNA about 10-fold, strongly suggesting that CF I_m68 is present in the 3' processing complex and that CF I_m68 remains associated with some of the processed mRNA.

DISCUSSION

Our observations provide strong evidence for a new role of CF I_m68 in histone RNA 3' end processing. Although several other components of the cleavage and polyadenylation machinery, including all five CPSF subunits, symplekin, as well as two CStF subunits (CStF-64 and -77) have been found to constitute the heat-labile histone RNA processing factor (HLF), other components, including CF I_m, have not been detected in that complex (16), and have also not been reported to contribute to histone RNA processing before. In this work, we have shown that CF I_m68 can be found in highly purified U7 snRNP fractions, and that it interacts with the U7-specific Sm-like protein Lsm11. This interaction was revealed in cell extracts by co-immunoprecipitation (Figure 2), *in vitro* by GST-pulldown experiments (Figure 3) as well as *in vivo* by the bimolecular fluorescence complementation (BiFC) technique (Figure 4). Interestingly, this interaction was not observed with a mutant of Lsm11 (MPL mutant) which, when assembled with U7 snRNA, produces U7 snRNPs that are non-functional in histone RNA processing (23). This finding suggested that this interaction might have a role in the 3' processing reaction. In line with this idea, we have found that both depletion and overexpression of CF I_m68 leads to significant decreases in the processing efficiency *in vivo* (Figure 5). Finally, the fact that histone 3' end formation can be stimulated by the addition of His-tagged CF I_m68 (Figure 6) and the finding that histone mRNA precursors

are enriched ~14-fold by immunoprecipitation of CF I_m68 (Figure 7) also argues for a role in histone mRNA 3' end processing.

Interestingly, while the small CF I_m, subunit, CF I_m25, can form trimeric complexes with CF I_m68 and Lsm11 *in vitro*, it does not appear to be involved in this interaction *in vivo* (Figure 4B, Supplementary Figure S1). This negative finding suggests that CF I_m68 may exist in two different states: one, associated with CF I_m25, that is involved in cleavage/polyadenylation and the other, free of CF I_m25, that participates in histone mRNA metabolism. How these two states of CF I_m68 are controlled will be an interesting topic for future investigations.

Work on the role of CF I_m in cleavage/polyadenylation has shown that it is one of the earliest factors to bind to a cleavage/polyadenylation substrate (19;20). It can be crosslinked to the pre-mRNA and stabilises the binding of several other processing factors, in particular that of CPSF, thereby enhancing the kinetics of the processing reaction.

CF I_m additionally plays a role in the definition of 3'-terminal exons. The exon definition model postulates that splicing factors bound to the 3' and 5' splice sites (ss) of an exon interact with each other and that this defines the exon and selects it for inclusion in the mRNA (37). Mechanistically, this interaction is now known to be mediated by proteins of the serine/argininine-rich family (SR proteins) which bind to exonic splicing enhancer sequences and establish contacts via protein:protein interactions with each other, with U2 auxiliary

factor (U2AF) bound at the 3' ss and with the U1 snRNP at the 5' ss (reviewed in (38). However, in terminal exons, this model needs to be modified. While in 5'-terminal exons the mRNA cap is added co-transcriptionally and the nuclear cap-binding complex appears to stimulate the use of the downstream 5' ss (reviewed in (39), in 3'-terminal exons both the 3' ss and the polyadenylation site need to be defined. This might be achieved by a direct interaction between CPSF 100 and the U2 snRNP that was shown to stimulate both splicing and pre-mRNA processing in a coupled assay (18). However, since CF I_m68 shares structural features with SR proteins (an RNA recognition motif and an alternating charge domain rich in serines and arginines), and because of its already mentioned early binding to cleavage/polyadenylation substrates, it is also an excellent candidate for an integrating role in 3'-terminal exon definition. In agreement with this idea, CF I_m was found in purified human spliceosomes (40;41). Moreover, CF I_m68, and possibly the other large CF I_m subunits as well, can interact with several members of the SR family of splicing factors such as SRp20, 9G8, and hTra2beta via the C-terminal alternating charge domain (21). Finally, a stimulation of 3' end processing of human β-globin mRNA by U2AF-65 bound to the polypyrimidine tract of the 3'-terminal exon (42) was recently shown to be mediated by an interaction between U2AF65 and CF I_m59 (43).

However, replication-dependent metazoan histone mRNAs are intronless and one could therefore argue that no interactions defining the "terminal exon" are needed. However,

although a histone 3' processing signal by itself may be efficiently recognised in an *in vitro* processing system, it is not certain whether the same signal is sufficiently well defined to achieve efficient cleavage *in vivo*. Aided by a local concentration within histone processing bodies (44), HBP and the U7 snRNP, with the help of ZFP100, may bind efficiently to nascent histone pre-mRNAs. However, the interaction of these basic cleavage site recognition components with HLF has not been characterised and may require additional helpers *in vivo*. Along these lines it is interesting that an RNA element in the coding sequence of histone genes was shown to act as a binding site for U2 snRNPs and that this binding could stimulate U7-dependent RNA 3' cleavage (17). It has not yet been clarified how this stimulation works, but, based on a study on 3'-terminal exon definition in polyadenylation substrates cited above (18), an interaction between the U2 snRNP and CPSF could be the mechanism. Moreover, CF I_m68 might also make an important contribution to this process *in vivo* by tethering HLF/CPSF to the U7 snRNP. Thus CF I_m68 could aid the U7 snRNP to attract the cleavage effector HLF to the cleavage site that has already been defined by the U7 snRNP, HBP and ZFP100. Together with the already mentioned function of the U2 snRNP, this could result in an enhancement of 3' end cleavage not unlike the one seen in 3'-terminal exon definition. To underline these parallels between polyadenylation substrates and metazoan histone pre-mRNAs, one should perhaps refer to them as "3' cleavage exons".

Additionally to the U2 snRNP, also SR proteins such as SRp20 and 9G8 can bind to the sequence element in the coding region of histone mRNAs, and this interaction was found to stimulate histone mRNA export (45). Since CF I_m68 is known to bind to these SR proteins via its C-terminal alternating charge domain (21), it is also possible that CF I_m68 links the U7 snRNP to this mRNA internal element. Such an interaction could also contribute to the stimulation of 3' end processing discussed above. However, it might also have implications for the nucleo-cytoplasmic transport of histone mRNA. Our observation that not only histone pre-mRNAs, but also a fraction of mature mRNAs, are immunoprecipitated along with CF I_m68 (Figure 7) indicates that an interaction exists at least for a subpopulation of cleaved histone mRNAs. Important in this respect, we have recently described a function of CF I_m68 in promoting the export of polyadenylated mRNAs from the nucleus (Ruepp, Aringhieri et al. 2009). A similar role for the export of histone mRNAs therefore appears possible, but it could not be tested with the experiments described here, because of the effect that CF I_m68 has on *in vivo* processing. Further experiments more specifically measuring nucleo-cytoplasmic transport will be required to explore this possibility.

In conclusion, our data indicate that CF I_m68 plays one or more important role(s) in the expression of histone mRNAs. It increases the efficiency of 3' end processing in vivo, presumably by helping to attract HLF to the factors directly recognising the processing substrate and thereby improving the

definition of the "3' cleavage exon". Moreover, it may also stimulate histone mRNA export.

Funding

This work was supported by the Canton Bern and Swiss National Science Foundation grants 3100A0-065225, -105547 and -120064 to D.S. as well as by grants from MIUR-PRIN 2006 and the Cariplo Foundation To S.M.L.B.

Acknowledgements

We thank Walter Keller and Georges Martin (Biozentrum Basel) for generous gifts of clones antibodies, and bacculovirus hexahistidine-tagged CF I_m68. Chang-Deng Hu (Purdue University) for the BiFC plasmids and Karin Schranz for excellent technical support.

FIGURES

Figure 1. Domain organisation of CF I_m68.

CF I_m68 has a structure reminiscent to spliceosomal SR proteins. It contains an N-terminal RNA recognition motif (RRM) and a C-terminal charged domain. Over its RRM it interacts with the small subunit of CF I_m.Its C-terminal charged domain can bind to RNA and interacts with a subset of spliceosomal SR proteins. The positions of the peptides identified by microsequencing are indicated with bars.

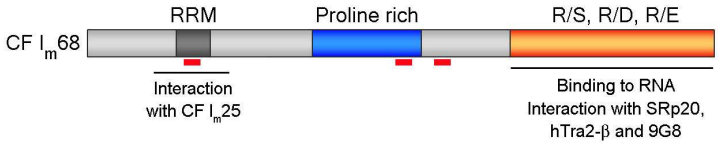

Figure 2. CF I_m68 interacts with Lsm10 and Lsm11.

(A) HA-tagged CF I_m68 was expressed in human 293-T cells and its ability to interact with Lsm11 and Lsm10 was assessed by immunoprecipitation with antibodies specific for Lsm11 (lane 3) and Lsm10 (lane 4). Negative control (lane 2), beads incubated with bovine serum albumin. Input, 1/30 of the amount used in the co-immunoprecipitation.

(B) Flag-tagged Lsm11 was expressed in HeLa cells and its ability to interact with CF I_m68 was assessed by immunoprecipitation with an antibody specific for CF I_m68. Anti-Actin served as negative control (lane 3). In both cases, the extracts had been treated with RNAse A. Lanes 1 and 2 are

1/10 and 1/15 of the amount used in the co-immunoprecipitation, respectively.

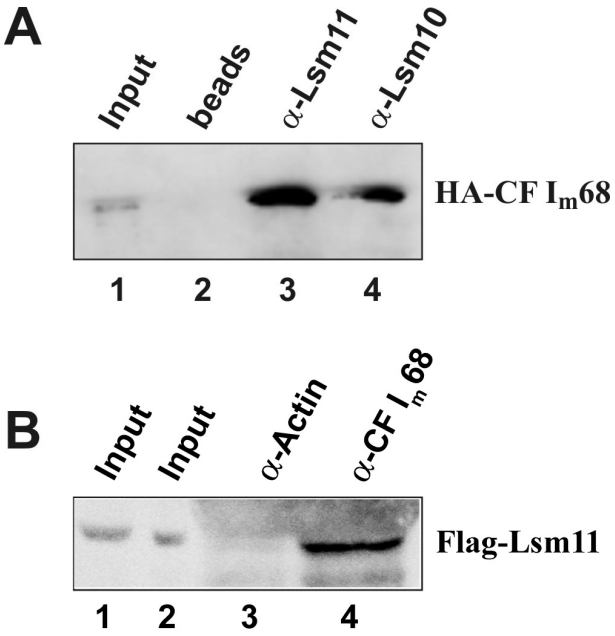

Figure 3. The interaction with CF I_m68 is specific for the wild-type N-terminus of Lsm11.

(A) Analysis of the binding of hexahistidine-tagged CF I_m68 to glutathione beads containing GST-NXF1-202 (lane 2) or GST fused to the first 157 amino acids of wild-type mouse Lsm11 (lane 3) or of a processing-deficient mutant thereof in which the amino acids 149-151 (MPL) are replaced by three alanines (23); lane 4). The beads were washed, and the bound material was analysed by western blotting (upper panel). To confirm that the absence of CF I_m68 in lane 4 is not due to an absence of GST-Nt-MPL, the blot was stained using Ponceau S (lower

panel). Input (lane 1), 1/3 the amount used in the binding assays was analysed directly. (B) Analysis of the binding of the hexahistidine-tagged CF I_m68 and HA-tagged CF I_m25 to glutathione beads containing GST fused to the first 157 amino acids of wild-type Lsm11. (Lane 1) is the same as in (A), (lanes 2 and 3) are the negative controls where equimolar amounts of His- CF I_m68 or HA-CF I_m25, repectively were incubated with GST. (Lane 4-8) glutathione beads containing GST fused to the first 157 amino acids of wild-type mouse Lsm11 that was incubated with HA-CF I_m25 (lane 4), His-CF I_m68 (lane 5), or both subunits with different ratios of HA-CF I_m25 to His-CF I_m68. The bound material was analysed by western blotting using anti-His and anti-HA antibodies, respectively.

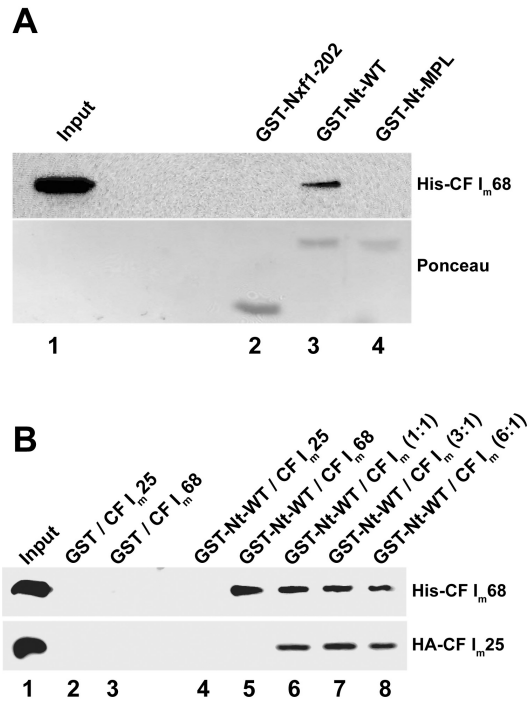

Figure 4. Interaction of CF I_m68 with Lsm11 in live, unperturbed cells.

The left column shows immunostaining images of HA-CF I_m68-VC, HA-CF I_m25-VC, Flag-Lsm11-VN, and Flag-MPL-VN after transient transfection of HeLa cells with the corresponding expression plasmids. The right column shows bimolecular fluorescence complementation (green) that occurs when the two proteins fused to the N- and C-terminal halves interact one each other. The first row in A-D shows the negative controls, where the fusion proteins are co-expressed with the empty vector expressing only the other half of the tagged fluorescent protein Venus (VN and VC, respectively) (A and C) Analysis of Lsm11/CF I_m68 heterodimerisation by confocal microscopy. (B) Analysis of Lsm11/CF I_m25 interaction. The immunostaining in the first row was performed with anti-HA, whereas the second and third row shows an immunostaining with anti-Flag (D) Analysis of Lsm11-MPL/CF I_m68 interaction.

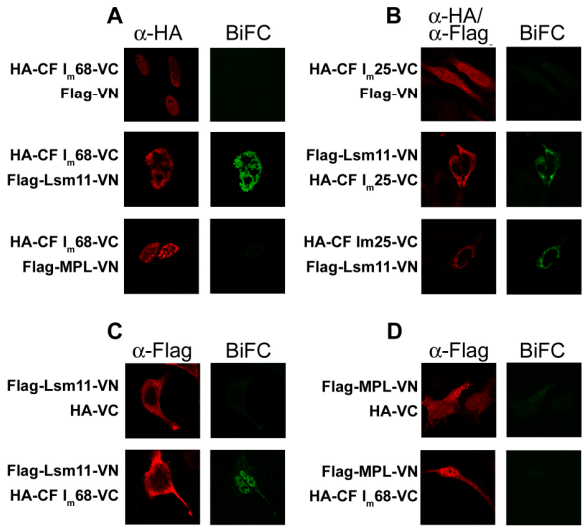

Figure 5. Effects of CF I_m68 depletion and overexpression on apparent histone RNA 3' end processing *in vivo*.

(A) Schematic representation of quantitative (real-time) reverse transcription-PCR (qRT-PCR) assay. Total mRNA (tot) of histone H3C is measured with a primer-probe set spanning the translation start codon. To measure the unprocessed precursors (pre), the primer-probe set spans the 3' cleavage site. (B) RNA 3' end processing efficiency in Hela cells depleted of CF I_m68 or Lsm11. The Western blots show endogenous CF I_m68 detected with anti-CF I_m68 antibody. SmB/B' served as loading control. The RT-PCR shows Lsm11 mRNA detected in total RNA. Depletion of Lsm11 seemed to be toxic to the cells, and a shift in the cell cycle distribution compatible with a G1 arrest could be detected by cytofluorometry of propidium iodide stained cells (supplementary Figure 4) in agreement with data published by others (35).

(C) RNA 3' end processing efficiency in Hela cells overexpressing CF I_m68. The Western blots show endogenous and HA-tagged CF I_m68 detected with anti-CF I_m68 antibody. SmB/B' served as loading control.

The relative *in vivo* processing efficiency was calculated as ratio of pre-mRNA to total mRNA and then normalised with respect to the ratio obtained in cells treated with either control siRNA, Tcr□-specific shRNA or pcDNA-puro. The data shown represent means ± standard deviations. Number of independent measurements (CF I_m68 depletion, 5; Lsm11 depletion, 3; CF

I_m68 overexpression, 4) p, significance values determined by Student's *t* test.

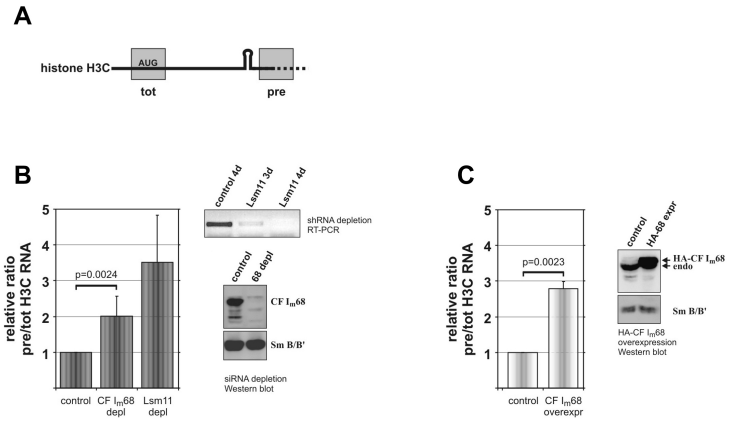

Figure 6. In vitro processing (A) Westernblot detecting CFI$_m$68 in 24 ul nuclear extract and a dilution series of hexahistidine-tagged CFI$_m$68.

(B) Graph showing the effect on the processing efficiency upon addition of recombinant His- CFI$_m$68 in comparison to the addition of the same amount of BSA. (C) Autoradiography of an *in vitro* processing time course with the addition of 30 ng BSA or 30 ng CFI$_m$68 to the processing reaction. (D) Graph showing the accumulation of processed substrate from experiment shown in C. (E) Autoradiography of an *in vitro* processing time course with the addition of 600 ng BSA or 600 ng CFI$_m$68 to the processing reaction. (F) Graph showing the accumulation of processed substrate from experiment shown in E. One representative experiment is shown.

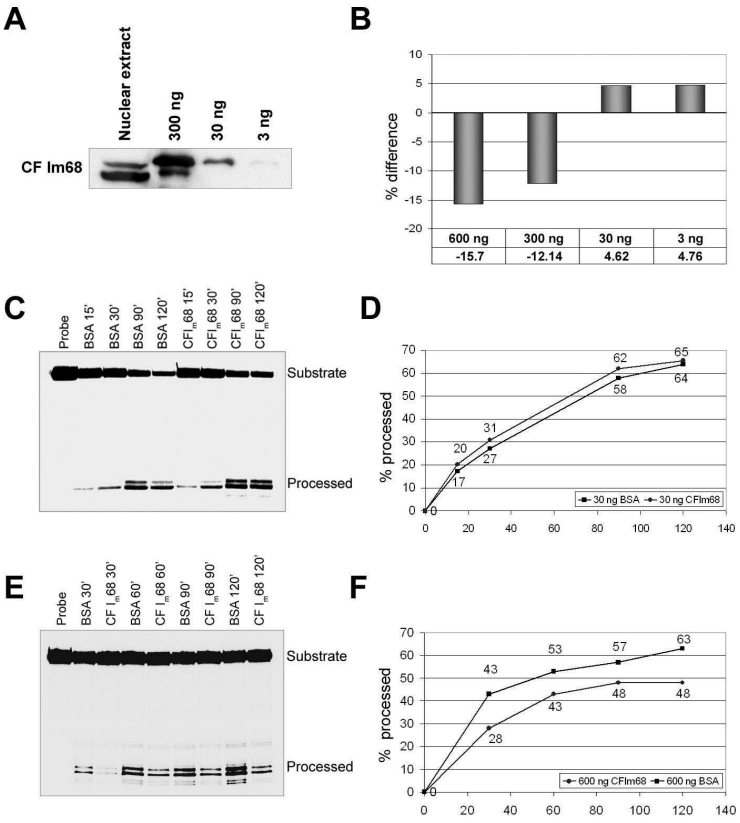

Figure 7. Co-immunoprecipitation of histone H3C pre-mRNA and total RNA with CF I_m68.

The graph shows the ratio between pre-mRNA and total histone H3C RNAs either in the input sample (light columns) or after co-immunprecipitation with anti-CF I_m68 (dark columns) as determined in three independent experiments. In Experiment 1 and 3 no RNA contamination was detected in the negative controls (n.c.), whereas for experiment 2 the contamination is shown as grey column. The cells were fixed with formaldehyde prior to extract preparation and immunprecipitation.

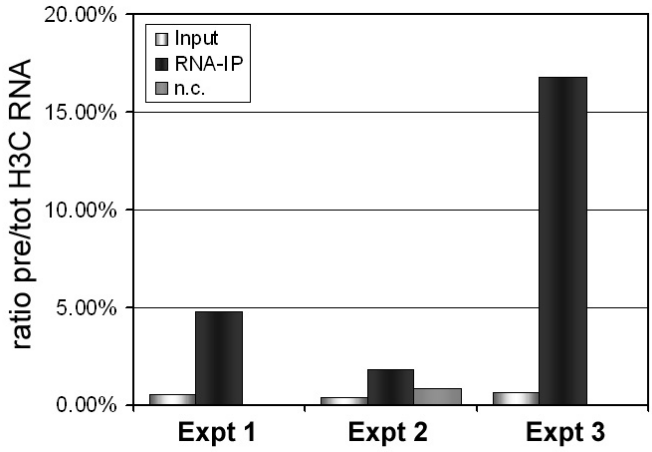

SUPPLEMENTAL MATERIALS

Supplementary Table S1. Sequences of oligonucleotides used for reverse-transcription-PCR.

Regular oligonucleotides

Lsm11 forward primer: 5'-AAGTTGGCTTCAGTGTGGGGAAG-3'

Lsm11 reverse primer: 5'-TCACTGTGCAAGATGAACCAGC-3'

TaqMan oligonucleotides for quantitative RT-PCR [a]

H3 pre *Taq*Man probe: 5'-FAM-CACCCACATCAGCACTT-NFQ-3'

H3 pre forward primer: 5'-TTCCATCGTATCCAAAAGGCTCTT-3'

H3 pre reverse primer: 5'-CAAGCGGTACAGCTTCTTCC-3'

H3 tot *Taq*Man probe: 5'-FAM-TCGCTATGGCCCGTACTAA-NFQ-3'

H3 tot for:	5'-GCTGGTAAGCCTGTGTTTTGG-3'
H3 tot rev:	5'-GCCGCCGGTCGACTT-3'

Abbreviations: FAM, 6-carboxyfluorescein; NFQ, non-fluorescent quencher. [a] The assays were designed by using File Builder of Applied Biosystems.

Supplementary Figure S1. Lack of evidence for an interaction of CF I_m25 with the U7 snRNP.

Flag-tagged Lsm11 was expressed in human 293-T cells and its ability to interact with CF I_m25 was assessed by immunoprecipitation with anti-CF I_m25 **(A)** or anti-Flag **(B)** antibodies. Relevant proteins were revealed by anti-Flag HRP (A and B, top) and anti-CF I_m25 (B, bottom). Negative controls (lanes 2), beads incubated with bovine serum albumin. Input, 1/30 of the amount used in the co-immunoprecipitation. Note that additional experiments also did not reveal any co-precipitation of Flag-tagged CF I_m25 by anti-Lsm11 antibody (data not shown).

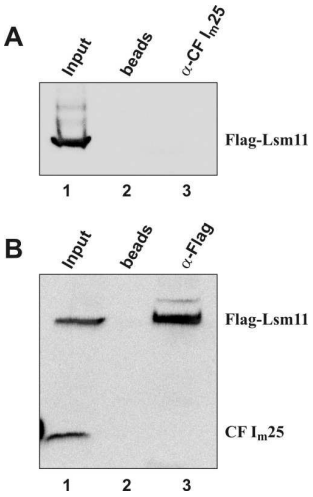

Supplementary Figure S2. Immunolocalisation of Lsm11.

Lsm11 (green) and coilin (red) were revealed in HeLa cells by indirect immunofluorescence: Methods were as described (Pillai *et al.*, 2001), except that Lsm11 was detected with affinity-purified rabbit polyclonal anti-Lsm11 antibodies (1:66).

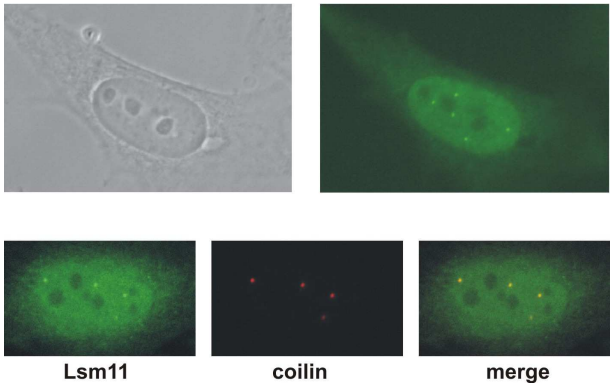

Supplementary Figure S3. Expression of fusion proteins in the same cell batches determined by immunoblotting with anti-Flag and anti-HA antibodies.

Note that a lane between lanes 8 and 9 has been omitted from the right hand panel.

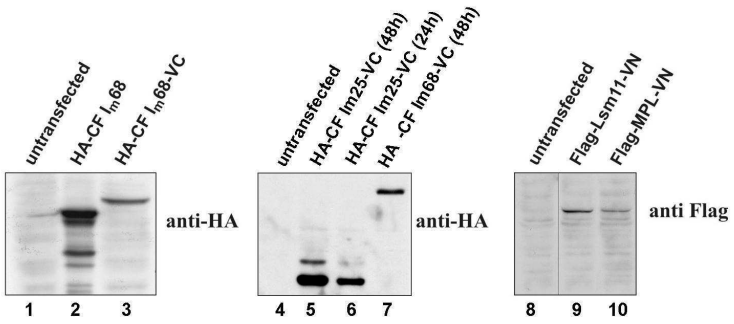

Supplementary Figure S4. Cytofluorometric analysis of HeLa cells depleted of Lsm11.

Hela cells were depleted from T-cell receptor β (Tcr beta) or Lsm11 by shRNA expression (see Materials and Methods of main manuscript). Four days after transfection, the cells were trypsinised and washed with phosphate buffered saline (PBS, 137 mM NaCl, 2.7 mM KCl, 10 mM Na2HPO4, 2 mM KH2PO4, pH 7.4) followed by resuspension in 400 µl PBS. For fixation, the cell suspension was added dropwise into 3ml precooled 70% EtOH under constant swirling. The fixed cells were then washed twice with PBS followed by incubation in 1 ml Propidium staining solution (PBS supplemented with 0.1% Triton-X-100, 2mg/ml RNAse A, 0.2 mg/ml propidium iodide) for 30 minutes at room temperature. Cell cycle stages were measured by cytofluorometry (Becton Dickinson BD FACS

Calibur), and Data were analysed using FlowJo software. The peaks corresponding to G1 and G2 are coloured in green and cyan, respectively. Cells in S-phase are coloured in yellow.

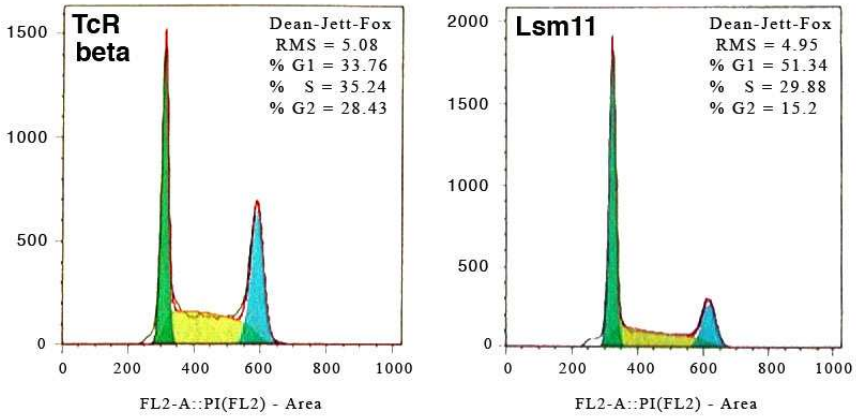

Reference

Pillai,R.S., Will,C.L., Lührmann,R., Schümperli,D., and Müller,B. (2001). Purified U7 snRNPs lack the Sm proteins D1 and D2 but contain Lsm10, a new 14 kDa Sm D1-like protein. EMBO J. *20*, 5470-5479.

REFERENCES

1. Mandel,C.R., Bai,Y. and Tong,L. (2008) Protein factors in pre-mRNA 3'-end processing. *Cell Mol. Life Sci.*, **65**, 1099-1122.
2. Dominski,Z. and Marzluff,W.F. (2007) Formation of the 3' end of histone mRNA: Getting closer to the end. *Gene*, **396**, 373-390.
3. Keller,W., Bienroth,S., Lang,K.M. and Christofori,G. (1991) Cleavage and polyadenylation factor CPF specifically interacts with the pre-mRNA 3' processing signal AAUAAA. *EMBO J.*, **10**, 4241-4249.
4. MacDonald,C.C., Wilusz,J. and Shenk,T. (1994) The 64-kilodalton subunit of the CstF polyadenylation factor binds to pre-mRNAs downstream of the cleavage site and influences cleavage site location. *Mol. Cell. Biol.*, **14**, 6647-6654.
5. Pillai,R.S., Will,C.L., Lührmann,R., Schümperli,D. and Müller,B. (2001) Purified U7 snRNPs lack the Sm proteins D1 and D2 but contain Lsm10, a new 14 kDa Sm D1-like protein. *EMBO J.*, **20**, 5470-5479.
6. Pillai,R.S., Grimmler,M., Meister,G., Will,C.L., Lührmann,R., Fischer,U. and Schümperli,D. (2003) Unique Sm core structure of U7 snRNPs: assembly by a specialized SMN complex and the role of a new component, Lsm11, in histone RNA processing. *Genes Dev.*, **17**, 2321-2333.

7. Wang,Z.F., Whitfield,M.L., Ingledue,T.C., Dominski,Z. and Marzluff,W.F. (1996) The protein that binds the 3' end of histone mRNA: a novel RNA-binding protein required for histone pre-mRNA processing. *Genes Dev.*, **10**, 3028-3040.
8. Martin,F., Schaller,A., Eglite,S., Schümperli,D. and Müller,B. (1997) The gene for histone RNA hairpin binding protein is located on human chromosome 4 and encodes a novel type of RNA binding protein. *EMBO J.*, **15**, 769-778.
9. Dominski,Z., Erkmann,J.A., Yang,X., Sanchez,R. and Marzluff,W.F. (2002) A novel zinc finger protein is associated with U7 snRNP and interacts with the stem-loop binding protein in the histone pre-mRNP to stimulate 3'-end processing. *Genes Dev.*, **16**, 58-71.
10. Gick,O., Krämer,A., Vasserot,A. and Birnstiel,M.L. (1987) Heat-labile regulatory factor is required for 3' processing of histone precursor mRNAs. *Proc. Natl. Acad. Sci. USA*, **84**, 8937-8940.
11. Lüscher,B. and Schümperli,D. (1987) RNA 3' processing regulates histone mRNA levels in a mammalian cell cycle mutant. A processing factor becomes limiting in G1-arrested cells. *EMBO J.*, **6**, 1721-1726.
12. Chen,F., MacDonald,C.C. and Wilusz,J. (1995) Cleavage site determinants in the mammalian polyadenylation signal. *Nucleic Acids Res.*, **23**, 2614-2620.

13. Müller,B. and Schümperli,D. (1997) The U7 snRNP and the hairpin binding protein: Key players in histone mRNA metabolism. *Semin. Cell Dev. Biol.*, **8**, 567-576.
14. Furger,A., Schaller,A. and Schümperli,D. (1998) Functional importance of conserved nucleotides at the histone RNA 3' processing site. *RNA*, **4**, 246-256.
15. Dominski,Z., Yang,X.C. and Marzluff,W.F. (2005) The polyadenylation factor CPSF-73 is involved in histone-pre-mRNA processing. *Cell*, **123**, 37-48.
16. Kolev,N.G. and Steitz,J.A. (2005) Symplekin and multiple other polyadenylation factors participate in 3'-end maturation of histone mRNAs. *Genes Dev.*, **19**, 2583-2592.
17. Friend,K., Lovejoy,A.F. and Steitz,J.A. (2007) U2 snRNP Binds Intronless Histone Pre-mRNAs to Facilitate U7-snRNP-Dependent 3' End Formation. *Molecular Cell*, **28**, 240-252.
18. Kyburz,A., Friedlein,A., Langen,H. and Keller,W. (2006) Direct Interactions between Subunits of CPSF and the U2 snRNP Contribute to the Coupling of Pre-mRNA 3' End Processing and Splicing. *Molecular Cell*, **23**, 195-205.
19. Rüegsegger,U., Blank,D. and Keller,W. (1998) Human pre-mRNA cleavage factor Im is related to spliceosomal SR proteins and can be reconstituted in vitro from recombinant subunits. *Mol. Cell*, **1**, 243-253.
20. Rüegsegger,U., Beyer,K. and Keller,W. (1996) Purification and Characterization of Human Cleavage Factor I(m)

Involved in the 3` End Processing of Messenger RNA Precursors. *J. Biol. Chem.*, **271**, 6107-6113.

21. Dettwiler,S., Aringhieri,C., Cardinale,S., Keller,W. and Barabino,S.M.L. (2004) Distinct Sequence Motifs within the 68-kDa Subunit of Cleavage Factor Im Mediate RNA Binding, Protein-Protein Interactions, and Subcellular Localization. *J. Biol. Chem.*, **279**, 35788-35797.
22. Cardinale,S., Cisterna,B., Bonetti,P., Aringhieri,C., Biggiogera,M. and Barabino,S.M.L. (2007) Subnuclear Localization and Dynamics of the Pre-mRNA 3' End Processing Factor Mammalian Cleavage Factor I 68-kDa Subunit. *Mol. Biol. Cell*, **18**, 1282-1292.
23. Azzouz,T.N., Gruber,A. and Schümperli,D. (2005) U7 snRNP-specific Lsm11 protein: dual binding contacts with the 100 kDa zinc finger processing factor (ZFP100) and a ZFP100-independent function in histone RNA 3' end processing. *Nucl. Acids. Res.*, **33**, 2106-2117.
24. Shyu,Y.J., Liu,H., Deng,X. and Hu,C.D. (2006) Identification of new fluorescent protein fragments for bimolecular fluorescence complementation analysis under physiological conditions. *Biotechniques.*, **40**, 61-66.
25. Brummelkamp,T.R., Bernards,R. and Agami,R. (2002) A system for stable expression of short interfering RNAs in mammalian cells. *Science*, **296**, 550-553.
26. Paillusson,A., Hirschi,N., Vallan,C., Azzalin,C.M. and Muhlemann,O. (2005) A GFP-based reporter system to

monitor nonsense-mediated mRNA decay. *Nucl. Acids. Res.*, **33**, e54.

27. Will,C.L., Kastner,B. and Lührmann,R. (1994) Analysis of ribonucleoprotein interactions. In Higgins,S.J. and Hames,B.D. (eds.), *RNA processing, Vol. 1*. Oxford University Press, Oxford, pp. 141-177.
28. Hu,C.D. and Kerppola,T.K. (2003) Simultaneous visualization of multiple protein interactions in living cells using multicolor fluorescence complementation analysis. *Nat Biotech*, **21**, 539-545.
29. Gilbert,C., Kristjuhan,A., Winkler,G.S. and Svejstrup,J.Q. (2004) Elongator Interactions with Nascent mRNA Revealed by RNA Immunoprecipitation. *Molecular Cell*, **14**, 457-464.
30. Chittum,H.S., Lane,W.S., Carlson,B.A., Roller,P.P., Lung,F.D., Lee,B.J. and Hatfield,D.L. (1998) Rabbit beta-globin is extended beyond its UGA stop codon by multiple suppressions and translational reading gaps. *Biochemistry*, **37**, 10866-10870.
31. Lomant,A.J. and Fairbanks,G. (1976) Chemical probes of extended biological structures: Synthesis and properties of the cleavable protein cross-linking reagent [35S]dithiobis(succinimidyl propionate). *J. Mol. Biol.*, **104**, 243-261.
32. Azzouz,T.N. and Schümperli,D. (2003) Evolutionary conservation of the U7 small nuclear ribonucleoprotein in Drosophila melanogaster. *RNA.*, **9**, 1532-1541.

33. Hu,C.D., Chinenov,Y. and Kerppola,T.K. (2002) Visualization of Interactions among bZIP and Rel Family Proteins in Living Cells Using Bimolecular Fluorescence Complementation. *Molecular Cell*, **9**, 789-798.
34. Frey,M.R. and Matera,A.G. (1995) Coiled bodies contain U7 small nuclear RNA and associate with specific DNA sequences in interphase human cells [published erratum appears in Proc Natl Acad Sci U S A 1995 Aug 29;92(18):8532]. *Proc. Natl. Acad. Sci. USA*, **92**, 5915-5919.
35. Wagner,E.J. and Marzluff,W.F. (2006) ZFP100, a Component of the Active U7 snRNP Limiting for Histone Pre-mRNA Processing, Is Required for Entry into S Phase. *Mol. Cell. Biol.*, **26**, 6702-6712.
36. Ruepp,M.D., Aringhieri,C., Vivarelli,S., Cardinale,S., Paro,S., Schumperli,D. and Barabino,S.M.L. (2009) Mammalian pre-mRNA 3' End Processing Factor CF Im68 Functions in mRNA Export. *Mol. Biol. Cell*, E09-05.
37. Berget,S.M. (1995) Exon recognition in vertebrate splicing. *J. Biol. Chem.*, **270**, 2411-2414.
38. Long,J.C. and Caceres,J.F. (2009) The SR protein family of splicing factors: master regulators of gene expression. *Biochem J*, **417**, 15-27.
39. Lewis,J.D. and Izaurralde,E. (1997) The role of the cap structure in RNA processing and nuclear export. *Eur. J Biochem*, **247**, 461-469.

40. Rappsilber,J., Ryder,U., Lamond,A.I. and Mann,M. (2002) Large-scale proteomic analysis of the human spliceosome. *Genome Res.*, **12**, 1231-1245.
41. Zhou,Z., Licklider,L.J., Gygi,S.P. and Reed,R. (2002) Comprehensive proteomic analysis of the human spliceosome. *Nature*, **419**, 182-185.
42. Millevoi,S., Geraghty,F., Idowu,B., Tam,J.L., Antoniou,M. and Vagner,S. (2002) A novel function for the U2AF 65 splicing factor in promoting pre-mRNA 3'-end processing. *EMBO Rep.*, **3**, 869-874.
43. Millevoi,S., Loulergue,C., Dettwiler,S., Karaa,S.Z., Keller,W., Antoniou,M. and Vagner,S. (2006) An interaction between U2AF 65 and CF I(m) links the splicing and 3' end processing machineries. *EMBO J*, **25**, 4854-4864.
44. Marzluff,W.F. (2005) Metazoan replication-dependent histone mRNAs: a distinct set of RNA polymerase II transcripts. *Current Opinion in Cell Biology*, **17**, 274-280.
45. Huang,Y. and Steitz,J.A. (2001) Splicing factors SRp20 and 9G8 promote the nucleocytoplasmic export of mRNA. *Mol. Cell*, **7**, 899-905.
46. Lerner,E.A., Lerner,M.R., Janeway,C.A. and Steitz,J.A. (1981) Monoclonal antibodies to nucleic acid-containing cellular constituents: probes for molecular biology and autoimmune disease. *Proc. Natl. Acad. Sci. U. S. A.*, **78**, 2737-2741.

Chapter 5

SUMMARY

The aim of the first work (presented in the Chapter 2) was to investigate the role performed by SRPK2 kinase in the regulation of alternative splicing in SH-SY5Y neuroblastoma cells after paraquat treatment (a complex I mitochondrial respiratory chain inhibitor). Alternative splicing is a versatile form of genetic control whereby a common precursor messenger RNA (pre-mRNA) is processed into multiple mRNA isoforms differing in their precise combination of exon sequences. This process is particularly important in the nervous system and its essential nature is underscored by the finding that its misregulation is a common feature of human diseases, including neurodegenerative pathologies. Our approach to gain insight the regulation of neuron specific pre-mRNA splicing brought us to the characterization of SRPK2 kinase because this protein phosphorylates Serine/Arginine-rich domain (RS-domain)-containing proteins and it is expressed almost exclusively in the nervous system. In order to understand how SRPK2 intracellular localization and activity are regulated, in first instance we performed a mutational analysis. These mutants have been characterized by transient transfection in SH-SY5Y neuroblastoma cells. We analysed SRPK2 intracellular localization both under physiological condition and after generating stress through mitochondrial damage, since

mitochondrial damage and oxidative stress are found in many neurodegenerative diseases. We also determined the effect of this stress treatment on SRPK2 phosphorylation and its nuclear translocation. We did this first by using the minigene E1A, an alternative splicing reporter system, and also by analysing both SR proteins intracellular localization and their phosphorylation status. This work showed that not only paraquat treatment increased the phosphorylated SRPK2 fraction, but also that a specific phosphorylation at its 581 residue could be connected with the nuclear translocation of SRPK2. Consequently, this nuclear translocation brought to a splicing change in the isoform ratio of the minigene reporter system. After the drug treatment we also observed a specific speckled enlarged pattern coupled with an increase in the phosphorylation level for the SR classical proteins, known targets of SR protein kinase 2. These findings supported a functional link between the nuclear translocation and the activity of this neuronal specific kinase.

In the second line of our research (presented in the Chapter 3) we performed experiments assessing the function of the mammalian 3' end processing factor CFIm68 in the mRNA export, thus confirming its action as an adaptor for TAP/NXF1 mRNA export receptor. In particular I helped to demonstrate that the tethering of CFIm68 promoted mRNA export by designing and performing an RNA FISH assay. I used a RNA-biotinylated probe that detected the intracellular localisation of an mRNA reporter construct co-transfected with the CFIm68 protein or control proteins. Therefore we observed an increase

of the probe fluorescent cytoplasmic signal only in the presence of the overexpressed CFIm68 but not with other control proteins, observation confirmed by further Real Time PCR data. In the third line of our research (presented in the Chapter 4) we reported that CFIm68 was also involved in the 3' end cleavage of mammalian histone transcripts (not polyadenylated) by interacting with the LSM11 U7 snRNP component both in vitro and in vivo thus increasing the efficiency of the 3' end processing in vivo. In this context I performed the Bimolecular Fluorescence Complementation (BiFC) analysis. I co-transfected the CFIm68 and the LSM11 proteins (or its MPL loss-of-function mutant) fused respectively with the C-terminus and the N-terminus of a Venus-Yellow Fluorescent Protein. Thus I detected a nuclear fluorescent complementation in more than 90% of the cells (or not complementation with the MPL mutant counterpart). This data supported our whole characterized observation concerning the involvement of this mammalian cleavage factor in 3' histone mRNAs processing.

GENERAL CONCLUSIONS AND FUTURE AIMS

While the results gained on the role assessed for CFIm68 both in mRNA export and 3'-end processing of animal histone mRNAs are discussed in details in the individual results and discussion sections (see Chapter 2 and 3), I would like to summarize the reached insights for the SRPK2 regulation after paraquat treatment (reported in Chapter 1), because it has been my main project. I would set them into a larger context, thereby discussing what can be the translational future perspectives.

In fact, we observed a SRPK2 mediated response after paraquat treatment involving SRPK2 upstream phosphorylation, which brought to a nuclear translocation and consequently to a spatial controlled function of the kinase. Strikingly, it appear clear that the understanding of this pathway will be a possible way to identify new drug targets useful in disease aimed therapy.

The emerging inhibitors of the signal transduction pathways regulating pre-mRNA alternative splicing may open the way to therapies against diseases caused by missplicing. In fact an increasing number of diseases caused by missplicing have been reported; in some cases, mutation(s) found around splice sites appear to be responsible for changing the splicing pattern of a transcript by unusual exon inclusion or exclusion, and/or alteration of 5' or 3' splicing sites [1]. A typical example is β-

thalassemia, an autosomal recessive disease, which is often associated with mutations in intron 2 of the β-globin gene. The generation of aberrant 5' splice sites activates a common 3' cryptic site upstream of the mutations and induces inclusion of a fragment of the intron-containing stop codon. As a result, the amount of functional β-globin protein is reduced.

For therapeutic modulation of alternative splicing, several trials with antisense oligonucleotide [2], peptide nucleic acid (PNA) oligonucleotide [3], and RNAi [4] have been reported. These approaches could be useful for manipulating a specific splice site selection of a known target sequence like β-globin [2].

However, the aberrant splicing, found in patients with breast cancer, Wilm's tumour, and Amyotrophic Lateral Sclerosis (ALS), are not always accompanied by mutations around splice sites. In fact, in sporadic ALS patients, EAAT2 (excitatory amino acid transporters 2) RNA processing is often aberrant in the motor cortex and in the spinal cord, the regions specifically affected by the disease. As exon 9 is aberrantly skipped in some ALS patients without any mutation in the gene [5], the disorders could be attributed to abnormalities in regulatory factors of splicing. Actually, the balance of alternative splicing products can be affected by changes in the ratio of hnRNPs and SR proteins [6], and in the phosphorylation state and localization of SR proteins [7].

During these years many laboratories in the world have been involved in the development of small molecules that affect the patterns of alternative splicing.

An example can be the study of SRPKs as new drug target. Inhibitors of SRPKs, such as SRPIN-340, may become novel therapeutic drugs broadly applicable for viral infections. In fact, Hagiwara group tried screening of specific SRPK inhibitors in a chemical library by an in vitro kinase assay, using an RS-repeat peptide as the substrate, and found that an isonicotinamide compound (N-[2-(1-piperidinyl)-5-(trifluoromethyl)phenyl] isonicotinamide), specifically suppresses the kinase activity of SRPK1 and was named SRPIN-340 (SR phosphorylation inhibitor 340) [8].

SRPK1 and SRPK2 were identified as the major cellular protein kinases able to phosphorylate Hepatitis B virus (HBV) core protein [9]. Herpes simplex virus 1 (HSV-1) protein ICP27 (infected cell protein 27), which contributes to host shut-off by inhibiting pre-mRNA splicing, was shown to interact with SRPK1 [10]. Interestingly, propagation of human immunodeficiency virus 1 (HIV-1) is suppressed by SRPIN-340 in MT-4 cells [8], indicating that SRPK-mediated phosphorylation of SR protein(s) play essential role(s) in the viral multiplication cycle. In addition to SRPIN-340, it was reported that a series of tricyclic quinoxaline derivatives have inhibitory activities against SRPKs [11].

In our study (Chapter 1) we examined the involvement of neuron-specific SRPK2 in neuronal cellular stress response. Also in this case the development and screening of small molecules specifically targeting SRPK2 should have interesting applications. First they could be used as tools to uncover new

functions gained by SRPK2 and also to study *in vivo* models of neurodegeneration. Second, once assessed the functional role gained by this kinase and once defined what would be the whole of alteration of alternative splicing regulation involved in neurodegeneration, these molecules could be employed in drug design and development.

Finally, I want to mention that the possibility to develop new therapies aimed to manipulate alternative splicing of specific genes with chemical compounds has been already proposed, notably for neuronal diseases, neoplastic diseases, and viral infections. However, signal transduction pathways that regulate alternative splicing have not been fully identified. Therefore, more basic research in this area is required.

REFERENCES

1. Faustino, N.A. and T.A. Cooper, *Pre-mRNA splicing and human disease.* Genes Dev, 2003. **17**(4): p. 419-37.
2. Sazani, P. and R. Kole, *Therapeutic potential of antisense oligonucleotides as modulators of alternative splicing.* J Clin Invest, 2003. **112**(4): p. 481-6.
3. Cartegni, L. and A.R. Krainer, *Correction of disease-associated exon skipping by synthetic exon-specific activators.* Nat Struct Biol, 2003. **10**(2): p. 120-5.
4. Celotto, A.M., J.W. Lee, and B.R. Graveley, *Exon-specific RNA interference: a tool to determine the functional relevance of proteins encoded by alternatively spliced mRNAs.* Methods Mol Biol, 2005. **309**: p. 273-82.
5. Lin, C.L., et al., *Aberrant RNA processing in a neurodegenerative disease: the cause for absent EAAT2, a glutamate transporter, in amyotrophic lateral sclerosis.* Neuron, 1998. **20**(3): p. 589-602.
6. Mayeda, A. and A.R. Krainer, *Regulation of alternative pre-mRNA splicing by hnRNP A1 and splicing factor SF2.* Cell, 1992. **68**(2): p. 365-75.
7. Nayler, O., et al., *The cellular localization of the murine serine/arginine-rich protein kinase CLK2 is regulated by serine 141 autophosphorylation.* J Biol Chem, 1998. **273**(51): p. 34341-8.

8. Hagiwara, M., *[Development of protein kinase inhibitors and their applications for chemical biology].* Nippon Yakurigaku Zasshi, 2008. **132**(1): p. 22-5.
9. Daub, H., et al., *Identification of SRPK1 and SRPK2 as the major cellular protein kinases phosphorylating hepatitis B virus core protein.* J Virol, 2002. **76**(16): p. 8124-37.
10. Sciabica, K.S., Q.J. Dai, and R.M. Sandri-Goldin, *ICP27 interacts with SRPK1 to mediate HSV splicing inhibition by altering SR protein phosphorylation.* EMBO J, 2003. **22**(7): p. 1608-19.
11. Szekelyhidi, Z., et al., *Synthesis of selective SRPK-1 inhibitors: novel tricyclic quinoxaline derivatives.* Bioorg Med Chem Lett, 2005. **15**(13): p. 3241-6.

RINGRAZIAMENTI

Gracias a la Vida cantava Violeta Parra...
Ed è così che comincio questi ringraziamenti perché se sono qui ora, se ho avuto tutte queste fortune, lo devo alla Vita, che mi ha regalato dei giorni intensi, ricchi di gioie, di dolori, ma soprattutto di amore, in tutte le sue forme, sentimento che purtroppo non tutti hanno la fortuna di avere dalla Vita ed è per tutto questo che ringrazio.
Grazie alla mia mamma Elsa: con te ne abbiamo passate tantissime di belle e di brutte in questi anni e sono felice di avere camminato accanto a te, anche nelle vie più difficili e sofferenti, mano nella mano, senza lasciare mai la presa. Ora ti vedo così sorridente e nonna felice che mi sembra tutto un brutto sogno quello che hai passato, ma cara mamma, la Vita ci ha dato sofferenze e ci ha dato anche i mezzi per superarle.
Grazie a Ginetta, senza di te come farei? Sei la mia seconda mamma e a te dovrò sempre tantissimo.
Grazie ai miei fratelli e ai loro consorti: Ugo, Rita, Isabella, Gianni, Danilo, Noemi. Voi siete stati per me papà e mamme e fratelli allo stesso tempo: non potrei essere più fortunata di così, grazie.
Grazie ai miei splendidi nipotini e nipotoni: Laura, Andrea, Sara, Valentina, Francesca, Gabriele, Chiara. Siete in sette, il numero perfetto; basta un vostro sorriso e passa ogni indugio.
Grazie al mio amore Nunzio: sei sempre al mio fianco e mi sostieni, specchiarmi nei tuoi occhi mi fa sentire unica.
Grazie ai miei cari e tanti Amici, nuovi e vecchi: Amici che ci sono sempre stati, Amici ritrovati, Amici nuovi conosciuti in questi anni e diventati così importanti, così unici e insostituibili.
Grazie al mio papà Agostino, che non è qua fra noi, che se ne è andato due giorni prima che io facessi il concorso per cominciare questa avventura del dottorato DIMET, che mi è mancato tanto, che mi manca sempre, ogni momento, e che paradossalmente sento sempre così vicino, anche se fisicamente non c'è più, ogni volta che devo fare delle scelte o ogni volta che devo andare avanti a muso duro, senza perdere la concentrazione, senza perdere la forza, senza perdere la passione.
Grazie a tutti i ragazzi del mio laboratorio: il capo, Silvia Barabino per i suoi insegnamenti. Reinaldo, Carolina, Vale: voi siete stati più che colleghi, ma amici: nei momenti in cui avevo bisogno, nei momenti in cui avete sopportato anche i lati più oscuri del mio carattere, perché stare assieme tante ore al giorno, praticamente tutto

il giorno, significa condividere; ed è davvero confortante avere con voi la conferma che anche sul lavoro si possono trovare amici veri e che le due cose siano tutt'altro che inconciliabili. Grazie anche ai relativamente neoarrivati, Gabriele, Andrea, Francesco, che hanno portato in laboratorio una ventata di testosterone, per la gioia di Reinaldo, che si sentiva in minoranza: siete tutti e tre delle bravissime persone.
Grazie a tutte le persone che ho incontrato sulla mia strada. Grazie agli amici e colleghi dei laboratori limitrofi con cui ho scambiato chiacchiere, reagenti, consigli e utili ragionamenti. Grazie agli amici e colleghi che ho incontrato nelle mie esperienze all'estero: in particolare Marc e Nicole, due ottime persone e ricercatori.
Grazie a tutti i lettori della mia tesi di dottorato.